Chapter 10: Detection and Attribution of Climate Change: from Global to Regional

Coordinating Lead Authors: Nathaniel Bindoff (Australia), Peter Stott (UK)

Lead Authors: Krishna Mirle AchutaRao (India), Myles Allen (UK), Nathan Gillett (Canada), David Gutzler (USA), Kabumbwe Hansingo (Zambia), Gabriele Hegerl (UK), Yongyun Hu (China), Suman Jain (Zambia), Igor Mokhov (Russia), James Overland (USA), Judith Perlwitz (USA), Rachid Sebbari (Morocco), Xuebin Zhang (Canada)

Contributing Authors: Ping Chang, Paul Durack, Jara Imbers Quintana, Gareth S. Jones, Georg Kaser, Alison Kay, Reto Knutti, James Kossin, Mike Lockwood, Fraser Lott, Jian Lu, Seung-Ki Min, Thomas Moelg, Pardeep Pall, Aurelien Ribes, Peter Thorne, Rong Zhang

Review Editors: Judit Bartholy (Hungary), Robert Vautard (France), Tetsuzo Yasunari (Japan)

Date of Draft: 15 April 2011

Notes: TSU Compiled Version

Table of Contents

Executive Summary

Evidence of the effects of human influence on the climate system has continued to accumulate and strengthen since the AR4. In particular a wealth of new evidence has emerged from across the climate system, including regional temperature changes, changes in the water cycle and the cryosphere, and oceanic changes, that points to a warming world resulting from increased greenhouse gas concentrations. The evidence for human influence on the intensity and frequency of extreme weather events [extremes] has strengthened. Evidence is emerging that changes in precipitation could be larger than predicted by current climate models, although uncertainties in data and analysis are large.

Evidence for Warming
Anthropogenic warming has been detected in temperature observations taken at the surface, in the atmosphere and beneath the surface of the ocean. Analyses of new data and a new generation of models, supports previous assessments for a strong robust detection of the effects of anthropogenic greenhouse gases concentrations on warming of the climate system. The anthropogenic fingerprints as observed in surface temperature (including greater warming at high latitudes and over land areas), in the free atmosphere (cooling in the stratosphere and warming in the troposphere) and in the ocean (warming spreading from the surface to depth) are distinctive in their patterns in space and time from the dominant modes of decadal variability and the expected response to natural forcings from changes in solar output and from explosive volcanic eruptions. Quantification of the contributions of anthropogenic and natural forcing using multi-signal detection and attribution analyses show that the largest contributor to the overall warming trend since the early and mid 20th century is greenhouse gases. Other forcings, including variability in tropospheric and stratospheric aerosols, stratospheric water, and solar output, as well as internal modes of variability, may have contributed to the year to year and decade to decade variability of the climate system, but cannot explain the systematic warming trends in the climate system since the early and mid 20th century.

From Global to Regional
Further evidence has accumulated on the detection and attribution of anthropogenic influence on warming in different regions of the world. The effects of human influence have been detected on warming over the Antarctic continent in addition to the other six continental regions of the world. Human influence has also been detected on many sub-continental scale regions (dividing the continental regions into 2 to 4 sub-regions depending on the size of the continent). Detection and attribution of changes at regional scales due to greenhouse gas increases is complicated by the greater role played by dynamical factors (circulation changes) and a greater range of forcings. These factors, while not dominant at global scales, can be much more important in particular regions of the world. Examples of such forcings include land use changes and the effects of sulphate and carbonaceous aerosols. Nevertheless, detection and attribution studies of specific regions for particular time periods have shown that in some cases a human influence on local warming can be detected.

The Water Cycle
New evidence has emerged for the detection of anthropogenic influence on aspects of the water cycle. While observational and modelling uncertainties remain, the consistency of the evidence from both atmosphere and ocean, points to robust evidence of anthropogenic influence on the water cycle. This is seen in the detection of human influence on the zonal pattern of global rainfall changes and on high northern latitude rainfall changes, on the increasing atmospheric humidity seen in multiple datasets and expected from theoretical considerations under a warming atmosphere, and on changes in runoff and drought. Detection and attribution of changes in these aspects of the water cycle are additionally supported by detection of systematic changes in oceanic salinity properties that are attributable to human influence and that are consistent with an amplified global water cycle. In addition, there is some evidence that changes in precipitation could be happening faster than predicted by current climate models.

The Cryosphere
Reductions in Arctic sea ice and northern hemisphere snow cover extent, and permafrost degradation are evidence of systematic changes in the cryosphere linked to anthropogenic climate change. Antarctic sea ice extent has increased by 1% with some regions increasing in area being balanced by regional decreases. Stratospheric ozone depletion and the consequent radiative and dynamical changes are a major factor in the observed variability of Antarctic sea ice. Expert assessments show that Greenland and Antarctica are

thinning at the edges, loosing mass and volume and thickening in the centre regions, through warmer oceans and by a warmer atmosphere over Greenland. Expert judgement implies that these responses of the ice sheets are consistent with climate change and likely to be larger than the natural variations. Mountain glaciers are systematically receding in response to the warming atmosphere and changed rainfall and exceeds the observed natural variations of these systems.

A Millennia to Multi-Century Perspective

Taking a longer term perspective shows the substantial role played by external forcings in driving climate variability on hemispheric scales, even in pre-industrial times. While internal variability of the climate system, with its ability to move heat around the climate system is important at the largest hemispheric scales, solar and volcanic forcing play a significant part in driving climate variability in the pre-industrial era. Climate models when they include natural forcings can explain a substantial part of the pre-industrial inter-decadal temperature variability on Hemispheric scales, and to some extent on smaller scales. However, these same climate models fail to explain more recent warming without the inclusion of anthropogenic increases in greenhouse gas concentrations. Analyses of the pre-industrial era also support the conclusion based on instrumental data that climate models are capable of adequately simulating natural internal variability required for detection studies.

Extreme Events

There has been a strengthening of the evidence for human influence on an increased frequency of extreme events. Evidence since the AR4 further supports a human influence on cold and warm temperature extremes, and this evidence has shown that very hot days have a detectable human influence. New detection and attribution studies show that human-induced increases in greenhouse gases have contributed to the intensification of heavy precipitation events observed over a large fraction of northern hemisphere continents. There is evidence that anthropogenic influence may have substantially increased the risk of extremely warm conditions regionally including the 2003 European heatwave, and may have significantly increased the underlying risk of flooding events associated with heavy precipitation events.

Implications for Projections

New analyses, particularly based on Top of Atmosphere radiative budget, are broadly consistent with the overall conclusion from the AR4 that equilibrium climate sensitivity (ECS) is very unlikely to be less than 1.5°C and that the upper tail of ECS is more difficult to constrain. New analyses further constrain net aerosol forcing and, there is evidence that models overestimate the rate of deep ocean heat uptake compared to constraints based on 20th century ocean and atmospheric data.

Remaining Uncertainties

While climate models successfully simulate many global and hemispheric scale aspects of climate variability and change, there is some evidence that climate models may overestimate warming trends over the past 30 years in the free troposphere tropics and Southern Hemisphere. Such discrepancies are not apparent in the surface temperature or radiosonde record over longer periods. At regional scales, considerable challenges remain in attributing observed variability and change to external forcing. Modelling uncertainties related to model resolution and incorporation of relevant processes become more important at regional scales, and the effects of internal variability become more significant in masking or enhancing externally forced changes.

10.1 Introduction

This chapter seeks to understand the causes of the observed changes that were assessed in Chapters 2 to 5. The chapter uses physical understanding, climate models and statistical approaches to understand what the observations are telling us about the causes of climate variability and change. It seeks to determine whether changes can be detected as being significantly outside the range expected from natural internal variability and assesses to what extent observed changes can be attributed to external drivers of climate change, both human induced and naturally occurring. It looks across the climate system as a whole, seeking to determine whether there are coherent changes being observed that are consistent with expectations of how the global climate would be predicted to behave, and what this tells us about the ability of climate models to predict future changes. The chapter also takes a regional perspective in seeking to understand why changes differ from place to place across the planet.

To achieve its objectives, this chapter looks right across the climate system, from the upper atmosphere to beneath the surface of the ocean. Its remit goes beyond temperature to assess also changes in the water cycle, circulation and climate phenomena (Section 10.3), ocean properties, including ocean temperature and salinity and sea level (Section 10.4), and the cryosphere, including sea ice, ice sheets, ice shelves and glaciers, and snow cover and permafrost (Section 10.5). The chapter considers not just how mean climate has changed but also how extremes are changing (Section 10.6) and, while it has a particular focus on the period for which instrumental data are available it also takes a multi-century perspective, including using non-instrumental data from paleoclimate archives (Section 10.7). It also considers the implications of new understanding of observed changes for climate projections both on the near-term and the long-term (Section 10.9).

There is increased focus on the extent to which the climate system as a whole is responding in a coherent way across a suite of climate indices such as surface mean temperature, temperature extremes, ocean heat content, river run off and precipitation change. To this end some recent literature has sought to analyse multiple variables in a single analysis and these studies are reviewed in a section on whole system attribution (Section 10.8). This whole system perspective is also taken in the final section which makes a synthesis of the evidence presented throughout the chapter (Section 10.10) to summarise the evidence for human influence on climate.

Research on the impacts of observed changes is assessed by Working Group II, which includes a chapter on detection and attribution of impacts. To try to ensure consistency across the Working Groups, here we adopt the terminology proposed by the IPCC good practice guidance paper on attribution (Hegerl et al., 2010) in describing the different approaches to attribution practised in the literature. Methodological approaches to detection and attribution are evaluated in Section 10.2.

There are additional challenges for attribution in proceeding from global to regional scales. Distinguishing signals of changes from the noise of natural internal variability generally becomes more difficult as spatial scale reduces. There is incomplete observational coverage of climate going back in time and observational uncertainties can be a greater problem for some regions than others. Models need to be assessed for their reliability at representing climate variability and change in the particular region in question, and local forcings such as changes in land use, that have little effect on large scales, may be important on regional scales. Extremes may be infrequently observed and dynamical or statistical models may be required to characterise the underlying variability of such rare events.

Evidence of a human influence on climate has progressively accumulated during the period of the four previous assessment reports of the IPCC. There was little observational evidence for a detectable human influence on climate at the time of the first IPCC Assessment report but by the time of the second report there was sufficient additional evidence for it to conclude that there was a “discernible” human influence on the climate of the 20th century. By the time of the third Assessment report attribution studies had begun to determine whether there was evidence that the responses to several different forcing agents were simultaneously present in temperature observations. The report found that a distinct greenhouse gas signal was robustly detected in the observed temperature record and that the estimated rate and magnitude of warming over the 2nd half of the 20th century due to greenhouse gases alone was comparable with, or larger than, the observed warming. It concluded that “most of the observed warming over the last fifty years is *likely* to have been due to the increase in greenhouse gas concentrations.”

With the additional evidence available by the time of the Fourth Assessment report, the conclusions were strengthened. This evidence included a wider range of observational data, a greater variety of more sophisticated climate models including improved representations of forcings and processes, and a wider variety of analysis techniques. This enabled the report to conclude that "most of the observed increase in global average temperatures since the mid-20th century is *very likely* due to the observed increase in anthropogenic greenhouse gas concentrations". The AR4 also concluded that "discernible human influences now extend to other aspects of climate, including ocean warming, continental-average temperatures, temperature extremes and wind patterns." This was based on quantitative attribution studies that had been conducted on climate variables other than global scale mean air temperature and that showed clear evidence of a response to anthropogenic forcing in these other aspects of climate.

A number of uncertainties remained at the time of AR4. It noted that difficulties remained in attributing temperatures on smaller than continental scales and over timescales of less than 50 years. Evidence for significant anthropogenic warming on continental scales excluded Antarctica for which no formal attribution studies were available at that time. Temperatures of the most extreme hot nights, cold nights and cold days were assessed to have likely increased due to anthropogenic forcing, but evidence for human influence on the hottest day was lacking. Formal attribution studies had found that there was a detectable volcanic influence on mean precipitation for some models, a result supported by theoretical understanding, but the result was not robust between model fingerprints, and an anthropogenic fingerprint on global precipitation changes had not been detected. While observed increases in heavy precipitation were consistent with expectations of the response to anthropogenic forcings, formal attribution studies had not been carried out. Such studies had not been widely carried out on other aspects of climate, with observational and modelling uncertainties and internal variability, making partitioning of the observed response into different anthropogenic and natural factors difficult. Inconsistencies between models and observations reduced the robustness of attribution results in some cases. Whereas there was a clear identification of an anthropogenic fingerprint in the pattern of tropospheric and stratospheric cooling that was observed, differential warming of the tropical free troposphere and surface was significantly larger in models than in some observational datasets, though this discrepancy was assessed to be most probably due to residual observational errors. The observed changes in sea level pressure in the NH were also substantially larger than those simulated, although the pattern of reduced pressure over the very high Northern latitudes was qualitatively consistent between models and observations. The observed variability of ocean temperatures appeared inconsistent with climate models reducing the confidence with which observed ocean warming could be attributed.

Since the AR4, improvements have been made to observational datasets, taking more complete account of systematic biases and inhomogeneities in observational systems, further developing uncertainty estimates, and correcting detected data problems (Domingues et al., 2008; Kennedy et al., 2011a, 2011b) There have been considerable advances in climate modelling, resulting in more climate models including a greater variety of forcings and processes including a better representation of aerosols, land surface properties and the carbon cycle. A more comprehensive set of simulations, including runs made with individual forcing combinations is now available as part of the CMIP5 archive. There has been an additional six years of data adding to climate records, which, for example, with the satellite era starting in 1979, has substantially lengthened records thereby providing a greater chance for signals of change to emerge from the noise of natural internal variability. With this greater wealth of observational and model data the opportunities have expanded to interrogate the observational record and thereby improve the extent to which observed changes can be partitioned into externally forced components and internal variability. These advances are assessed in this chapter.

10.2 Evaluation of Detection and Attribution Methodologies

Detection and attribution methods have been discussed in previous assessment reports; and the AR4 contains a detailed methods appendix (Hegerl et al., 2007b), which we refer to. For completeness, this section reiterates key points and further discusses new methodological developments and challenges, including in attributing smaller scale climate change. Methods are also summarized and discussed, including a cross-Working Group context, in the IPCC Good Practice Guidance Paper (Hegerl et al., 2010).

10.2.1 Chaos and Climate: The Context of Detection and Attribution

Detection and attribution describes the scientific activity concerned with quantifying the evidence for a causal link between external drivers of climate change and observed changes in climatic variables. It provides the central, although not the only, line of evidence that has supported statements such as "the balance of evidence suggests a discernible human influence on global climate" or "most of the observed increase in global average temperatures since the mid-20th century is very likely due to the observed increase in anthropogenic greenhouse gas concentrations."

There are four core elements to any detection and attribution study:
1. An estimate of how external drivers of climate change have evolved before and during the period under investigation, including both the driver whose influence is being investigated (such as rising greenhouse gas levels) and other external drivers which may have a confounding influence (such as solar activity);
2. A quantitative understanding, normally encapsulated in a model, of how these external drivers affect observable climate indicators, such as surface temperature change;
3. Real-world observations of those indicators; and
4. An estimate, often but not always derived from a physically-based model, of the characteristics of variability expected in those observations due to chaotic fluctuations generated in the climate system in the absence of any externally-driven climate change.

The Earth's climate is a chaotic system, generating effectively random variability on all time-scales through interactions within and between the system's components, including the atmosphere, oceans, biosphere and cryosphere. An apparent change or trend in a climate variable does not necessarily require an explanation in terms of an external driver: it may simply be a manifestation of chaotic variability. Therefore, a warming trend within a decade, or the occurrence of a single very warm year, is not by itself sufficient evidence for attribution to a particular external driver. Likewise, the absence of warming in the short term, or the occurrence of cold year or season, does not in itself call into question the existence of an attributable long-term warming trend in global climate. Hence, in contrast to the statement that the world is warming, no statement of why it is warming in a system as complex as the Earth's climate will ever be entirely unequivocal. The challenge in detection and attribution is to establish what can be said and at what level of confidence. The response to a particular forcing is said to be detected at the 5% confidence level if its magnitude in the observations is greater than would be expected from internal variability alone in at least 95% of cases. The same response is said to be attributable to that forcing if it can be detected despite allowing for uncertainty in other potentially confounding factors and if the observed response is consistent with the magnitude of the expected response to that forcing.

10.2.2 Methods: A Simple Demonstration of Common Principles

In this section, we demonstrate the common principles of detection and attribution using the simplest possible implementation comparing the observed surface temperature record with the CMIP5 ensemble [current figure based on 3 members of the CMIP3 ensemble].

The simplest evidence for attribution is the consistency test: climate model simulations that account for human influence on climate are found to be consistent with observations of a particular climate variable, while simulations that do not account for human influence are not. This is illustrated by Panels a) and c) of Figure 10.1 (Allen, 2007), which shows observed northern and southern hemisphere mean temperature anomalies from 1851 to present (dots) compared with the response of the members of the multi-model ensemble to the combination of anthropogenic and natural forcing, and to natural forcing alone respectively, with all time-series expressed relative to the mean of 1880-1920. It is evident from the figure that the observations are consistent with (meaning statistically indistinguishable from a member of) the ensemble that includes human influence and are not consistent with the ensemble that does not [results from statistical tests of consistency with CMIP5 need to be discussed here]. Such consistency tests are affected by uncertainties in forcing, in climate sensitivity (if the model's sensitivity is not correct, the test will be unreliable), and care should be taken in interpreting results from multiple hypothesis testing (Berliner et al., 2000).

[INSERT FIGURE 10.1 HERE]

Figure 10.1: Schematic demonstration of optimal detection (Allen et al., 2007; to be updated to CMIP5 models by Imbers et al., 2011). A simple attribution analysis, comparing model simulations with observed temperature changes over the 20th century. **a)** Observed northern and southern hemisphere area-averaged near-surface temperature anomalies during the period 1901–2005 relative to average temperatures between 1900–1940. Colour scale indicates time, with redder being more recent. Black lines: Corresponding simulated temperatures from six of the models shown in Figure 1 driven by the combination of GHG increase, anthropogenic sulfate aerosols, and natural (solar and volcanic) variability. Southern Hemisphere points are offset by 1^{o}C. **b)** Same data, plotting model simulations (horizontal) against observations (vertical). Colour scale indicates time, as in Panel a). **c)** and **d)** show the same but where the models only include natural forcings. **e)** Observed temperature anomalies after removing the best-fit contribution from sulfate and natural forcing. Best-fit is obtained from a three-way, least-squares multiple linear regression between the observations and model-simulated responses to GHGs, sulfate, and natural forcing, obtained from simulations in which drivers are prescribed separately (ensemble means smoothed with a five-point running mean). Black lines: Simulated temperatures from three models driven by GHGs alone. **f)** Simulated greenhouse response versus observed temperatures after removing best-fit sulfate and natural contributions. Regression fits are obtained for the models separately, hence allowing the models to make different errors in the magnitudes of their responses. Fitted points are plotted separately in Panel f) and averaged together before being removed from the observation in Panel e). **g)** and **h)**: same as in e) and f), but showing the response to anthropogenic sulfates. **i)** and **j)**: the response to natural (solar and volcanic) variability. Formal uncertainty analysis of regression slopes requires a more sophisticated treatment. The fact that the dots in Panel f) lie along the leading diagonal indicates that these models are neither overestimating nor underestimating the response to GHG increase (Allen, 2007).

If we could be confident that all the uncertainties in climate simulation were represented in the multi-model ensemble, then consistency of the observations with the ensemble that includes human influence, and inconsistency with the ensemble that does not, would be sufficient for attribution. The detection and attribution community has, however, always taken a more conservative approach, to allow for the possibility that all available models might be consistently over- or under-estimating the magnitude of the response to climate forcing, either due to uncertainty in forcing or response, for example due to erroneous climate sensitivity or transient climate response.

Panels b) and d) in Figure 10.1 demonstrate there is a good fit between observed surface temperature changes and the ensemble mean when human influence is included, and a poor fit when it is not, indicating that no amount of re-scaling of the response to natural forcing would account for the changes observed.

An even more conservative approach is to allow for the possibility that models may over- or under-estimate the magnitude of the response to individual forcings by different factors. To allow for this, it is normally assumed that the responses to different forcings add linearly, and that internal climate variability is independent of the response to external forcing, so the response to any one forcing can be scaled up or down without affecting any of the others. This linearity assumption has been tested and found to hold for large-scale temperature changes, but there are reasons in principle to suspect it might not hold for other variables like precipitation (see discussion in Hegerl et al. (2007b) and Hegerl and Zwiers (2011)). Attribution does not require linearity, but assuming it simplifies the analysis.

The hypothesis that the response to individual forcings may be over- or under-estimated can be tested by plotting the response to a particular forcing against observed changes from which the estimated response to other forcings, defined here simply as the least-squares fit to the multi-model ensemble mean, has been subtracted. This is essentially what is done when a multiple regression is performed to distinguish the impact of a particular factor from various potentially confounding factors in any field of the natural or social sciences. It must be stressed that Figure 10.1 does not present a new approach, but is provided to allow readers to visualise the essential principles common to the majority of attribution studies since Hasselman(1997). Dots in Panels e), g) and i) in Figure 10.1 show observed northern and southern hemisphere temperatures from which the estimated responses to e) sulphate and natural, g) greenhouse and natural, and i) greenhouse and sulphate forcing have been subtracted. Lines show model responses to e) greenhouse, g) sulphate and i) natural forcing alone for members of the multi-model ensemble (sulphate is used here as shorthand for anthropogenic aerosols in general). The observed response to these individual forcings is consistent with the corresponding responses in the multi-model ensemble, as well as the response to all forcings taken together (Panel a).

The analysis of individual forcings is important, because only if forcings are estimated individually, can fortuitous cancellation of errors be avoided. Such a cancellation of errors between climate sensitivity and the magnitude of the sulphate forcing in models may have led to an underestimated spread of climate model simulations of the 20th century (Kiehl, 2007; Knutti, 2008). This cancellation of errors was never an issue for the core attribution conclusions of the 4th Assessment because these relied on studies that estimated the responses to greenhouse and sulphate forcing separately, although if models were conditioned with observations of 20th century climate change (Knutti, 2008) then the amplitudes of the simulated and observed responses to each forcing would be more likely to be found consistent . Panels f), h) and j) in Figure 10.1 show the multi-model mean response to greenhouse, sulphate and natural forcing respectively, plotted against observed changes from which confounding variability (i.e., changes correlated with the estimated response to either of the other two forcings) has been subtracted. The strength of the relationship between modelled and observed response in these panels provides a visual indication of the strength of the evidence for a response to these various factors.

Quantitative tests of the null-hypothesis of no relationship between forcing and response, and estimates of uncertainty in estimated best-fit scaling of models to data requires a detailed statistical model. This section and Figure 10.1 is intended to demonstrate the simple principles that are common to all detection and attribution studies. Consistent with standard statistical practice, a model-simulated response to external forcing is deemed consistent with the observations at a given confidence level if the hypothesis that the observations were generated by an identical response plus internal climate variability cannot be rejected at that confidence level. Hence the estimated properties of internal climate variability play a central role in this assessment. These are either estimated empirically from the observations (Section 10.2.3) or derived from control simulations of coupled models (Section 10.2.4).

10.2.3 Time-Series Methods and Granger Causality

A number of studies have applied methods developed in the econometrics literature to assess the evidence for a causal link between external drivers of climate and observed climate change using the observations themselves to estimate the expected properties of internal climate variability (e.g., Kaufman and Stern, 1997). The advantage of these approaches is that they do not depend on the accuracy of any particular climate model's simulation of variability. The price is that some kind of statistical model of variability must be assumed to allow information on timescales that are not thought to be strongly affected by external climate forcing to be used to predict the properties of internal climate variability on timescales that are affected by external forcing.

Time-series methods applied to the detection and attribution problem can generally be cast in the overall framework of testing for Granger causality. This is essentially a least-squares likelihood-maximisation approach in which an observed series y_t is modelled as a (linear or non-linear, depending on the complexity of the application) function of earlier values of both itself and any candidate series x_{it} that is suspected to have had a causal influence on y_t, together with an additive uncorrelated Gaussian noise z_t: hence the statistical model is $y_t = f(y_{t-1}, y_{t-2}, ..., y_{t-k_0}, x_{it-1}, x_{it-2}, ..., x_{it-k_1}, x_{jt-1}, x_{jt-2}, ..., x_{jt-k_2}, ..., z_t)$.

Although attractively general, this model potentially contains more undetermined parameters than there are data-points, particularly if the function f is allowed to be non-linear. Hence physical arguments have to be used to limit the number of lags (k_0, k_1 etc.) to consider and in some cases to constrain relationships between parameters to avoid overfitting and spurious conclusions.

In conventional tests of Granger causality, a variable x_{it} is said to "Granger cause" y_t if the omission of x_{it} significantly increases the magnitude of the estimated noise required in the statistical model. This can lead to an over-emphasis on short-term fluctuations when the main interest is in understanding the origins of a long-term trend. Smirnov and Mokhov (2009) propose an alternative characterisation that allows them to distinguish between conventional Granger causality and a "long-term causality" that focuses on low-frequency changes. Lockwood (2008) uses a similar approach, following (Douglass et al., 2004; Lean, 2006; Stone and Allen, 2005a). Although not always couched in terms of Granger causality, these analyses nevertheless conform to the same general statistical model.

Time-series methods are ultimately limited by the structural accuracy of the statistical model used, or equivalently the validity of the constraints imposed on the very general form of the Granger causality model. Many studies use a simple AR(1) model of residual variability, which implies an exponential decay of correlation between successive fluctuations with lag time. On timescales longer than the correlation decay time, AR(1) noise is essentially uncorrelated, implying no further increase of power with timescale.

Given limited data, it may be impossible to reject an AR(1) model for residual variability, but in most climate indicators for which long time-series exist, power is generally found to continue to increase with timescale even all the way out to millennial timescales. It is impossible to assess on the basis of the time-series alone whether this is a consequence of external forcing or arises from the properties of internal climate variability, but it has been shown (Franzke, 2010) that trends that appear significant when tested against an AR(1) model are not significant when tested against a process which supports this "long-range dependence." Hence it is generally desirable to explore sensitivity of results to the specification of the statistical model in any time-series based analysis.

10.2.4 Methods Based on General Circulation Models and Optimal Fingerprinting

Fingerprinting methods are able to use more complete information about the observed climate change, including spatial information. This can particularly help to separate the pattern of forced change from patterns of climate variability. Fingerprint methods also generally use climate model data to estimate the uncertainty due to variability generated within the climate system, which avoids assumptions such as long-range dependence or AR(1), but leaves uncertainty due to questions about the realism of model variability. Figure 10.1 provides a visualisation of the relationship between simulated and observed temperature responses to various climate forcing factors, but translating this into a quantitative estimate of the fraction of recent warming attributable to different factors, and an uncertainty range therein, requires two further components. First, a quantitative measure of the strength of an association or correlation between observed changes and fingerprints, is required. This essentially defines how much weight is given to different combinations of points in the scatter plots in Figure 10.1 in defining the correlation, down-weighting (in many studies) combinations which are subject to high levels of "climate noise". Second, a measure of internal climate variability, possibly augmented by a measure of uncertainty in the model-simulated response patterns, is required to define the null-hypothesis of no relationship between the observations and any particular model-simulated signal.

When the signal of a particular external forcing is strong relative to the noise of internal variability, results are not particularly sensitive to the precise specification of variability in either step. When the signal-to-noise ratio is low, however, as is often the case with regional or non-temperature indicators, the accuracy of the specification of variability becomes a central factor in the reliability of any detection and attribution study. In studies cited in the IPCC 4th Assessment, variability was typically represented by the sample covariance matrix of segments of control runs of climate models. Since these control runs are generally much too short to estimate the full covariance matrix, a truncated version is used retaining only a small number, typically of order 10–20, of high-variance principal components.

A full description of optimal fingerprinting is provided in Appendix 9.A of (Hegerl et al., 2007b) and further discussion of the methods is to be found in Hegerl and Zwiers (2011). The key elements of an optimal fingerprinting analysis are illustrated in the schematic shown in Figure 10.2. Typically these analyses are of patterns in space and time since both facets are needed to describe fingerprints of forcings and to distinguish between them. Model data are masked by observational data so that analyses are only carried out where observational data are available. The observed and modelled space time patterns are compared in a linear regression where the signal patterns and observations are normalized by the climate's internal variability. This normalization, standard in linear regression, is used in most detection and attribution studies to improve the signal-to-noise ratio. Signal estimates are obtained by averaging across ensembles of forced climate model simulations so as to reduce the contamination of the signal by internal variability noise.

[INSERT FIGURE 10.2 HERE]

Figure 10.2: Schematic of a detection and attribution analysis on multiple signals employing a linear regression based approach. In the example given here two signals are employed (anthropogenic and natural) and five spatial patterns make up each fingerprint.

The main innovation in optimal fingerprinting since the 4th Assessment is the introduction by Ribes et al. (2009) of a regularized estimate of the covariance matrix, being an optimally-weighted linear combination of the sample covariance matrix and the corresponding unit matrix. This has been shown (Ledoit and Wolf, 2004) to provide a more accurate estimate of the true covariance matrix (that which would have been obtained if an infinitely long stationary realisation of control variability were available) than the sample covariance matrix. The regularized covariance also has substantial advantages in being well-conditioned and invertible, avoiding dependence on the truncation step which can have a substantial and relatively arbitrary impact on results. The advantages of the regularized covariance matrix were demonstrated in a detection study focussing on regional temperature change over France, but this method has yet to be applied to the standard global attribution problem [Note this needs to be done for results to be included in summary figures].

The next step in an attribution study is to check that the residual variability, after the responses to external drivers have been estimated and removed, is consistent with the expected properties of internal climate variability, and that the estimated magnitude of the externally-driven responses are consistent between model and observations (equivalent to the slopes of the scatter plots in Figure 10.1) falling on the unit diagonal). If either of these checks fails, the attribution result is treated with caution, because it suggests there are processes or feedbacks affecting the observations that are not adequately represented by the model. However, ‘passing’ the test is not a safeguard against unrealistic variability assumptions, which is why estimates of internal variability are discussed in detail in this chapter and assessments of models characterization of internal variability are made in Chapter 9.

Finally, Ribes et al. (2010) propose a hybrid of the model-based optimal fingerprinting and time-series approaches, referred to as “temporal optimal detection”, under which the overall shape of the response to external forcing is estimated from a climate model, but instead of using model-simulated variability to down-weight components of the signal that are subject to high levels of noise, each signal is simply assumed to consist of a single spatial pattern modulated by a single, smoothly varying time-series. Climate variability in these time-series is then modelled with an AR(1) process, avoiding the problem of ill-conditioned estimates of the covariance matrix which they apply to regional temperature and precipitation data over France.

10.2.5 Single-Step, Multi-Step and Associative Attribution

Attribution studies have traditionally involved explicit simulation of the response to external forcing of an observable variable, such as surface temperature change, and comparison with corresponding observations of that variable. Attribution is claimed when the simulated response is consistent with the observations at some confidence level, not consistent with internal variability and not consistent with any plausible alternative response. This, so-called single-step attribution, has the advantage of simplicity, but restricts attention to variables for which long and consistent time-series of observations are available and which can be simulated explicitly in current models driven solely with external climate forcing.

To address attribution questions for variables for which these conditions are not satisfied, Hegerl et al. (2010) introduced the notation of multi-step attribution, formalising existing practice in a number of studies (Stott et al., 2004a). In a multi-step attribution study, the attributable change in a variable such as large-scale surface temperature is estimated with a single-step procedure, along with its associated uncertainty, and the implications of this change are then explored in a further (physically- or statistically-based) modelling step. Conclusions of a multi-step attribution study can only be as robust as the least certain link in the multi-step procedure. For an example of multi-step attribution, see Section 10.6.2. Furthermore, as the focus shifts towards more noisy regional changes, it can be difficult to separate the effect of different external forcings. In such cases, it can be useful to detect the response to all external forcings in the variable in question, and then determine the most important factors underlying the attribution results by reference to a closely related variable for which full attribution analyses considering the partitioning into separate forcings are available (see e.g., Morak et al. (2011).

Hegerl et al. (2010) also introduced a definition of associative attribution, under which a global attribution claim is made if a consistent pattern of change emerges across a range of variables (possibly from a wide range of sources). This approach has not been extensively used in physical climate science, and will not be further reviewed here.

10.2.6 Linking Detection and Attribution to Model Evaluation and Prediction: Bayesian and Frequentist Approaches

The majority of attribution studies take the most conservative possible approach to prior knowledge, in that no prior knowledge is assumed of the magnitude, or even the sign, of the response to an external climate driver. Tighter uncertainty estimates can be obtained if prior knowledge (for example, that volcanoes can only cause a net cooling) is incorporated into the constraints, normally using a Bayesian approach. The price of this reduced uncertainty is that results then depend on those prior assumptions in addition to the evidence provided by the observations. Bayesian approaches to detection and attribution are discussed in Hegerl et al. (2007b).

When attribution results are reported, they are typically derived from conventional hypothesis tests that minimise reliance on prior assumptions: hence when it is reported that the response to anthropogenic greenhouse gas increase is very likely greater than half the total observed warming, it means that the null-hypothesis that the greenhouse-gas-induced warming is less than half the total can be rejected with the data available at the 10% confidence level at least. It may well be the case that all available models, and the prior knowledge of practicing climate scientists, indicate a higher greenhouse-induced warming, but this information is deliberately set aside to provide a conservative attribution assessment. Expert judgment is still required in attribution, particularly in assessing whether internal variability and potential confounding factors have been adequately accounted for, but it plays a less central role. Hence it may be the case that prediction statements, which combine expert judgment explicitly with observations, appear more confident than attribution statements, even when they refer to the same variable on successive decades. This is not a contradiction, and simply reflects the relative weight given the expert judgment in the two cases.

10.3 Atmosphere and Surface

[PLACEHOLDER FOR FIRST ORDER DRAFT]

10.3.1 Temperature

[PLACEHOLDER FOR FIRST ORDER DRAFT]

10.3.1.1 Surface (Air Temperature and SST)

[PLACEHOLDER FOR FIRST ORDER DRAFT]

10.3.1.1.1 Observations of surface temperature change

Global mean temperatures warmed strongly over the period 1900–1940 (Figure 10.4, see Section 10.7.4), followed by a period with little significant trend, and strong warming since the mid-1970s (Section 2.2.3.2). Since the 1970s, global mean temperature in each successive decade has been warmer than the previous decade by an amount larger than that associated with observational uncertainty (Section 2.2.3.2). Early 20th century warming was dominated by warmth in the Northern Hemisphere extratropics, while warming since 1970 has been more global in extent, albeit with a maximum in the Arctic and a minimum in the Southern Ocean (Section 2.2.3.2). Correction of residual instrumental biases (Kennedy et al., 2011a, 2011b; Thompson et al., 2008) causes a warming of global mean SST by up to 0.2°C over the period 1945–1970. These bias corrections have the effect of reducing the best estimate of the warming trend over the latter half of the 20th century, but have little effect on the 1900–1999 trend, or on trends calculated over the period since 1970 (Kennedy et al., 2011a). This corrected SST data set has yet to be included in a global near surface air temperature dataset.

The global mean temperature in each of the five years since the period assessed in the AR4 (2006–2010) has been among the 12 warmest years on record, based on either the HadCRUT3 (Brohan et al., 2006), GISS (Hansen et al., 2010; Hansen et al., 2001) or NOAA/NCDC records (Vose, 2011). Nonetheless there has been some apparent reduction in the rate of warming over the past decade. Compared to HadCRUT3, this reduction in the rate of warming is less apparent in the GISS record, in which missing data over the Arctic are infilled (Hansen et al., 2010; Chapter 2; Hansen et al., 2001), since the Arctic has continued to warm strongly over the past decade (Hansen et al., 2010; Section 2.2.3.2).

10.3.1.1.2 Simulations of surface temperature change

Since the AR4, a new set of simulations from a greater number of AOGCMs have been performed as part of the Fifth Coupled Model Intercomparison project (CMIP5). The simulations of most relevance to this chapter are the prescribed CO_2 historical simulations including a comprehensive range of anthropogenic and natural forcings, the simulations with natural forcings only, simulations with other individual forcings, and the control simulations. These new simulations have several advantages over the CMIP3 simulations assessed in the AR4 (Hegerl et al., 2007b). Firstly, the models used are in general more advanced, with moderate increases in resolution and improved parameterisations (Chapter 9). Secondly the set of forcings included in the historical simulations is in general more complete, with many models including an interactive sulphur cycle, and thus able to simulate the indirect aerosol effect, an important forcing missing from many of the CMIP3 simulations. In addition most models include tropospheric and stratospheric ozone changes, as well as solar and volcanic forcing, and some models include black carbon aerosols. Some models also include realistic changes in land use. While the main historical simulations end in 2005, these may be extended with RCP scenario simulations, which include greenhouse gas and aerosol forcing changes that are very close to those which have actually occurred since 2005. Moreover many of these RCP simulations generally also include realistic solar cycle changes. This, and the fact that forcing uncertainty has only a small contribution to uncertainty in near future changes (Hawkins and Sutton, 2009) allows simulations to be compared with observations up to the end of 2010, potentially improving the ability of detection and attribution analyses to constrain the regression coefficients that relate observed climate change to simulated climate change. Most importantly for attribution, most models have been used to simulate the response to natural forcings only. These simulations are needed in order to separate anthropogenic and natural forcing effects in any attribution analysis. Many modelling centres will also submit simulations with historical greenhouse gas changes alone, or with other individual forcings, allowing the effects of these forcings to be separated in attribution analyses.

Figure 10.3 (upper panel) shows that when the effects of anthropogenic and natural forcings are included the spread of model simulations in this ensemble [update this statement when CMIP5 simulations incorporated] broadly spans the observational estimates of global mean temperature whereas this is not the case for simulations in which only natural forcings are included (Figure 10.3, lower panel). Better agreement between models and observations when the models include anthropogenic forcings is also seen in the CMIP3 simulations, although some individual models including anthropogenic forcings overestimate the warming trend, while others underestimate it (Fyfe et al., 2010). The CMIP5 simulations from HadGEM2-ES and CanESM2 appear to be cooler on average than the CMIP3 simulations over the period 1950–1990, which may be related to the inclusion of indirect aerosols in both CMIP5 models, but only some CMIP3 models. Over the decade 2000–2010 some separation can be seen between the CanESM2 simulations which are generally warmer than the observations and at the upper end of the CMIP3 range, and the HadGEM2-ES simulations, which are at the lower end or below the CMIP3 range.

[INSERT FIGURE 10.3 HERE]

Figure 10.3: [PLACEHOLDER FOR FIRST ORDER DRAFT, to be updated with more CMIP5 model data and new observational datasets when available] Three observational estimates of global mean temperature (dark grey lines) from HadCRUT3, NASA GISS, and NOAA NCDC, compared to model CMIP3 simulations (light grey) and CMIP5 simulations from HadGEM2-ES and CanESM2 (red) with natural forcings only (lower panel) and anthropogenic and natural forcings (upper panel). All data were masked using the HadCRUT3 coverage, and global average anomalies are shown with respect to 1881–1920, where all data are first calculated as anomalies relative to 1961–1990 in each grid box.

Knutti (2008) and others argue that the agreement between observed 20th century global mean temperature and temperature changes simulated in response to anthropogenic and natural forcings, should not in itself be taken as an attribution of global mean temperature change to human influence. Kiehl et al. (2007), Knutti (2008) and Huybers (2010) identify correlations between forcings and feedbacks across ensembles of earlier generation climate models which they argue are suggestive that parameter values in the models have been chosen in order to reproduce 20th century climate change. For example Kiehl et al. (2007) finds that models with a larger sulphate aerosol forcing tend to have a higher climate sensitivity, such that the spread of their simulated 20th century temperature changes is reduced. Stainforth et al. (2005) find that the spread of climate sensitivity in the CMIP3 models is smaller than the spread derived by perturbing parameters across plausible ranges in a single model, even after applying simple constraints based on the models' mean climate. Schwartz et al. (2007) demonstrate that the range of simulated warming in the CMIP3 models is smaller than would be implied by the uncertainty in radiative forcing.

The top left panel of Figure 10.4 shows the pattern of temperature trends observed over the period 1901–2010, based on the HadCRUT3v, NASA GISS and NCDC datasets. Warming has been observed almost everywhere, with the exception of only a few regions. Rates of warming are generally higher over land areas and in high latitudes, compared to oceans and lower latitude regions. The middle left panel of Figure 10.4 demonstrates that a similar pattern of warming is simulated in the combined CMIP3 and CMIP5 simulations with natural and anthropogenic forcing over this period. Over most regions, simulated and observed trends are consistent: Exceptions are parts of central Asia, and the Southern Hemisphere mid-latitudes, where the simulations warm less than the observations, and parts of the tropical Pacific, where the simulations warm more than the observations. Trends simulated in response to natural forcings only (lower panel) are generally close to zero, and inconsistent with observed trends.

Over the period 1979–2010 (right column, Figure 10.4) the observed trend pattern is similar to that over the 1901–2010 period, except that much of the eastern Pacific cooled over this period, and Southern Hemisphere mid-latitude trends exhibited less warming. These differences are not reflected in the simulated trends over this period in response to anthropogenic and natural forcing (right middle panel, Figure 10.4). This reduced warming in observations over the Southern mid-latitudes over the 1979–2010 period can also be seen in Figure 10.5 (lower panel), which also shows that the models appear to warm too much in this region over this period. However, examining Figure 10.5, upper panel, we see that there is no discrepancy in zonal mean temperature trends over the longer 1901–2010 period in this region, suggesting that the discrepancy over the 1979–2010 period may either be a manifestation of internal variability or relate to regionally-important forcings which are not included in the simulations, such as sea salt aerosol (Korhonen et al., 2010; Santer and Coauthors, 2011a).

[INSERT FIGURE 10.4 HERE]
Figure 10.4: [PLACEHOLDER FOR FIRST ORDER DRAFT, to be updated with more CMIP5 model data and new observational datasets when available] Trends in observed and simulated changes (oC per decade) over the 1901–2010 period (left hand column) and the 1979–2010 periods (right hand column). Top row: Trends in observed temperature changes averaged over the HadCRUT3, NASA GISS, and NCDC datasets. Second row: Trends averaged over the CMIP3 and available CMIP5 datasets when they include anthropogenic and natural forcings. Third row: Trends averaged over the model datasets when they include natural forcings only. Data shown only where observational data are available in the HadCRUT3 dataset. Boxes in 2nd and 3rd rows show where 5 to 95 percentile of model range lies above or below observational value at that grid box.

[INSERT FIGURE 10.5 HERE]
Figure 10.5: [PLACEHOLDER FOR FIRST ORDER DRAFT, to be updated with more CMIP5 model data and new observational datasets when available] Zonal mean temperature trends over 1901–2010 period (top) and 1979–2010 period (bottom). Black lines show HadCRUT3, NASA GIS and NCDC observational datasets, orange lines models with anthropogenic and natural forcings, blue lines models with natural forcings only. All data masked to HadRUT3 mask.

Since in standard detection and attribution analyses the amplitude of the responses to various forcings is estimated by regression, the possible tuning of models to reproduce 20th century global mean temperature changes will have almost no effect on the detectability of the various forcings. Similarly this will have almost no effect on estimates of future warming constrained using a regression of observed climate change onto simulated historical changes. The spatial and temporal patterns of temperature changes simulated in response to the various forcings would be hard to tune in a model development setting, and it is these which form the basis of most detection and attribution analyses. Nonetheless, these results do suggest some caution in interpreting simulated and observed forced responses of consistent magnitude as positive evidence of model fidelity, since there is some evidence that this might arise partly from conditioning the model ensemble using historical observations of climate change (Huybers, 2010; Knutti, 2008).

[START BOX 10.1 HERE]

Box 10.1: Understanding the Increased Spread of 20th Century Simulations

[To be updated once CMIP5 ensemble is available] As shown in Figure 10.3 the spread of global mean temperatures as simulated by the climate models now available is greater than at the time of the AR4. Why is this and what are the implications for attribution of warming to human influence and for our confidence in estimates of future warming?

The newer generation of models included in the CMIP5 ensemble are in general more advanced than those in the CMIP3 ensemble (see Chapter 9). They include a greater variety of forcings and a more complete description of interactions between different components of the climate system. Many more models now include an interactive sulphur cycle and simulate the indirect aerosol effects on clouds, by which clouds can become brighter and longer lasting. Some models now also include other aerosol species such as carbonaceous aerosols, and some include interactive land surface schemes in which vegetation responds to changes in carbon dioxide and climate. As a result models have even more degrees of freedom than previously. For example, climate models are provided with observationally based estimates of sulphur emissions from which they then internally calculate the oxidation of sulphur dioxide to sulphate aerosols, its transport through the atmosphere, its interaction with clouds, and its deposition in precipitation.

There is evidence that the uncertainty range of 20th century global temperature change simulated by the CMIP3 ensemble, whether by design (through some element of model tuning) or by chance, is smaller than that implied by the uncertainty in radiative forcing (Schwartz et al., 2007). However, in standard detection and attribution analyses, the amplitude of the responses to various forcings is estimated by regression, and therefore this does not have a first order effect on estimates of global warming attributable to greenhouse gases and other forcings. Such analyses, which considers space time patterns of change, are able to discriminate between models, as is illustrated in Box 10.1, Figure 1 in which, whereas all three models look rather similar in terms of their global mean temperature (solid lines in Box 10.1, Figure 1a), they differ markedly in their ability to represent the observed evolution of hemispheric temperature contrast, land ocean temperature contrast, and meridional temperature gradient [update with CMIP5 simulations]. Observational constraints therefore go beyond global mean temperature and provide a means to test a model's ability to represent the response to greenhouse gas forcing, and therefore the fidelity of its transient climate response. Detection and attribution analyses carried out on the CMIP5 ensemble, [update when more simulations available] which has a wider spread of global mean temperatures, produce broadly consistent estimates of attributable greenhouse warming, as shown in Figure 10.6c right hand panel [update with more CMIP5 simulations].

As a consequence a wider range of simulations of past global temperature does not necessarily imply that observationally constrained estimates of future warming, according to a particular emissions scenario, should be wider and more uncertain. In fact as more observational data are obtained, and the climate change signal strengthens, observationally constrained uncertainties of future global warming would be expected to narrow over time, regardless of any increase of spread of the raw model ensemble (Stott and Kettleborough, 2002) although the expression of internal variability in the observed evolution means that the overall increase in signal to noise may not be smoothly linear.

[INSERT FIGURE BOX 10.1, FIGURE 1 HERE]

Box 10.1, Figure 1: [PLACEHOLDER FOR FIRST ORDER DRAFT, to be updated with CMIP5 models] Components of large scale temperature response a) global mean, b) northern hemisphere average minus southern hemisphere average, c) land average minus ocean average, d) meridional temperature gradient) for three models (HadCM3, GFDL, PCM, solid lines) and after scaling by optimal detection using observational constraints (dashed lines). Adapted from (Stott et al., 2006).

[END BOX 10.1 HERE]

[Briefly discuss temperature variability comparisons between CMIP5 models and observations that have been assessed in Chapter 9, and implications for attribution.]

10.3.1.1.3 Attribution of observed global scale temperature changes

The AR4 concluded that most of the observed increase in global average temperatures since the mid-20th century was *very likely* due to the observed increase in anthropogenic greenhouse gas concentrations. As discussed in Section 10.2, the robustness of this conclusion was not affected by any fortuitous cancellation of errors between climate sensitivity and the magnitude of aerosol forcing present in the CMIP3 ensemble. Additional studies made since AR4 (Christidis et al., 2010; Jones et al., 2010) applied to a new generation of models that samples a wider range of forcing, modelling and observational uncertainty support previous studies that concluded that greenhouse gases are the largest contributor to global mean temperature increases since the mid 20th century. [Update when more studies available] The implications of a wider spread of simulations in CMIP5 than CMIP3 when the models include both natural and anthropogenic forcings (Figure 10.4) are discussed further in Box 10.1.

With more sophisticated models that include a greater number of forcings and improved representation of processes, including the indirect effects of anthropogenic aerosols, comes the opportunity to investigate if fingerprints of forcings hitherto not detected can be identified in the observed record. The influence of black carbon aerosols (from fossil and bio fuel sources) has been detected in the recent temperature record, though the warming attributable to black carbon is small compared to that attributable to greenhouse gas increases (Jones et al., 2010). This warming is simulated mainly over the Northern Hemisphere with a sufficiently distinct spatio-temporal pattern that it can be separated from the response to other forcings in the regression. The estimated warming attributable to black carbon aerosols is consistent with the simulated response of 0.14 ± 0.1 K/century over the 1900–2007 period.

Figure 10.6 shows an update of Figure 9.9 in Hegerl et al.(2007b). Scaling factors derived from four CMIP3 models over the period 1900–2000 are compared to those derived using HadGEM2-ES over the period 1900–2009. The 1900–2009 HadGEM2-ES analysis indicates a consistent but somewhat smaller GHG regression coefficient than that derived from the CMIP3 models over the period 1900–1999, and a regression coefficient on the non greenhouse gas anthropogenic component smaller than one, suggesting that HadGEM2-ES overestimates the temperature response to these forcings (the response to ozone and land-use change are also included with the aerosol response in this analysis). Figure 10.6b compares the attributable warming trends over the 1900–1999 period based on the CMIP3 models with the attributable warming trend over the same period based on HadGEM2-ES. Results are broadly consistent with the CMIP3 results. Figure 10.6c compares the CMIP3 attributable warming over 1950–1999 with the attributable warming over 1960–2009 calculated using HadGEM2-ES. Whereas the greenhouse-gas-attributable warming over the 1950–1999 period was significantly larger than the observed warming based on all four models, over the 1960–2009 period, the greenhouse-gas-attributable warming is found to be consistent with estimates from the CMIP3 models for the 1950–1999 period and is not significantly larger than the observed trend for the later period (dashed line), a trend that has increased relative to the earlier period (solid line).

Figure 10.6d shows the results of an optimal detection analysis using HadCM3 over the period 1900–1999 with five different observational datasets. Regression coefficients are broadly consistent, and conclusions regarding the detectability of the greenhouse gas and aerosol response are not sensitive to the choice of dataset. However, best guess regression coefficients vary from dataset to dataset by an amount comparable to the uncertainties associated with internal climate variability. This suggests that observational uncertainty, to the extent that this is reflected in differences between these five datasets, may be comparably important to internal climate variability as a source of uncertainty in greenhouse-gas attributable warming or aerosol-attributable cooling.

[INSERT FIGURE 10.6 HERE]

Figure 10.6: [PLACEHOLDER FOR FIRST ORDER DRAFT**,** to be updated with CMIP5 model analyses for updated period to include 21st century data] Estimated contributions from greenhouse gas (red), other anthropogenic (green) and natural (blue) components to observed global surface temperature changes. **a)** 5 to 95% uncertainty limits on scaling factors based on an analysis over the 1900–1999 period (leftmost 4 sets of bars) and 1900–2009 period (rightmost set of bars). **b)** The corresponding estimated contributions of forced changes to temperature changes over the 20th century expressed as the difference between 1990 to 1999 mean temperature and 1900 to 1909 mean temperature. **c)** Estimated contribution to temperature trend over 1950–1999 (leftmost 4 sets of bars) and over 1960–2009 (rightmost set of bars). The solid horizontal black lines in b) and c) show the corresponding observed temperature changes from HadCRUT2v (Parker et al., 2004) and the dashed line in c) show the observed temperature trend over 1960–2009 HadCRUT3v (Brohan et al., 2006). Five different analyses are shown using different models (MIROC3.2, PCM, HadCM3, GFDL-R30, HadGEM2-ES) which are explained in more detail in the text. From (Stott et al., 2010) adapted from (Hegerl et al., 2007). **d)** to **f)** Parallel plots to a) to c) but entirely for 1900–1999 period, for HadCM3 model and for five different observational datasets; (HadCRUT2v, HadCRUT3v, NASA GISS, NCDC, JMA). From (Jones et al., 2011, in prep). (Jones, G. S., The sensitivity of the choice of observational dataset on the detection of anthropogenic changes to near surface temperatures).

Fyfe et al. (2010) compare simulated and observed trends in global mean temperature over the period 1950–1999 before and after removing volcanic, ENSO, and COWL (Cold Ocean/Warm Land pattern, a statistical construct whose removal reduces short term fluctuations in global temperature due to atmospheric circulation variability) signals using a regression method following Thompson et al. (2008). Removing these natural variability components reduced the estimated uncertainty in the trends. While the observed trends were very clearly inconsistent with zero, Fyfe et al. (2010) find that only eight of the 24 CMIP3 models' historical simulations exhibit trends consistent with that observed, with nine models overestimating the trend, and seven underestimating it. However, uncertainties are estimated in this study using a first-order autoregressive model based on monthly means, which may underestimate internal variability on decadal timescales. Stott et al. (2006b) apply an attribution analysis to greenhouse gas, aerosol and natural forcing responses using three models. They find consistency in the magnitudes of simulated and observed greenhouse gas and aerosol responses in HadCM3 and GFDL, but the magnitudes of the responses to both of these forcings are significantly underestimated in PCM. While a greenhouse gas response can be detected using global mean information only with all three models, they find that regional information helps to constrain the magnitudes of these responses.

The clustering of very warm years in the last decade is very unlikely to have occurred by chance (Zorita et al., 2008). Smirnov and Mokhov (2009), adopting an approach that allows them to distinguish between conventional Granger causality and a "long-term causality" that focuses on low-frequency changes (see Section 10.2) find that increasing CO_2 concentrations are the principle determining factor in the rise of global mean surface temperature over recent decades. However global mean temperatures have not increased strongly over the past decade, a time when the multi-model mean temperature continued to increase in response to steadily increasing greenhouse gas concentrations and constant or declining aerosol forcing. A key question, therefore, is whether the recent apparent slowdown in the rate of observed global warming is consistent with internal variability superposed on an anthropogenic warming trend (for example, as represented by the spread of model trends over the same time), whether it has been driven by changes in radiative forcing.

Easterling and Wehner (2009) compare the distribution of observed decadal trends with simulated distributions from CMIP3 historical simulations, and conclude that the observed decadal trends are consistent with the range of decadal trends simulated over the 20th century. Liebmann et al. (2010) conclude that observed HadCRUT3 global mean temperature trends of 2 years and longer ending in 2009 are not unusual in the context of the record since 1850. Knight et al. (2009) conclude that observed global mean temperature changes over a range of periods to 2008 are within the 90% range of simulated temperature changes in HadCM3. Consistent with Hansen et al. (2010), they find smaller warming in HadCRUT3 than in the GISS and NCDC records over periods of 4–14 years ending in 2008 (see also Section 2.2.3.2). Over the period 1999–2008, ENSO contributed a warming influence, so the lack of warming seen in the global mean temperature over this period cannot be attributed to ENSO (Fyfe and Merryfield, 2011; Knight et al., 2009). For decadal temperature trends in the lower troposphere calculated over overlapping 10-year periods from the past 32 years, Santer et al. (2011b) demonstrate that the differences between simulated and observed trends are not significant. In summary, while the trend in global mean temperature over the past decade is not significantly different from zero, it is also not inconsistent with internal variability superposed on an anthropogenic warming trend.

Several studies have discussed possible contributions to the less rapid warming over the past decade. Solomon et al. (2010) show, based on satellite measurements, that stratospheric water vapour declined abruptly by about 10% after 2000 for unknown reasons. Based on radiative forcing calculations and a simple climate model they estimate that this change in stratospheric water vapour reduced the 2000–2009 temperature trend by 0.04 K/decade, though the net effect of this and the other forcings was still a strongly positive trend.

Lean and Rind (2009) argue that the evolution of global mean temperature since 2000 can be well-simulated by a lagged regression model based on ENSO, volcanic aerosol, anthropogenic forcing and solar irradiance forcing components, with solar forcing contributing about 0.1°C cooling between the solar maximum in 2001–2002 and the 2009 minimum, which was unusually deep and extended. This is consistent with Hegerl et al. (2007b), who suggest that the peak-to-trough amplitude of the response to the solar cycle is estimated to be 0.1°C.

Lockwood et al. (2008) also demonstrate that a multiple regression approach based on volcanic aerosol, solar variations, ENSO and anthropogenic forcing reproduces the evolution of global mean temperature well over the period 1953–2006, including during the period after 2000. Each forcing factor is passed through a low-pass filter characterised by a time-constant which represents the delayed response of the climate system arising from of thermal inertia, providing a set of responses shown in Panels a) to d) in Figure 10.7. These are related to observed global mean surface temperature anomalies (the blue line in the top panel of Figure 10.7) using a multiple linear regression with an first-order autoregressive, or AR(1), noise model. This approach draws attention to the role of ENSO and the recent solar minimum in explaining temperature changes over the past decade. The fit between observed and predicted temperatures indicates that these four factors between them can explain a substantial fraction of recent interannual temperature fluctuations throughout this period. Moreover, there is no indication that the fit is any different in the most recent decade. The fact that 1998 remains the warmest year on record is explained by a combination of low solar activity in recent years and the exceptional El Nino event that occurred in that year, providing no indication of any reduction in long-term warming trend between the 1990s and 2000s.

More generally, Scafetta and West (2007) argue that climate models may underestimate the temperature response to solar forcing, and that up to 50% of the warming since 1900 may be solar-induced. This result is contested by Benestad and Schmidt (2009) who find that only 7% of the warming since 1900 is attributable to solar forcing, and argue that the approach adopted by Scafetta and West (2007) is not robust, since it disregards forcings other than solar in the preindustrial period, and assumes a high and precisely-known value for climate sensitivity. Lean and Rind (2008) conclude that solar forcing explains only 10% of the warming over the past 100 years, while contributing a small cooling contribution over the past 25 years, based on another approach.

Ingram (2006) cautions against the use of regression on climate forcings in attribution studies, and argues that climate models are needed to realistically translate forcings into the climate response.

[INSERT FIGURE 10.7 HERE]

Figure 10.7: Top: the variations of the observed global mean air surface temperature anomaly (blue line) and the best multivariate fit (red line). Below: the contributions to the fit from a) ENSO, b) volcanoes, c) solar contribution, d) a linear drift. From Lockwood (2008).

Another possible cause of the reduced warming since 2000 is increased aerosol concentrations. Hofmann et al. (2009) report an increase of background stratospheric aerosol concentration since 2000 by 4–7%, which they attribute mainly to an increase in coal burning in China. Based on the cooling observed following the

Pinatubo eruption, they estimate that this may have cooled the troposphere by about 0.03°C, a small effect. Korhonen et al. (2010) suggest that an increase in sea salt aerosol over the high latitude Southern Ocean, driven by an increase and poleward shift in the mid-latitude jet, may have led through its indirect effect to a summertime negative radiative forcing between 50°S and 65°S comparable to the positive radiative forcing due to CO_2 increases. This effect, not included in most models, could contribute to discrepancies between simulated and observed trends over the past 30–40 years (Figure 10.5).

The scaling factors on the responses to greenhouse gas and aerosol forcing derived using global detection and attribution analyses may be used to scale projected future change (Section 10.9). Analyses carried out using an additional decade of observational data beyond that considered by the studies assessed by Hegerl et al. (2007b) may allow greenhouse gas and aerosol scaling factors to be more tightly constrained (Figure 10.6), helping to constrain projections (Padilla et al., 2011).

10.3.1.1.4 Attribution of regional surface temperature change

[Review observed regional temperature changes based on Chapter 2 and Figure 10.8]

Anthropogenic influence on climate has been robustly detected on the global scale, but for many applications it is useful to know whether anthropogenic influence may also be detected using data from a single region only. Based on several studies, Hegerl et al. (2007b) conclude that anthropogenic influence is detectable in every continent except Antarctica. Since then Gillett et al. (2008b) have applied an attribution analysis to Antarctic land temperatures over the period 1950–1999 and have been able to separately detect natural and anthropogenic influence, which was found to be of consistent magnitude in simulations and observations. Averaging over all observed locations, Antarctica as a whole has warmed over the observed period (Gillett et al., 2008b), even though some individual locations have cooled, particularly in summer and autumn, and over the shorter 1960–1999 period (Thompson and Solomon, 2002; Turner et al., 2005). Thus anthropogenic influence on climate has now been detected on all seven continents, although the evidence for human influence on warming over Antarctica is weaker than for the other six continental regions, being based on only one study for a region with greater observational uncertainty than the other regions, with very few data before 1950, and sparse coverage that is mainly limited to the coast and the Antarctic peninsula. Also due to the short observational record in this region it is difficult to check the models' ability to represent decadal-scale internal variability over this region.

Since the publication of the AR4 several other studies have detected anthropogenic influence on continental or sub-continental regions.[Discuss CMIP5 models and observations on Giorgi sub-continental scale regions]

[INSERT FIGURE 10.8 HERE]

Figure 10.8: [PLACEHOLDER FOR FIRST ORDER DRAFT, to include CMIP5 simulations] Plot of temperature and precipitation on sub-continental regions illustrating greater signal to noise and separation of anthropogenically and naturally forced CMIP climate model simulations.

Min and Hense (2007) apply a Bayesian decision analysis to continental-scale temperatures using the CMIP3 multi-model ensemble and conclude that either anthropogenic forcings or combined anthropogenic and natural forcings provide the best explanation of observed changes in temperature, consistent with earlier studies reviewed in the AR4.

Jones et al. (2008) detect anthropogenic influence on summer temperatures, in a multi variable optimal detection analysis on the temperature responses to anthropogenic and natural forcings, over all Northern Hemisphere continents and in many subcontinental Northern Hemisphere land regions. Christidis et al. (2010) use a multi-model ensemble constrained by global-scale observed temperature changes to estimate the changes in probability of occurrence of warming or cooling trends over the 1950–1997 period over various sub-continental scale regions. They conclude that the probability of occurrence of warming trends has been at least doubled by anthropogenic forcing over all such regions except Central North America.

Several recent studies have applied attribution analyses to specific sub-continental regions. Bonfils et al. (2008) apply an attribution analysis to winter minimum temperature over the Western USA. They find a detectable anthropogenic response which is robust to changes in the details of their analysis. Pierce et al. (2009) reach similar conclusions based on a larger multi-model ensemble. They also conclude that weighting models according to various aspects of their climatology does not significantly change the detection results, and that a simple multi-model average gives the most robust results. Dean and Stott (2009) demonstrate that while anthropogenic influence on raw temperature trends over New Zealand is not detectable, after circulation-related variability is removed as in Gillett et al. (2000), an anthropogenic signal is detectable, and residual trends are not consistent with a response to natural forcings alone. Human-caused changes in greenhouse gases are found to be the main driver of the 20th-century SST increases in both Atlantic and Pacific tropical cyclogenesis regions (Gillett et al., 2008a; Santer, 2006). Over both regions, the responses to anthropogenic forcings are detected when the responses to natural forcings are also included in the analysis (Gillett et al., 2008a). Ribes et al. (2010) detect a change in temperature over France, using a first order autoregressive model of internal variability. However, the noise model used by the authors may underestimate internal variability on decadal timescales. These authors derive very low estimates of uncertainty based on this approach compared to uncertainty estimated using internal variability from climate models for climate change on similar scales.

Gillett et al. (2008b) detect anthropogenic influence on near-surface Arctic temperatures over land, with a consistent magnitude in simulations and observations. After deriving mid-latitude and tropical changes in aerosol forcing from surface temperature changes using an inverse approach, Shindell and Faluvegi (2009) infer a large contribution to both mid-century Arctic cooling and late century warming from aerosol forcing changes. Lean and Rind (2008) argue, based on a lagged regression of observed temperatures onto forcings, that climate models overestimate high-latitude amplification of the response to anthropogenic forcing. Stott and Jones (2009) find that internal variability makes the estimate of high latitude amplification based on the observed period very uncertain, and therefore that observations and climate models are not significantly different in this respect.

Karoly and Stott (2006) apply an attribution analysis to Central England temperature, a record which extends back to 1700, and which corresponds to a single grid box in the model they use, HadCM3. After demonstrating that the model simulates realistic temperature variability compared to the observed record, they compare observed trends with those simulated in response to natural forcings alone, anthropogenic forcings and internal variability. They find that the observed trend is inconsistent with either internal variability or the simulated response to natural forcings, but is consistent with the simulated response when anthropogenic forcings are included. To date, formal attribution studies of this type have not been applied at other individual locations, which do not have such long instrumental series as for CET and therefore for which it is more difficult to assess the ability of the models to represent observed variability in the pre-industrial era. When applying an attribution analysis at a particular location, care needs to be taken firstly to ensure that all plausible local climate forcings are considered as possible explanations of the observed warming, and also that the model or models used simulate realistic variability and response to forcings at the grid box scale at the location concerned (Stott et al., 2010).

Wu and Karoly (2007) calculate the statistical significance of temperature trends in individual grid cells over the 1951–2000 period, using control simulations from climate models. They find that 60% of grid cells exhibit significant warming trends, a much larger number than expected by chance, consistent with an earlier analysis (Karoly and Wu, 2005). Similar results apply when circulation-related variability is first regressed out. Nonetheless, as discussed in the AR4, when a global field significance test is applied, this becomes a global attribution study: Since not all grid cells exhibit significant warming trends the overall interpretation of the results in terms of attribution at individual locations remains problematic.

10.3.1.2 Atmosphere

This section presents an assessment of the causes of global and regional temperature changes in the free atmosphere, and advances in the understanding of discrepancies between observed and simulated differential warming in the free troposphere and at the surface. Hegerl et al. (2007b) concluded that 'the observed pattern of tropospheric warming and stratospheric cooling is very likely due to the influence of anthropogenic forcing, particularly greenhouse gases and stratospheric ozone depletion.' An apparent inconsistency between differential warming of the troposphere and surface in models with some observational records was assessed to be more likely related to observational errors than to model errors.

10.3.1.2.1 Observations

Newer radiosonde datasets and radiosonde data sets considered in the IPCC Forth Assessment Report show consistently that over the period from 1958 to present, tropospheric temperatures increased while stratospheric temperatures decreased (Figure 10.9).

[INSERT FIGURE 10.9 HERE]

Figure 10.9: [PLACEHOLDER FOR FIRST ORDER DRAFT, to be updated with CMIP5 models] Latitude-height sections of simulated and observed zonal mean temperatures trends from December 1957 to November 2009 for all data except for IUK which is only available to 2006. Shown are the ensemble mean of all forcing and natural forcing simulations for HadGEM1 (top row), and four radiosonde data sets. One data point at a given latitude is considered sufficient to generate zonal means in this figure. From Lott et al., 2011 (in preparation).

Since the publication of the AR4, more attention has been paid to homogenization of radiosonde temperature records of tropospheric temperature, and to derivation of uncertainty estimates. Over the period 1979–2005 these newer datasets generally exhibit more tropospheric warming that those considered in the AR4 (Thorne et al., 2010), and since the 1960s, each successive decade has exhibited warmer tropospheric temperatures than the previous one (Section 2.2.5.7). Further attention has also been paid to the homogenization of satellite-borne MSU tropospheric temperature records, and one group has derived a new record (STAR; Zou et al., 2006) showing more warming than those reviewed in the AR4 (Thorne et al., 2010). Since 2000, lower tropospheric temperatures have exhibited little trend (Santer et al., 2011b).

Stratospheric radiosonde and MSU temperature records have also benefited from increased scrutiny in recent years (Seidel et al., 2011), resulting in a convergence of estimates of lower stratospheric cooling to 0.3–0.6°C/decade over the 1979–2009 period, with closer agreement between satellite-derived and radiosonde estimates (Seidel et al., 2011), though radiosonde records still indicate more cooling than MSU (Section 2.2.5.7). Trends in the middle and upper stratosphere amount to -0.5°C to -1.5°C per decade during 1979 to 2005 with the greatest cooling in the upper stratosphere near 40–50km. However, these trend estimates rely primarily on a single data set derived from operational SSU satellite data. The rate of cooling of the mid-stratosphere with values of 0.5^{o}C per decade since 1979 is considerably higher than indicated in earlier assessments as a result of the inclusion of a correction for the effect of changes in atmospheric CO_2 on the satellite weighting function. The SSU data have also recently received attention from additional groups, and their work has highlighted uncertainties in the resulting trends (Seidel et al., 2011). Temperature anomalies throughout the stratosphere were relatively constant since 1995 (Randel et al., 2009).

10.3.1.2.2 Tropospheric temperature change

Climate models forced with increasing greenhouse gas concentration simulate a vertical structure of temperature trends in the troposphere, characterized by a general warming from the surface to the troposphere together with an enhanced warming in the tropical upper troposphere (Figure 10.9). The AR4, which assesses the main findings of Karl et al.(2006), states that on a global scale, near surface temperature and lower and mid-tropospheric temperature have warming rates similar to near surface temperature and that this small lapse rate change is consistent with model simulations. It was pointed out, however, that in the tropics differential warming rates between the surface and free troposphere in models are inconsistent with some observational records.

Since the AR4 a number of studies have investigated the consistency of simulated and observed trends in the tropical free tropospheric temperature, and differential warming between the surface and free troposphere in the tropics. Most of these studies have used the CMIP3 simulations which ended in 1999. Research has focused on assessing biases and uncertainties in large-scale radiosonde and satellite temperature trends (Allen and Sherwood, 2008; Thorne et al., 2007; Titchner et al., 2009), assessing differences between simulations and observations (Douglass et al., 2008; Santer et al., 2008; Thorne et al., 2007), recalculating trends based on updated observational datasets (Allen and Sherwood, 2008; Christy et al., 2010; Santer et al., 2008; Thorne et al., 2011), and assessing the impact of natural variability (Bengtsson and Hodges, 2009) and impact of specific statistical methodologies for trend estimates and their uncertainties. Klotzbach et al. (2009) suggest that there are differences between observed surface and satellite data trends over land, which they attribute to enhanced warming near the surface in the stable nighttime boundary layer. The claim by Douglass et al. (2008) that modeled and observed trends in the tropical troposphere for the period from 1979 to 1999 are significantly different is contradicted by Santer et al. (2008) and McKitrick et al. (2010). The findings of Santer et al. (2008) are based on analyzing updated radiosonde and satellite datasets, considering observed and simulated trend uncertainties due to natural variability. Santer et al. (2008) also provide evidence based on synthetic data that the consistency test applied by Douglass et al. (2008) leads to incorrect conclusions. Christy et al. (2010) find differences between differential warming rates in observations and the ensemble average CMIP3 differential warming rates over the period 1979–1999. However, Thorne et al. (2007) and Santer et al. (2008) conclude that after fully accounting for observational uncertainty, there is no significant discrepancy between the observed differential warming rates and the full spread of the CMIP3 ensemble. Taking these studies together, we conclude, that apparent differences between tropical free tropospheric temperature trends in models and observations and differential warming in the tropics over the period 1979–1999 are unlikely to be statistically significant after fully accounting for observational uncertainties.

However, two recent studies have compared observed free tropospheric temperature trends with simulated trends over the period 1979–2009, by merging historical CMIP3 simulations to 1999 with scenario simulations to 2009, allowing a more exacting test of model-observation consistency (McKitrick et al., 2010; Santer et al., 2011a). For the period from 1979 to 2009 they show that both on global scale, and over much of the tropics and Southern Hemisphere mid-latitudes, the CMIP3 models produce a larger warming trend than observations (see Figure 10.10). This difference is statistically significant at the 5% level averaged over the Southern Hemisphere for both the mid-troposphere and lower-troposphere, and on the global scale for the mid-troposphere, based on two separate MSU datasets datasets (Figure 10.10). According to Santer et al. (2011a) potential causes for the model-observation discrepancies in recent 30-year trends are the neglect of negative forcings in many of the CMIP3 simulations of forced climate change, forcing discontinuities at the splice points between 20th and 21st century climate change simulations, model response errors, and an unusual manifestation of natural internal variability in the observations. For the period from 1958–2003, on the other hand, Thorne et al. (2011) shows consistent model-data agreement of tropospheric lapse rate from the surface to the tropopause indicating that the disagreement in the more recent period is not necessarily evidence of a general problem in simulating long-term global warming trends.

Other studies since the AR4 have examined the zonal mean temperature response to a broader range of forcings. Hansen et al. (2007) analyze a series of individual forcing runs for the period from 1880–2003 using the GISS climate model. Distinct zonal mean temperature response patterns were derived both for the whole period as well as individual periods 1880–1940, 1940–1979, 1979–2003 and also 1950–2003. They note that substantial temperature changes in the troposphere are often accompanied by temperature changes of opposite sign in the stratosphere. The main results of Hansen et al. (2007) are consistent with the study by Yoshimori and Broccoli (2008) who carry out individual forcing experiments using the GFDL AM2.1 model coupled to a mixed layer ocean model. Their analysis of the zonal mean temperature identifies a hemispherically asymmetric temperature response in the troposphere due to black carbon, organic carbon and tropospheric aerosol affecting mostly the extratropical Northern Hemisphere.

[Assess attribution studies using zonal mean temperature changes in the CMIP5 models. Discuss final Figure 10.10].

[INSERT FIGURE 10.10 HERE]

Figure 10.10: [PLACEHOLDER FOR FIRST ORDER DRAFT, to be updated with CMIP5 models] Comparison of the latitude/altitude structure of 30-year temperature trends in observations and in CMIP3 models. Results are for the lower stratosphere (TLS; A), the mid- to upper troposphere (TMT; B), the lower troposphere (TLT; C), and SST (D). Modeled and observed trends were calculated over the common period 1979–2009. The analysis period contains only two samples of overlapping 30-year trends (for the periods 1979–2008 and 1980–2009). Each observed trend (bo) is the average of these two trend samples. Since 50 individual realizations of the 1979–2009 period are available from the spliced 20CEN/SRES A1B runs, each multi-model average trend, << bm >>, is based on 50 × 2 samples of overlapping 30-year trends. The 5–95 percentiles of these sampling distributions are shaded. Results in the left column are for individual latitude bands (82.5°N-70°N, 70°N-50°N, 50°N-30°N, 30°N- 10°N, 10°N-0°N, etc.), and are plotted on the sine of the center of the latitude band. Results in the right column are for temperatures averaged over 4 different regions: the NH, the tropics (20◦N-20◦S), the SH, and the globe. Because of differences in the latitudinal extent of observational MSU datasets, the RSS spatial coverage was used as the basis for calculating all

spatial averages of TLS, TMT, and TLT (see SI Appendix). Spatial averages in A-C data use both land and ocean data. The model TLS and TMT results were stratified according to the presence or absence of stratospheric ozone depletion in the CMIP3 20CEN runs. Since “with O3” and “no O3” trends are virtually identical lower in the atmosphere, “ozone-stratified” results are not shown for TLT and SST. From Santer et al., 2011 (in preparation).

10.3.1.2.3 Stratospheric temperature change

Schwarzkopf and Ramaswamy (2008) investigate the evolution of stratospheric temperature in the 20th century in GFDL CM2.1 1861–2003 simulations with natural, anthropogenic and combined natural and anthropogenic forcing agents as well as based on well-mixed greenhouse gases and ozone-only simulations. They find that over the whole simulation period the total warming effect of natural forcing is negligible compared to the cooling simulated by anthropogenic forcings. The study further infers a signal of human influence on the atmosphere in the global mean lower to middle stratosphere by early in the 20th century in the model. The larger values of regional and seasonal interannual variability for stratospheric temperatures compared to the global-mean values affects the emergence of a statistically significant signal. However, Schwarzkopf and Ramaswamy (2008) find early significance in the Arctic summer (by about 1890 at 30km and by about 1950 at about 21km) and Antarctic summer (by about 1940).

Chemistry climate models (CCMs) forced with observed concentrations of anthropogenic halogenated Ozone Depleting Substances (ODS), well-mixed greenhouse gases, and natural forcings simulate the historical evolution of stratospheric temperature broadly consistently with observations (Chapter 3 of Eyring et al., 2010) Gillett et al. (2011) use the suite of CCMVal version 2 simulations for an attribution study of observed changes in stratospheric zonal mean temperatures. They partition 1979–2005 MSU temperature trends into ODS induced and GHG induced changes which takes into account that GHG-cooling induced increase in ozone concentration cancel out part of the cooling due to the GHGs themselves (Shepherd and Jonsson, 2008). Gillett et al. (2011) find that both ODSs and natural forcing contributed to the observed stratospheric cooling in the lower stratosphere with the impact of ODS dominating. The cooling contribution of natural forcings results most likely from the fact that El Chichón warmed the stratosphere in the first half of the record while there were no volcanic eruptions in the second half of the record resulting in a cooling trend due to the stratospheric aerosol forcing. The influence of GHGs on stratospheric temperature could not be detected independently of ODSs. [Assessment of studies based on CMIP5]

Lin et al. (2010) explain the observed lower stratosphere wave 1 temperature trend structure in austral spring with the overlapping influence of ozone depletion causing cooling and response of the Brewer Dobson Circulation (BDC) to observed increase in sea surface temperatures causing stratospheric warming (Hu and Fu, 2009). The CMIP3 models do not capture the observed spatial trend pattern in the Southern Hemisphere high-latitude stratosphere in the winter and spring seasons. They fail to simulate the response of the BDC to global warming in this region. The long-term changes in these waves are completely missed (Lin et al., 2010). [The analysis will be repeated for CMIP5 and CCMVal 2 simulations which can be assessed]

10.3.2 Water Cycle

Water cycle changes are among the most important potential climate changes in terms of potential vulnerability of societies and ecosystems in water-limited environments. Recent reviews of detection and attribution of trends in various components of the water cycle have been published by Huntington (2006) and Stott et al. (2010).

The surface water budget is affected directly by both temperature and precipitation. Thus surface water variables have the potential for exhibiting more detectable climate change signals than precipitation. The large interannual and decadal variability associated with regional temperature and precipitation still make it difficult to reach definitive detection and attribution results.

10.3.2.1 Changes in Atmospheric Water Vapour

Detection of humidity trends is important for validating climate change projections because the positive feedback associated with water vapor is a robust feature of the climate model response to radiative forcing (Chapter 9). According to the Clausius–Clapeyron (CC) relation, the saturation vapor pressure increases approximately exponentially with temperature. Therefore the maximum possible water vapour content of the troposphere increases in a warmer world. As moisture condenses out of supersaturated air from time to time, it is physically plausible, and has been assumed in many studies, that the distribution of relative humidity would remain roughly constant under climate change. In this case, the CC-relation implies a roughly exponential increase in specific humidity with temperature at a rate of about 7%/K (Allen and Ingram, 2002).

The direct consequences of such a water vapor increase would include a decrease in convective mass flux, an increase in horizontal moisture transport, associated enhancement of the pattern of evaporation minus precipitation and its temporal variance, and a decrease in horizontal sensible heat transport in the extratropics (Held and Soden, 2006b). An anticipated consequence of these flux and transport changes is that wet regions should become wetter and dry regions drier (Held and Soden, 2006a). Many of these anticipated changes, reasoned from physical principles, have been simulated by climate models.

Lack of appropriate data has been a significant limiting factor in the analysis of humidity changes, although there has been some recent progress with the development of the HadCRUH Surface Humidity dataset (Willett et al., 2007a) (2008). This dataset (see Figure 10.11) indicates significant increases between 1973 and 2003 in surface specific humidity over the globe, the tropics, and the Northern Hemisphere, with consistently larger trends in the tropics and in the Northern Hemisphere during summer, and negative or nonsignificant trends in relative humidity. This is in accord with the nonlinearity in the CC-relation: warmer regions should exhibit larger increases in specific humidity for a given temperature change. Anthropogenic influence has been clearly detected in this surface humidity dataset (Willett et al., 2007b).

[INSERT FIGURE 10.11 HERE]

Figure 10.11: Observed (top row) and simulated (bottom row) trends in specific humidity over the period 1973–1999 in g/kg per decade. Observed specific humidity trends a) and the sum of trends simulated in response to anthropogenic and natural forcings d) are compared with trends calculated from observed b) and simulated e) temperature changes under the assumption of constant relative humidity; the residual (actual trend minus temperature induced trend is shown in c) and f) (Willett et al., 2007).

Trenberth et al. (2005) analyze SSM/I column water vapor retrievals and find a significant global-average trend of about 1.3%/decade since 1988. The anthropogenic water vapor fingerprint simulated by an ensemble of 22 climate models has subsequently been identified in lower tropospheric moisture content estimates derived from SSM/I data covering the period 1988–2006 (Santer et al., 2007). Santer et al. (2009) finds that detection of an anthropogenic response in column water vapour is insensitive to the set of models used. They rank models based on their ability to simulate the observed mean total column water vapour, and its annual cycle and variability associated with ENSO. They find no appreciable differences between the fingerprints or detection results derived from the best or worst performing models. Simmons et al. (2010) analyze a suite of observed and assimilated humidity products, and also found that specific humidity has been increasing in recent decades. The upward trend in specific humidity over land areas, however, is modest over this period while land-based temperature trends are pronounced, such that relative humidity (a function of both temperature and specific humidity as described by the CC-relationship) has been declining over land.

Stratospheric water vapour exists in much smaller concentrations than near-surface vapour, but can play a disproportionately important role in the surface energy budget because greenhouse gases at this high altitude are extremely effective at enhancing the overall greenhouse effect. Randel et al. (2006) describe an abrupt decrease in stratospheric water vapour in the late 1990s. The relatively short and sparse record of stratospheric water vapour makes formal trend detection and attribution difficult for this variable. Rosenlof and Reid (2008) show that decreasing water vapour values in the equatorial lower stratosphere after 2000 are correlated with warmer ocean surface temperatures and colder tropopause temperatures. Solomon et al. (2010) also find that lower stratospheric water vapor concentration declined abruptly after 2000. Based on simulations with a model of intermediate complexity, they find that this abrupt decrease contributed a surface cooling of about 0.03°C by 2008, slowing the surface temperature increase that would be expected due to increasing greenhouse gas concentrations.

10.3.2.2 Changes in Global Precipitation

The availability of energy is a stronger constraint than the availability of moisture on the increase of global precipitation (Allen and Ingram, 2002). Warming the troposphere enhances the radiative cooling rate in the upper troposphere, thereby increasing precipitation, but this could be partly offset by a decrease in the efficiency of radiative cooling due to an increase in atmospheric greenhouse gases. As a result, global precipitation rates are expected to increase only at around 2%/K rather than following the 7%/K of the CC-relationship. Wentz et al. (2007) suggest that observed global precipitation in SSM/I data has increased according to the much faster CC-relation, but Liepert and Previdi (2009) show that the relatively short (20 yr) SSM/I record may not be sufficient to determine whether models and observations agree on the rainfall response to recent radiative forcing. This is because of various problems with observational data and because global precipitation change estimated over such a short time period may not be representative of changes that will occur on longer timescales. Observed changes in globally averaged land precipitation appear to be more consistent with the expected effects of both anthropogenic and natural forcings (including volcanic activity that affects short wave forcing) than with the effects of long wave forcing in isolation (Lambert et al., 2004; Lambert and Allen, 2009).

Another expected aspect of simulated precipitation change is a poleward redistribution of extratropical precipitation, including increasing precipitation at high latitudes and decreasing precipitation in the subtropics, and potentially changes in the distribution of precipitation within the tropics by shifting the position of the Intertropical Convergence Zone or the Walker Circulation in the Pacific. Comparisons between observed and modeled trends in land precipitation over two periods during the 20th century are shown in Figure 10.12. A comparison of observed trends averaged over latitudinal bands with those simulated by 14 climate models forced by the combined effects of anthropogenic and natural external forcing, and by 4 climate models forced by natural forcing alone, shows that anthropogenic forcing has had a detectable influence on observed changes in average precipitation (Zhang et al., 2007b). While these changes cannot be explained by internal climate variability or natural forcing, the magnitude of change in the observations is greater than simulated.

[INSERT FIGURE 10.12 HERE]

Figure 10.12: Comparison between observed (solid black) and simulated zonal mean land precipitation trends for 1925–1999 (left) and 1950–1999 (right). Black dotted lines indicate the multi-model means from all available models (ALL in top row, ANT in middle row, and NAT in bottom row), and black dash-dotted lines those from the subset of 4 models which simulated the response to each of the forcing scenarios (ALL4, ANT4 and NAT4). The model simulated range of trends is shown shaded. Black dashed lines indicate ensemble means of ALL and ANT simulations that have been scaled (SALL and SANT) to best fit the observations based on a 1-signal analysis. Coloured lines indicate individual model mean trends (Zhang et al., 2007).

The influence of anthropogenic greenhouse gases and sulfate aerosols on changes in precipitation over high-latitude land areas north of 55°N has also been detected (Min et al., 2008a). Detection is possible here, despite limited data coverage, in part because the response to forcing is relatively strong in the region, and because internal variability is low. Consistent with this argument, there has been some consistency in northern Europe winter precipitation between that from observations and that from simulations conducted by four different regional climate models (Bhend and von Storch, 2008). Generally, however, detection and attribution of regional precipitation changes remains difficult because of low signal-to-noise ratios and poor observational coverage. To date there have been no detection and attribution studies of precipitation over oceans because the available satellite datasets (such as that from the SSM/I) are short and not considered to be sufficiently reliable for this purpose.

In climates where seasonal snow storage and melting plays a significant role in annual runoff, the hydrologic regime changes with temperature. In a warmer world, less winter precipitation falls as snow and the melting of winter snow occurs earlier in spring, resulting in a shift in peak river runoff to winter and early spring. This has been observed in the western U.S. and in Canada (Zhang et al., 2001). The observed trends toward earlier timing of snowmelt-driven streamflows in the western US since 1950 are detectably different from natural variability (Hidalgo et al., 2009). A detection study of change in components of the hydrological cycle of the western US that are driven by temperature variables attributes up to 60% of observed climate related trends in river flow, winter air temperature, and snow pack over the 1950–1999 period in the region to human influence (Barnett et al., 2008), discussed further in Section 10.8.

10.3.2.3 Changes in Surface Water and Streamflow

The surface water budget involves precipitation (the flux of water from the atmosphere to the surface), evapotranspiration (ET, the water flux from surface to atmosphere) and runoff (the horizontal transport of water across the surface). Because ET is temperature-dependent, the surface water budget integrates temperature and precipitation trends. The projection of warmer temperatures across continents, together with the decrease in precipitation projected across dry subtropical latitudes, makes trends in the surface water budget of tremendous interest particularly in the subtropics.
Monitoring and understanding changes in runoff and drought is more difficult than for temperature and precipitation because soil moisture is poorly observed, and soil moisture and runoff changes are difficult to constrain from the residual difference between precipitation and evaporation, both of which are also relatively poorly observed. Many factors can cause soil moisture and runoff changes, including changes in climate, land use, stream management, water withdrawal, and water use efficiency by plants in high CO_2 environments (Gedney et al., 2006). Nevertheless, there has been an overall global increase in dry areas, as represented by the Palmer Drought Severity Index (PDSI), a commonly used drought indicator, and this increase has been attributed to anthropogenic influence (Burke et al., 2006) . It should be noted that the calculation of PDSI involves only surface temperature and precipitation, and so its characterization of ET involves a parameterization. The parameterization of ET in terms of temperature used in the standard formulation of PDSI is tuned to the current climate, and might overestimate ET in a warmer climate (Lockwood, 1999), so trends in PDSI must be viewed with caution.

Despite more intensive human water consumption, continental runoff has increased through the 20th century. Gedney et al. (2006), using a surface exchange scheme driven by observations and climate model simulations, detect anthropogenic influence on global runoff. They attribute the observed increase in runoff to a suppression of plant transpiration resulting from CO_2-induced stomatal closure although it has been argued that data limitations call the conclusions of this study into question (Gedney et al., 2006; Peel and McMahon, 2006).

Increases in evapotranspiration due to warming trends could be modulated by the land surface moisture available for ET. (Jung et al., 2010) examined a global network of land-based ET measurements and found that the observed increase in ET in the late 20th century ceased after 1998. They attributed the change in trend to diminished soil moisture in areas that have exhibited pronounced drought since that time. This conclusion is subject to the uncertainty noted above with regard to soil moisture monitoring.

10.3.3 Changes in Circulation and Climate Phenomena

The atmospheric circulation is driven by the uneven heating of the Earth's surface by solar radiation. The circulation transports heat from warm to cold regions and thereby acts to reduce temperature contrasts. Thus, atmospheric circulations are of critical importance for the climate system influencing regional climate and regional climate variability. Therefore, changes in atmospheric circulation are important for local climate change since they could act to reinforce or counteract the effects of external forcings on climate in a particular region. Observed changes in atmospheric circulation and patterns of variability are reviewed in Section 2.6. While there are new and improved datasets now available, changes in the large-scale circulation remain difficult to detect.

10.3.3.1 Tropical Circulation

Evidence for changes in the strength of the Hadley and Walker circulations are assessed in Section 2.6.5. While there is low confidence in trends in the strength of the Hadley circulation and limited evidence of any systematic trend in the strength of the Walker circulation, there is evidence from a variety of observed changes in atmospheric variables that the tropical belt as a whole has widened (see Figure 10.13). This evidence is based on independent datasets that show a poleward expansion of the Hadley circulation since the late 1970s (Fu et al., 2006; Hu and Fu, 2007) as well as surface, upper-tropospheric and stratospheric features (Forster, 2011; Hu et al., 2011; Hudson et al., 2006; Lu et al., 2009; Seidel and Randel, 2007; Seidel et al., 2008).

[INSERT FIGURE 10.13 HERE]
Figure 10.13: [PLACEHOLDER FOR FIRST ORDER DRAFT, will be replaced by a model-observation comparison figure] Changes in the tropical belt, estimated from different quantities as marked in the plot Adapted from (Seidel et al., 2008).

Recent studies have suggested that the observed widening of the tropical belt could be related to climate changes due to anthropogenic forcing, including stratospheric cooling due to stratospheric ozone depletion, tropospheric warming due to increasing GHGs, and warming of tropical SSTs (Johanson and Fu, 2009). However models appear to systematically under-estimate the observed widening. The observed widening of between about 2 and 5 degrees latitude between 1979 and 2005 is greater than climate model projections of expansion over the 20th century (Seidel et al., 2008) [update assessment with CMIP5 models if literature available]. This indicates that current models could systematically underestimate forced changes in the width of the tropical belt.

CMIP3 simulations for the 20th century, sensitivity experiments based on the NCAR CAM3 model and coupled chemistry-climate model simulations demonstrate that Antarctic ozone depletion is a major factor in causing poleward expansion of the Hadley circulation during austral summer (McLandress et al., 2011; Polvani et al., 2010; Son et al., 2009; Son et al., 2008; Son et al., 2010). Held (2000) postulates that the width of the Hadley circulation is determined by mid-latitude baroclinic wave activity. An increase in static stability due to increasing greenhouse gas concentrations suppresses baroclinic growth rates such that the onset of baroclinicity is shifted poleward. Thus, the Hadley circulation extends poleward. This relationship is supported by IPCC AR4 simulation results for the 21st century, in which mid-latitude static stability increases and the Hadley circulation extends poleward with the A1B scenario of GHG emission (Frierson et al., 2007; Frierson, 2006; Lu et al., 2007). Hu and Fu (2007) suggest that the observed poleward expansion of the Hadley circulation might be due to weakening of baroclinic wave activity because the observed global warming has stronger warming at higher latitudes and weaker warming at lower latitudes in the Northern Hemisphere, resulting in weakening of the meridional temperature gradient. SST warming, especially tropical SST warming, may also make an important contribution to the poleward expansion of the Hadley circulation. Several recent studies, focusing on atmospheric responses to tropical SSTs over interannual time scales, demonstrate that tropical SSTs have important impacts on the strength and width of the Hadley circulation (Hoerling and Kumar, 2003; Lau et al., 2006; Lau et al., 2005; Lu et al., 2008). That is, an El Nino-like spatial pattern of SST is associated with stronger and narrower Hadley cells, while anomalously warm SSTs over the Indian and western Pacific and Indian Oceans correspond to wider and weaker Hadley cells. AGCM simulations forced by observed time-varying SST indeed display total poleward expansion of the Hadley circulation by about 1° in latitude over 1979–2002 (Hu et al., 2011). Although the above results all suggest that the poleward expansion of the Hadley circulation is related to anthropogenic forcing, GCM simulations underestimate the observed magnitudes of poleward expansion (Hu et al., 2011; Johanson and Fu, 2009). Thus, what caused the poleward expansion of the Hadley circulation and how it is related to external forcing remains uncertain.

10.3.3.2 ENSO

Section 2.6.9 reviews the evidence for changes in ENSO and finds little robust evidence of long-term trends in NINO 3.4 SSTs or changes in ENSO variability. Some recent studies suggest that the change in ENSO activity over the late 20th century is likely caused by global warming because the increasing trend in ENSO amplitude remains, even after removing both the long-term trend and decadal change of the background climate (Zhang et al., 2008a). But caution needs to be excised in interpreting these results, because 1) large uncertainty exists in estimating the SST trend in the tropical Pacific using different observed data sets (Deser et al., 2010a) and 2) ENSO dynamics may be intrinsically nonlinear and the long-term variation in the background climate of the tropical Pacific may be a residual effect of naturally varying ENSO (Schopf and Burgman, 2006). In addition, climate model projections of future ENSO changes vary considerably from model to model: some projecting an increase in ENSO activity as warming continues (Guilyardi, 2006), some showing little or no change in ENSO activity (Guilyardi, 2006; Merryfield, 2006; Oldenborgh et al., 2005), some determining a decreased ENSO activity (Meehl et al., 2005b) reflecting the complex dynamics that control ENSO variability.

ENSO changes may also come from a variety of sources outside of the tropical Pacific, like changes in the midlatitude storm tracks, which may have a significant influence on ENSO variability (Anderson, 2004; Chang et al., 2007; Vimont et al., 2003), changes in the Atlantic Meridional Overturning Circulation (AMOC), changes in the global interhemispheric SST pattern (Feng et al., 2008), and Indian Ocean SST variability (Izumo et al., 2010). A recent study shows that the robust warming trend in the tropical Atlantic (Deser et al., 2010a) can lead to a La Nina-like response in the tropical Pacific (Kucharski et al., 2010).

There has been limited success in identifying changes in the character of ENSO variability from observations although there is some evidence that a different type of El Nino event has appeared more frequently from the mid-20 the century on (Section 2.6.9). There has been a tendency for El Nino-related SST anomalies to shift towards the central tropical Pacific from the mid 20th century on (Lee and McPhaden, 2010; Section 2.6) consistent with climate model projections (Yeh, 2010). The influence of this type of SST anomaly on the atmosphere appears to be different from that of the canonical ENSO SST (Ashok and Yamagata, 2009; Kim et al., 2009; Kim et al., 2010; Weng et al., 2009).

10.3.3.3 Atlantic Multi-Decadal Oscillation

The observed detrended 20th century multidecadal SST anomaly averaged over the North Atlantic, often called the Atlantic Multidecadal Oscillation (AMO), has significant regional and hemispheric climate impacts. The warm AMO phases occurred during 1925–1965 and the recent decade since 1995, and cold phases occurred during 1900–1925 and 1965–1995. The AMO which has a global temperature signature amplitude of about 0.49K (Knight et al., 2005) is highly correlated with multidecadal variations of the tropical North Atlantic (TNA) SST, and modeling studies indicate a causal link between the AMO and the multidecadal variability of the Atlantic hurricane activity (Knight et al., 2006; Zhang and Delworth, 2006). The AMO is also found to have played an important role in the multidecal variability of the Sahel summer monsoon rainfall (Shanahan et al., 2009; Tourre et al., 2010; Zhang and Delworth, 2006) and the Indian summer monsoon rainfall (Goswami et al., 2006; Li et al., 2008; Zhang and Delworth, 2006). Recent modeling studies (Knight et al., 2006; Sutton and Hodson, 2007) provide a clear assessment of the impact of the AMO over the Atlantic, North America, and Western Europe. Zhang et al. (2007a) demonstrate that AMO-like SST variations can contribute to NH mean surface temperature fluctuations, such as the early 20th century warming, the pause in hemispheric-scale warming in the mid-20th century, and the late 20th century rapid warming, in addition to the long-term warming trend induced by increasing GHGs. The AMO is often thought to be driven by the variability of the Atlantic Meridional Overturning Circulation (AMOC) (Knight et al., 2005; Latif et al., 2006) although some have suggested that the AMO is driven by changes in radiative forcing (Mann and Emanuel, 2006).

10.3.3.4 NAM/NAO

Since the publication of the AR4 the North Atlantic Oscillation has tended to be in a negative phase. In particular the winter of 2009–2010 exhibited a strong negative NAO anomaly, and the annual mean 2010 NAO anomaly is the most negative Jones NAO anomaly on record (Hoerling et al., 2011). This means that the positive trend in the NAO discussed in the AR4 has considerably weakened when evaluated up to 2011 (see also Section 2.6.9). Similar results apply to the closely-related Northern Annular Mode. Figure 10.14 shows that the DJF trend in a zonal index similar to the NAM is considerably weaker over the period 1961–2011 compared to the period 1955–2005 considered by Gillett (2005). Over the most recent 50-year period the observed trend based on the more reliable HadSLP2r data is no longer significant at the 5% level compared to simulated internal variability, although it remains significant at this level based on the NCEP reanalysis.

Other work (Woollings, 2008) demonstrate while the Northern Annular Mode is largely barotropic in structure, the simulated response to anthropogenic forcing has a strong baroclinic component, with an opposite geopotential height trends in the mid-troposphere compared to the surface in many models. Thus while the response to anthropogenic forcing may project onto the NAM, it is distinct from the NAM itself.

In contrast to most earlier studies reviewed in the AR4, Morgenstern et al. (2010) find a weakly negative winter NAO response to greenhouse gas increases in coupled chemistry climate models, along with a weak positive response to ozone depletion in spring. Taken together, these findings somewhat weaken the conclusion of the AR4 that the positive trend in the NAM is likely due in part to anthropogenic forcing.

10.3.3.5 SAM

The SAM index has remained mainly positive since the publication of the AR4, although it has not been as strongly positive as in the late 1990s. Nonetheless, a Southern Hemisphere zonal index similar to the SAM shows a larger trend in DJF over the period 1961–2011 compared to the 1955–2005 period (Figure 10.14). Recent modelling studies confirm earlier findings that the increase in greenhouse gas concentrations tend to lead to a strengthening and poleward shift of the Southern Hemisphere midlatitude jet (Karpechko et al., 2008; Sigmond et al., 2011; Son et al., 2008; Son et al., 2010) which projects onto the positive phase of the Southern Annular Mode. Stratospheric ozone depletion also induces a strengthening and poleward shift of the midlatitude jet, with the largest response in austral summer (Karpechko et al., 2008; McLandress et al., 2011; Polvani et al., 2010; Sigmond et al., 2011; Son et al., 2008; Son et al., 2010). Sigmond et al. (2011) find approximately equal contributions to simulated annual mean SAM trends from greenhouse gases and stratospheric ozone depletion up to the present. Fogt et al. (2009) demonstrate that observed SAM trends over the period 1957–2005 are positive in all seasons, but only statistically significant in DJF and MAM, based on simulated internal variability. Observed trends are also consistent with CMIP3 simulations including stratospheric ozone changes in all seasons, though in MAM observed trends are roughly twice as large as those simulated. Fogt et al. (2009) find that the largest forced response has likely occurred in DJF, the season in which stratospheric ozone depletion has been the dominant contributor to the observed trends. Taken together these findings strengthen the conclusion of the AR4 that the positive trend in the SAM is likely due in part to anthropogenic forcing, with the impact of ozone depletion on the DJF SAM being the clearest aspect of the anthropogenically-forced response.

[INSERT FIGURE 10.14 HERE]

Figure 10.14: DJF zonal index trends over 50-year periods. Panel a) shows the 50-year DJF trend in an index of meridional pressure gradient derived by subtracting mean SLP poleward of 45°N from mean SLP equatorward of 45°N in HadSLP2r (blue) and the NCEP reanalysis (green) over the period 1955–2005 (solid), and 1961–2011 (dotted). This zonal index is closely related to the NAM index. The black line shows a histogram of trends simulated in overlapping segments of control simulation from nine CMIP3 models, while the red line is a histogram of 1955–2005 trends in the historical simulations of nine CMIP3 models including greenhouse gas changes, sulphate aerosol changes, natural forcings and stratospheric ozone depletion. Panel b) shows equivalent 50-year DJF zonal index trends for the Southern Hemisphere, closely related to SAM index trends. Updated from Gillett (2005).

10.3.3.6 Indian Ocean Dipole

Ihara et al. (2008) suggest that shoaling of the thermocline in the Indian Ocean, due to warming may have increased the occurrence of positive IOD events. In a GCM simulation, Zheng et al. (2010) find that shoaling of the thermocline strengthens the thermocline feedback on the IOD. But while anthropogenic forcing leads to a shoaling of the thermocline, it also increases the static stability of the troposphere in the model – this compensates, and overall IOD variance doesn't change. Thus they conclude that the apparent increase in IOD variance observed is likely due to internal variability. In the 20th century simulations of the CMIP3 ensemble, the IOD exhbits an upward trend. Cai et al. (2009) therefore suggest that anthropogenic forcing may therefore have increased the chance of occurrence of successive positive IOD events. Taken together these studies suggest that there is little evidence to date of an anthropogenic influence on the IOD.

10.3.3.7 Monsoon

[PLACEHOLDER FOR FIRST ORDER DRAFT]

10.4 Changes in Ocean Properties

[PLACEHOLDER FOR FIRST ORDER DRAFT]

10.4.1 Ocean Temperature and Heat Content

The AR4 had concluded that the oceans had warmed (Bindoff et al., 2007) and that this warming could not be explained with natural climate variability (Hegerl et al., 2007b). Further, it is likely that anthropogenic forcing has contributed to the general warming observed in the upper several hundred meters of the ocean during the second half of the 20th century (Barnett et al., 2005) and (Pierce et al., 2006). They found that the vertical and basin-scale structure of ocean warming to be consistent with the response to anthropogenic forcing (well mixed greenhouse gases and sulphate aerosols) as simulated by two climate models (PCM and HadCM3). There were however, concerns regarding the ability of climate models (not restricted to PCM and HadCM3) to simulate the observed variability in ocean heat content.

Many factors contribute to differences between modelled and observed variability in ocean temperature. The first is the incomplete and time-varying coverage of the observations. Until the advent of Argo data in the early 21st century, our view of the mean state and variability of ocean temperature was based on incomplete observational coverage that varied geographically, with depth and time. Estimates of heat content variability can depend on assumptions made to infill data when and where measurements are lacking (AchutaRao et al., 2006; Gregory et al., 2004). It has been demonstrated that the variability of historically forced simulations agrees more closely with observations when the model data is "subsampled" in a manner consistent with that of the time evolving observational record (AchutaRao et al., 2007). It has also been shown that the inclusion of volcanic forcing in simulations of the 20th century contributes to the simulated variability of ocean heat content (AchutaRao et al., 2007) and that eruptions temporarily offset late 20th century upper ocean warming (Church et al., 2005; Delworth et al., 2005; Gleckler et al., 2006b). A few of the models analyzed in the AR4 did not use volcanic forcings in these simulations of the 20th century climate leading to an under-representation of the variability observed over the second half of the 20th century.

A second factor that influences variability in observational data sets is related to the documented biases in different types of instruments (Gouretski and Koltermann, 2007) and the systematic space–time changes in these biases to the overall observing system (AchutaRao et al., 2007). A large part of the discrepancy has since been shown to be a result of instrument errors (Wijffels et al., 2008). A comparison of AR4 models with the bias corrected observations (Domingues et al., 2008) found that the decadal variability of the climate models with volcanic forcing is in better agreement with the observations (Figure 10.15). However the modelled multi-decadal trends are smaller than observed trends of global heat content.

[INSERT FIGURE 10.15 HERE]
Figure 10.15: Comparison of observed and simulated ocean heat content (OHC) and thermosteric sea level (ThSL) estimates for the upper 700 m. a) and b): Models without volcanic forcing. c) and d): Models with volcanic forcing (Domingues et al., 2008).

Detection and attribution studies of ocean warming have typically analyzed the temperature change from the ocean surface down to a fixed depth. The average temperature of the water column at a particular location can change either due to changes in air-sea heat flux or as a result of advective redistribution of oceanic heat. The difficulty with analyses of ocean warming using the conventional ''fixed depth'' approach is that these advective and air-sea processes cannot be separated. The over-representation of North Atlantic and North Pacific oceans (when compared to other basins) in the observed record can easily bias a basin or global average warming rate. It is estimated that approximately 50% of the upper ocean warming signal in the North Atlantic could be associated purely with local changes in ocean circulation rather than air-sea interaction (Palmer and Haines, 2009).

A new approach has been adopted that seeks to isolate temperature changes occurring due to changes in air-sea heat flux from those caused by advective redistribution of oceanic heat (Palmer et al., 2009). They analyze changes in the average temperature above the 14˚C isotherm by comparing observed and climate model (HadCM3) simulated space-time patterns over non-overlapping 2-year periods for five ocean basins (Palmer and Haines, 2009; Palmer et al., 2007). The HadCM3 simulations describe remarkably well the temporal evolution of ocean temperatures in the World's ocean basins over the last five decades and the detected the effects of both anthropogenic and volcanic influences simultaneously (Palmer et al., 2007). The analyzed changes in the average temperature over the upper 220m (the average depth of the 14˚C isotherm) in the conventional way did not show a robust detection of either anthropogenic or volcanic influences.

These new approaches of using temperature or density surfaces (Downes et al., 2009, 2010; Palmer and Haines, 2009) may be leading to a more robust detection as a result of filtering of high frequency ocean dynamics (such as eddies and internal waves) thereby yielding reduced observational sampling noise and by reducing the impact of climate mode variability (such as ENSO) in model simulations. Further, by attributing the short-term cooling episodes to volcanic eruptions and the multi-decadal warming to anthropogenic forcing, this approach offers an improvement over previous studies that were only able to capture the secular change from anthropogenic forcings.

Until recently, ocean temperature detection and attribution analysis has been performed in a single-model framework, where one or two models have been used to estimate both the climate response to an imposed forcing change as well as the background noise of internal variability. In a recent study (Gleckler et al., 2011 in preparation) a multi-model analysis of upper ocean warming has been carried out, applying the same methodology used to evaluate atmospheric water vapor changes (Santer, 2007). Another issue that complicates the detection and attribution of OHC changes is that simulations with coupled atmosphere-ocean general circulation models (AOGCMs) generally exhibit a residual "drift" in deep ocean heat content resulting from a slow and incomplete spin up process associated with the coupling of model components (Gleckler et al., 2006a; Gregory et al., 2001). A concern is that model estimates of natural variability could be sensitive to the method of drift removal. This sensitivity of detection and attribution of ocean heat content changes has been tested to different measurement bias corrections, methods of drift removal, and the impact of volcanic forcing in a multi-model context (Gleckler et al., 2006a; Gregory et al., 2001).

10.4.2 Ocean Salinity and Freshwater Fluxes

There is increasing recognition of the importance of ocean salinity at an essential climate variable (Doherty et al., 2009), particularly for understanding the hydrological cycle. In the IPCC Fourth Assessment Report observed ocean salinity change in the oceans indicated that there was a systematic pattern of increased salinity in the shallow subtropics and a tendency to freshening of waters that originate in the polar regions (Bindoff et al., 2007), broadly consistent with an acceleration of the hydrological cycle. New atlases and revisions of the earlier work based on the increasing number of the ARGO profile data, and historical data have extended the observational salinity data sets for examining the long terms change at the surface and within the interior of the ocean.

Patterns of subsurface salinity changes on pressure surfaces also largely follow an enhancement of the existing mean pattern within the ocean. For example, the inter-basin contrast between the Atlantic (salty) and Pacific (fresh) intensifies over the observed record (Boyer et al., 2005; Durack and Wijffels, 2010; Hosoda et al., 2009; Roemmich and Gilson, 2009; von Schuckmann et al., 2009). These deep reaching salinity changes suggest that past changes in the surface freshwater fluxes have propagated into the ocean interior. These new analyses also show a clear enhancement of the high-salinity subtropical waters, and freshening of the high latitude waters (Helm et al., 2010). An example of the freshening of the high latitude waters is the coherent freshening expressed in the Antarctic Intermediate Water subduction pathway centred around 50°S (Bindoff and McDougall, 2000; Boyer et al., 2005; Curry et al., 2003; Durack and Wijffels, 2010; Helm et al., 2010; Hosoda et al., 2009; Johnson and Orsi, 1997; Roemmich and Gilson, 2009; Wong et al., 1999) including studies on density horizons (Curry et al., 2003; Helm et al., 2010; Wong et al., 1999). While this framework of density surfaces show that many changes are dominated by the subduction of changed properties into the deep ocean caused by the lateral movement of the gyres and can reflect a broad-scale warming (Durack and Wijffels, 2010). However, at the salinity minimum and shallow salinity maximum the interpretation of the observed changes in salinity are unambiguous (Bindoff and McDougall, 2000)

Observed surface salinity changes also suggest an increase in the global water cycle has occurred. The strong linear correlation of 0.7 of the the mean climate of the surface salinity with the pattern of multi-decadal changes in surface salinity is supports the acceleration of the hydrological cycle (Durack and Wijffels, 2011, in preparation). The robust global tendency towards an enhanced surface salinity pattern agrees with other regional studies (Curry et al., 2003) , and other global analyses of surface salinity change (Boyer et al., 2005; Hosoda et al., 2009; Roemmich and Gilson, 2009). The changes of surface salinity demonstrate that wet regions get fresher and dry regions saltier, following the expected response of an amplified water cycle.

While there are now many established detection studies of both surface salinity and sub-surface salinity changes, there are relatively few formal attribution studies of these salinity changes to anthropogenic forcing. Indeed, here we rely on expert judgment from the studies that have quantitatively examined the observed trends in ocean salinity with coupled ocean atmosphere general circulation models in response to all anthropogenic forcing. The global models project changes (Figure 10.16, Panel a) in the meridional variation of precipitation minus evaporation that broadly coincide with apparent freshwater fluxes inferred from the observed changes and these two estimates of freshwater flux coincide within error estimates (Figure 10.16, Panel b). The observed salinity changes imply a 3 ± 2% decrease in precipitation minus evaporation (P -E) over the mid and low latitude oceans in both hemispheres, a 7 ± 4% increase in the Northern Hemisphere high latitudes, and a 16 ± 6% increase in the Southern Ocean since 1970. Salinity amplification as a measure of the acceleration of the hydrological cycle has also been estimated from coupled general circulation models and from observations. Salinity amplification is defined as slope of the temporal changes (in space) and the mean spatial pattern. In terms of the salinity amplification the observations are relative to the global surface warming (Figure 10.16 Panel d) shows an amplification of the meridional hydrological cycle to be about 16 and very close to slope expected from the Clausius-Clapeyron equation (Durack and Wijffels, 2011, in preparation), while the models with SRES forcing are about half of this value (Figure 10.16 Panel d). The low value is of projections relative to the observed salinity amplification is consistent with detection and attributions studies precipitation over land (Wentz et al., 2007; Zhang et al., 2007b). Expert judgment now shows a broad consistency between the observed trends that are greater than natural variation and the mechanisms from models of anthropogenic forcing and is likely to be attributable to rising greenhouse gases and aerosols in the atmosphere.

[INSERT FIGURE 10.16 HERE]

Figure 10.16: Ocean salinity change observed in the ocean (Panel c) and estimated surface precipitation minus evaporation (Panel b), and comparison with coupled climate change model projections of precipitation minus evaporation from 10 IPCC AR4 models (Panel a), and the salinity pattern amplification (see text) from coupled GCM with all forcings and from 20th century simulations and observations as a function of global surface temperature change (Panel d). Panel a),b), and c) are from Helm et al. (2010) and Panel c) is from Durack and Wijffels (2011, in preparation).

10.4.3 Sea Level

At the time of the AR4, there were very few studies quantifying the contribution of anthropogenic forcing to steric sea-level rise and glacier melting. Therefore, an expert assessment had concluded that anthropogenic forcing had likely contributed to at least one-quarter to one-half of the sea level rise during the second half of the 20th century based on modelling and ocean heat content studies. The AR4 had observed that models that include anthropogenic and natural forcing simulated the observed thermal expansion since 1961 reasonably well and that it is very unlikely that the warming during the past half century is due only to known natural causes.

Since then, corrections applied to instrumental errors in ocean temperature measurement systems have significantly improved the balance in the overall sea level rise budget for the 1961–2003 period (Domingues et al., 2008). For models that do not include volcanic aerosols, the variations in simulated ocean heat content and thermosteric sea level has a smaller decadal variability than the observations and larger long-term trends. Climate models that include volcanic forcing agree reasonably with the observations of decadal variability, but underestimate the observed multi-decadal trends (Figure 10.15). The model trends with volcanic forcing are in greater agreement with the observations but are on average about 28% smaller in the upper 300m and about 10% smaller in the upper 700m. Although, the improved observed ocean-temperature time series produces less decadal variability in sea level owing to the correction of the time-varying biases (as described in Section 10.4.1), there are still significant unexplained signals in total sea-level variability. Closure of the global budget remains a challenge due to many uncertainties, including the human influence on land-based water storage, and a significant unmeasured deep-ocean temperature component (Milne et al., 2009).

While the global sea level shows a steady rise, regional patterns of sea level change are more complex with a rise in some regions accompanied by a fall in others. One such region is the Indian Ocean, where sea level has decreased markedly in the south tropical Indian Ocean but has increased elsewhere in the basin. Investigations of the possible drivers of sea level changes in this basin since the 1960s find that the sea level change pattern is driven by changing surface winds (Han et al., 2010). The sea level change patterns are well simulated by a wind driven linear ocean-model, a reduced gravity model, as well as two state of the art ocean models. The HYCOM and POP models capture the decadal variability seen in the longer in situ record (Peltier, 2004) and the agreement extends to the satellite records of sea-level. The changing surface winds associated with a combined invigoration of the Indian Ocean Hadley and Walker cells are tied to an SST warming trend in the Indo-Pacific warm pool during the past few decades using AGCMs forced by observed SST changes in the warm pool. In two climate models used in the AR4 (CCSM3 and PCM) the positive SST trend in the Indo-Pacific warm pool is caused primarily by anthropogenic forcing with natural forcing producing no regional SST increase. The possible role of multi-decadal natural (forced or internal) variability in enhancing such a pattern is unknown. It is probable that anthropogenic forcing (with long time scales) combined with natural variability explains the observed wind and sea-level changes.

10.4.4 Other Ocean Properties

[PLACEHOLDER FOR FIRST ORDER DRAFT]

10.4.4.1 Oxygen

Both modelled (Deutsch et al., 2005; Matear and Hirst, 2003; Plattner et al., 2002) and observed (Aoki et al., 2005; Bindoff and McDougall, 2000; Emerson et al., 2004; Keeling and Garcia, 2002; Mecking et al., 2006; Nakanowatari et al., 2007; Ono et al., 2001) regional oxygen decreases are largely explained by decreases in renewal rates, resulting in more time for biological oxygen utilisation to occur. Despite showing reasonably consistent patterns of change these observational studies tend to be limited to a few individual basins and cruise sections. The strongest decreases in oxygen occur in the mid-latitudes of both hemispheres, near regions where there is strong water renewal and exchange between the ocean interior and surface waters. Approximately 15% of this decrease can be explained by a warmer mixed-layer reducing the capacity of water to store oxygen, while the remainder is consistent (Matear et al., 2000) with decreased exchange of surface waters with the ocean interior (Helm et al., 2011 in preparation). The global scale decreases in oxygen suggests that such changes are not just the result of regional oscillations. The surface temperatures, increased ocean heat content (and surface salinity patterns) have been attributed human influence (Hegerl et al., 2007b) and projected stratification decreases suggest (as a multi-step attribution) it is likely these oxygen decreases can also be attributed to human influences through a reduction in water mass renewal rates.

10.5 Cryosphere

[PLACEHOLDER FOR FIRST ORDER DRAFT]

10.5.1 Sea Ice

[PLACEHOLDER FOR FIRST ORDER DRAFT]

10.5.1.1 Arctic and Antarctic Sea Ice

The decline of Arctic sea ice thickness and September sea ice extent has increased considerably in the first decade of the 21st century (Alekseev et al., 2009; Comiso and Nishio, 2008; Deser and Teng, 2008; Maslanik et al., 2007; Nghiem et al., 2007). There was a rapid reduction in September 2007 to 37% less extent relative to the 1979–2000 climatology (Figure 4.X, to be revealed in ZOD draft of Chapter 4). This compares to the previous minimum of 25% in 2005. Since 2007 the sea ice extent at the end of summer has remained at 30% or more below the reference climatology for the period 2007 through 2010. The amount of old thick multi-year sea ice in the Arctic has also decreased, by 42% from 2004 through 2008 (Giles et al., 2008; Kwok et al., 2009). The observed sea ice extent reduction exceeds the reductions simulated by the climate models available for the IPCC AR4 (Holland et al., 2010; Stroeve et al., 2007). It should be noted that this is a comparison of the single observed climate trajectory with a limited number of climate model projections with relatively few ensemble members to span the range of possible future conditions. The nearly stepwise drop in sea ice extent in 2007 to unprecedented and sustained low values combined with projected increase of Arctic temperatures, increases the chance of a nearly sea ice free Arctic in September (that is at the end of summer) in the next four decades — well ahead of most coupled model estimates (Boe et al., 2009; Wang and Overland, 2009).

The increase in the magnitude of recent Arctic temperature and sea ice changes are likely to be due to coupled Arctic amplification mechanisms (Miller et al., 2010; Serreze and Francis, 2006). Historically, sea ice formed rapidly on areas of open ocean in autumn causing a strong negative radiative feedback and causing a rapid seasonal cooling. But recently, the increased mobility and loss of multi-year sea ice, combined with enhanced heat storage in the sea-ice free regions of the Arctic ocean (and in turn returns this heat to the atmosphere in the following autumn), form a connected set of processes with positive feedback increasing Arctic temperatures and decreasing sea ice extent (Gascard and al, 2008; Serreze et al., 2009). In addition to the well known *ice albedo* feedback where decreased sea ice cover decreases the amount of *insolation* reflected from the surface, in recent years evidence has emerged for a late summer/early autumn positive *ice insulation* feedback due to additional ocean heat storage in the areas previously covered in sea-ice (Jackson et al., 2010). Arctic amplification is also a consequence of poleward heat transport in the atmosphere (Doscher et al., 2010; Graversen and Wang, 2009; Langen and Alexeev, 2007). These feedbacks in the Arctic climate system suggest that the Arctic is sensitive to external forcing. For example, when the 2007 sea ice minimum occurred, Arctic temperatures had been rising and sea ice extent had been decreasing over the previous two decades (Screen and Simmonds, 2010; Stroeve et al., 2008). Nevertheless, it took an unusually persistent southerly wind pattern over the summer months to initiate the loss event in 2007 (Wang et al., 2009a; Zhang et al., 2008b). Similar wind patterns in previous years did not initiate major reductions in sea ice extent because the sea ice was too thick to respond (Overland et al., 2008). Increased oceanic heat transport by the Barents Sea inflow in the first decade of the 20th century may also play a role in determining sea ice anomalies in the Atlantic Arctic (Dickson et al., 2000; Semenov, 2008). It is very likely that Arctic amplification mechanisms are currently affecting the regional Arctic climate, given the reduction of late summer sea ice extent in the Barents Sea, the Arctic Ocean north of Siberia, and especially the Chukchi and Beaufort Seas, in addition to the loss of old thick sea ice and the record air temperatures in autumn observed at adjacent coastal stations.

Attribution of Arctic change to anthropogenic forcing is difficult because one is assessing changes relative to large natural variability in a regionally small area with an energetic atmospheric circulation. A major question as recently as five years ago was whether the recent Arctic warming and sea-ice loss was unique in the instrumental record and whether the observed trend would continue (Serreze et al., 2007). Arctic temperature anomalies in the 1930s were apparently as large as those in the 1990s. The warming of the early 1990s was associated with a persistently positive Arctic Oscillation, which at the time was considered as either a natural variation or global warming (Feldstein, 2002; Overland and Wang, 2005; Overland et al., 2008; Palmer, 1999; Serreze et al., 2000). (Min et al., 2008b) compared the seasonal evolution of Arctic sea ice extent from the observations with those simulated by multiple GCMs for 1953–2006 (Figure 10.17). Comparing changes in both the amplitude and shape of the annual cycle of the sea ice extent reduces the likelihood of spurious detection due to coincidental agreement between the response to anthropogenic forcing and other factors, such as slow internal variability. They found that human influence on the sea ice extent changes can be robustly detected since the early 1990s. The detection result is also robust if the effect of AO on observed sea ice change is removed. The anthropogenic signal is also detectable for individual months from May to December, suggesting that human influence, strongest in late summer, now also extends into colder seasons.

[INSERT FIGURE 10.17 HERE]

Figure 10.17: Seasonal evolution of observed and simulated Arctic sea ice extent over 1953–2006. Anomalies are displayed relative to the 1953–1982 means from observations (OBS) and model simulations with anthropogenic only (ANT) and natural plus anthropogenic (ALL) forcings. These anomalies were obtained by computing non-overlapping 3-year mean sea ice anomalies for March, June, September, and December separately. Note different color scales between the observed and modeled patterns. Units: $\times 10^6$ km^2 (Min et al., 2008).

In the last five years evidence has continued to accumulate from both observations and model studies that systematic changes are occurring in the Arctic. Persistent trends in many Arctic variables, including sea ice extent, the timing of spring snow melt, increased shrubbiness in tundra regions, changes in permafrost, increased area coverage of forest fires, increased ocean temperatures, as well as Arctic-wide increases in air temperatures, can no longer be associated solely with dominate climate variability patterns such as the Arctic Oscillation or PNA (Overland, 2009; Quadrelli and Wallace, 2004; Vorosmarty et al., 2008) and (www.arctic.noaa.gov/reportcard). Global climate models subject to anthropogenic forcing generally project that the temperature increase in the Arctic will be larger than at more southerly latitudes and that the increase will be Arctic-wide in character (Chapman and Walsh, 2007). Figure 10.18 shows the annual near-surface air temperature anomalies in 2001–2010 for the high-latitude Northern Hemisphere. If the trend is broken down regionally and seasonally, the early part of the decade in spring had a minimum increase of +1°C relative to climatology throughout the Arctic, with a hot spot near eastern Siberia. Since then the Arctic-wide background temperatures has remained positive but the location of the hot spot has shifted to the Atlantic side of the Arctic. Autumn temperature anomalies have the greatest inter-seasonal value over much of the Arctic; this is also consistent with anthropogenic forcing in climate models. In contrast, during the period of positive AO (1989–1995) there were only regional positive temperature anomalies over Eurasia consistent with the footprint of AO on temperature (Quadrelli and Wallace, 2004).

[INSERT FIGURE 10.18 HERE]
Figure 10.18: Near surface (1000 hPa) air temperature anomaly multiyear composites (°C) for 2001–2010. Anomalies are relative to 1968–1996 mean and show an Arctic amplification of recent air temperatures. Data are from the NCEP–NCAR Reanalysis through the NOAA/Earth Systems Research Laboratory, generated online at www.cdc.noaa.gov.

There is still considerable discussion of the warm temperature anomalies that occurred in the Arctic in the 1920s and 1930s (Hegerl et al., 2007a; Ahlmann 1948; Veryard 1963). The early 20th century warm period, while reflected in the hemispheric average air temperature record (Brohan et al., 2006), did not appear consistently in the mid-latitudes nor on the Pacific side of the Arctic (Johannessen et al., 2004; Wood and Overland, 2010). (Polyakov et al., 2003) argued that the Arctic air temperature records reflected a natural cycle of about 50–80 years. However, (Bengtsson et al., 2004; Wood and Overland, 2010) Grant et al. (2009) instead link the 1930s temperatures to natural variability in the North Atlantic atmospheric circulation as a single episode that was potentially sustained by ocean and sea ice processes in the Arctic and mid-latitude Atlantic.

Another recent Arctic surprise was emergence of strong meridional atmospheric circulation in the winter 2009-2010 and the beginning of winter 2010-2011, which allowed cold air to advect southward into the eastern North America and Asia, and northern Europe (Cattiaux et al., 2010; L'Heureux et al., 2010; Seager et al., 2010). The NAO index for December 2009 to February 2010 was the most negative value in 145 years of data (www.cgd.ucar.edu/cas/jhurrell/indices.html). The corresponding AO index was also strongly negative indicating a breakdown of the climatological polar vortex. In fact for winter 2009-2010 the 850 mb geopotential height field over the central Arctic had a local maximum compared to the normal minimum associated with an established polar vortex. Warmer Arctic air in autumn is less dense and increases the geopotential thickness between constant pressure surfaces, thus working against the stability of the polar vortex (Overland and Wang, 2010; Schweiger et al., 2009; Serreze et al., 2009). There are also suggested Arctic-subarctic teleconnections from model results (Budikova, 2009; Deser et al., 2010b; Kumar et al., 2010; Petoukhov and Semenov, 2010; Seierstad and Bader, 2009; Singarayer et al., 2006; Sokolova et al., 2007).

A final comment is due with regard to the paradox of only minor sea ice changes near Antarctica in previous decades versus the substantial changes in the Arctic. Sea ice extent across the Southern Hemisphere over the year as a whole increased 1.0% per decade from 1978–2006 with the largest increase in the Ross Sea during the autumn (Comiso and Nishio, 2008; Turner et al., 2009). The bulk of the Antarctic has experienced little change in surface temperature over the last 50 years, although a slight cooling has been evident around the coast of East Antarctica since about 1980. The exception is the Antarctic Peninsula, where there has been warming (Steig et al., 2009; Turner and Overland, 2009). Many of the different changes observed between the two polar regions can be attributed to topographic factors and land/sea distribution. The Antarctic ozone hole may have had an influence on the circulation of the ocean and atmosphere, isolating the continent and increasing the westerly winds over the Southern Ocean, especially during the summer and winter. Because of a southward shift in the tropospheric jet, the ozone hole has been proposed a possible contributor to warming over the Antarctic Peninsula, cooling over the high plateau, increases in sea ice area averaged around Antarctica, and warming of the subsurface Southern Ocean at depths up to several hundred meters (WMO,

2011) (Goosse et al., 2009). However, recent work (Sigmond and Fyfe, 2010; Steig et al., 2009) take issue with the links between Antarctic ozone, circulation, and sea ice changes. Instead, in these works, regional changes in atmospheric circulation and associated changes in sea surface temperature are required to explain the enhanced warming in West Antarctica. Sigmond and Fyfe (2010) simulate an increase in Antarctic sea ice in response to stratospheric ozone depletion.

10.5.2 Ice Sheets and Ice Shelves, and Glaciers

[PLACEHOLDER FOR FIRST ORDER DRAFT]

10.5.2.1 Greenland and Antarctic Ice Sheet

The Greenland and Antarctic Ice Sheets are important to regional and global climate because along with other cryospheric elements such as sea ice and permafrost may cause an amplification of the surface warming and irreversible changes (HANSEN and LEBEDEFF, 1987). These two ice sheets are also important contributors to sea-level rise (Section13.X, PLACEHOLDER FOR FIRST ORDER DRAFT).

West Greenland climate in 2010 was marked by record-setting high air temperatures, ice loss by melting, and marine-terminating glacier area loss (www.arctic.noaa.gov/reportcard/greenland.html). In Nuuk (64.2°N along Greenland's west coast) temperatures in summer, spring, and winter were the warmest since record keeping began in 1873. A combination of a warm and dry 2009–2010 winter and the very warm summer resulted in the highest melt rates since at 1958 and an area and duration of ice sheet melting that was above any previous year on record since at least 1978 (Fettweis et al., 2011). The largest recorded glacier area loss observed in Greenland occurred at Petermann Glacier. The annual rate of area loss in marine-terminating glaciers was 3.4 times that of the previous 8 years, when regular observations became available. There is now clear evidence that the ice area loss rate of the past decade is greater than loss rates pre-2000. Greenland meteorological and ice data fits the conceptual model of a continued response to a slow rise in temperatures (Mernild et al., 2009) combined with a 2010 major melt of the surface ice sheet in response to these record temperatures. The 2010 record temperatures at least during the winter part of the year were in part due to near record negative extremes the AO and NAO climate patterns (L'Heureux et al., 2010). These results and the results from AOGCM simulations of Greenland surface melt in AR4 and since then (2007; Mernild et al., 2009) suggest that the surface mass balance of the Greenland is negative and consistent with climate change.

Attribution of the short term increases in surface melt and mass loss anthropogenic forcing is difficult because these changes are most likely started by a combination of slow increases in mean temperatures over a number of years and through extreme weather events. Ice loss or changes in glacial hydrology can remain for several years even though weather in subsequent years returns to more variable conditions. This is certainly true for the continued summer sea ice minimum in the central Arctic following the summer 2007 southerly wind event (Wang et al., 2009a), and initiation may be true for Greenland in 2010. Warm winter temperatures results in less heat required to raise ice temperatures to the melting point. Under these conditions, melt onset occurs earlier than normal and the snow cover duration is shorter. Mass loss and melt is also occurring in Greenland through the intrusion of warm water into the major glaciers such as Jacobshaven Glacier (Holland et al., 2008; Walker et al., 2009).

Antarctica also has long terms trends in its surface temperature with significant variations in these trends depending on the strength of the SAM and the impacts of ozone depletion in the stratosphere (Steig et al., 2009; Thompson and Solomon, 2002; Turner and Overland, 2009). Simulations using atmospheric general circulation models with observed surface boundary conditions over the last 50 years suggest that the contributions of from both ozone and rising greenhouse gases. It was concluded that the pattern of mean surface temperature trends in both West and East Antarctica are positive for 1957–2006, and this warming trend is difficult to explain without the radiative forcing associated with increasing greenhouse-gas concentrations (Steig et al., 2009). Satellite altimetry observations show that both Antarctic and Greenland are loosing mass. These estimates of mass losses have increased since 2000 and all show that the greatest mass losses are being lost at the edges and a tendency to increase in the interior (Section 4.X, PLACEHOLDER FOR FIRST ORDER DRAFT). Taken together, the ice sheets of Greenland and Antarctica are shrinking. Slight thickening in inland Greenland is more than compensated for by thinning near the coast (Section 4.X). Warming is expected to increase low-altitude melting and high-altitude precipitation in Greenland; altimetry data suggest that the former effect is dominant. However, because some portions of ice sheets respond only slowly to climate changes, past forcing may be influencing ongoing changes, complicating attribution of recent trends (Section 4.Y).

10.5.2.2 Mountain Glaciers

For the “modern” climate after the last maximum extent of mountain glaciers, known as “Little Ice Age” extent, there is reliable evidence from physical and/or statistical approaches that coupled atmosphere-ocean interactions (i.e., internal climate variability), such as ENSO, NAO, AMO, and PDO govern interannual to decadal variations in glacier mass (Hodge et al., 1998; Huss et al., 2010; Nesje et al., 2000; Vuille et al., 2008) and in length(Chinn et al., 2005). Regarding long-term changes in mountain glaciers during the modern climate fewer studies are available which allow careful evaluation of the long term trends of mass loss by glaciers and the direct attribution of this mass loss to climate change (Molg and Kaser, 2011). Reichert et al. (Reichert et al., 2002) show for two sample sites at mid and high latitude that natural climate variability over multiple millennia would not result in such short glacier lengths as observed in the 20th century. For a sample site at low latitude (Molg et al., 2009) (and refs. therein) found a close relation of glacier mass loss to the atmosphere-ocean circulation in the Indian Ocean since the late 19th century, observations of which could be reproduced by a global climate model with external forcing and agree with a regional response to global warming. However, these findings do not necessarily mean that the dominant local atmospheric driver (the direct cause of glacier mass loss) is warming (Molg et al., 2009). Based on a suite of methods (observations, multi-century global climate model runs, atmospheric modelling, glacier models, and proxy data) – conclude that mountain glacier shrinkage during the modern climate cannot be explained by natural internal variability and requires external climate forcing.

10.5.3 Snow Cover and Permafrost

Satellite measurement of annual snow cover extend over the Northern Hemisphere has substantially decreased in 1972–2006, with large decreases in summer and spring and small increase in winter (Dery and Brown, 2007). This seasonality in snow cover trend is also consistent with those obtained from in-situ measurement (Kitaev and Kislov, 2008; Kitaev et al., 2007) over the Northern Eurasia. Pan-Arctic snow melt has started about 0.5 day/year earlier, and snow cover duration has also decreased (Brown and Mote, 2009; Choi et al., 2010). Trends in snow cover and its duration have complicated responses to changes in both temperature and precipitation. Observed trends in snow cover and its duration for the satellite observation period are consistent with expected snow cover response to warming as simulated by a snowpack model, both in terms of overall pattern of changes and regions that are most sensitive to warming. They are also consistent with the spatial pattern of significant snow cover reduction simulated by the CMIP3 models 20th century simulations (Brown and Mote, 2009). The observed snow cover change is also consistent with simulations conducted with the IAP RAS Climate model under observed anthropogenic and natural forcing (Eliseev et al., 2009). A few formal detection and attribution study have also indicated anthropogenic influence on snow cover. Ma et al. (2011, a placeholder as the paper is still not published yet) detects anthropogenic signal in the changes in snow-cover extend over both the American and Eurasian continents. Pierce et al. (2008) detected anthropogenic influence in winter snowpack in Western United States over the 1950-99. They define snowpack as ratio of 1 April snow water equivalent (SWE) to water-year-to-date precipitation (*P*). They found that the observations and anthropogenically forced models have greater SWE/*P* reductions than can be explained by natural internal climate variability alone and that model-estimated effects of changes in solar and volcanic forcing likewise do not explain the SWE/*P* reductions.

Wide spread permafrost degradation and warming appear to be in part a response to atmospheric warming. The warming trend of permafrost temperature increase from 0.022^{o}C yr^{-1} to 0.034°C yr^{-1} in Russia during 1966–2005 reflects a similar magnitude of warming trend in surface air temperature (Pavlov and Malkova, 2010). In Qinghai-Tibet Plateau, altitudinal permafrost boundary has lowered up by 25 m in the north during last decades and by 50 to 80 m in the south (Cheng and Wu, 2007). Arzhanov (2007) used the ERA-40 reanalysis to drive a permafrost model and found that the simulated values of active layer depth are in agreement with measurement of active layer depth over the pan-Arctic. Changes in snow cover also play a critical role (Osterkamp, 2005; Zhang et al., 2005) in permafrost degradation. Trends towards earlier snowfall in autumn and thicker snow cover during winter have resulted in stronger snow insulation effect, and as a result a much warmer permafrost temperature than air temperature in the Arctic. The lengthening of the thaw season and increases in summer air temperature have resulted in changes in active layer thickness.

10.6 Extremes

[PLACEHOLDER FOR FIRST ORDER DRAFT]

10.6.1 Attribution of Changes in Frequency/Occurrence and Intensity of Extremes

[PLACEHOLDER FOR FIRST ORDER DRAFT]

10.6.1.1 Temperature

Observed changes in temperature extremes (Alexander et al., 2006) are consistent with changes expected with global warming. A warming of mean temperatures is expected to lead to an increased prevalence of warm temperature extremes and a reduction in cold temperature extremes although changes in variability can exacerbate or countermand this tendency. Nevertheless there are greater challenges in detection and attribution of extreme than of mean temperatures. There are fewer observations of sufficient quality and homogeneity at daily and sub-daily timescales than at monthly timescales. Also, extremes, by their nature, are rarely observed and therefore sampling becomes an issue. Statistical techniques have been used in some studies to extrapolate distributions and deduce underlying changes in rare events.

Examining rare but not particularly extreme temperatures, such as temperatures that would be expected to be exceeded one year in ten, avoids some of the challenges associated with more extreme temperatures. When averaged over sub-continental scale regions in the Northern hemisphere, Jones et al. (2008) showed that there has been a rapid increase in the frequency of such unusually warm summer temperatures and Stott et al. (2011) generalized this result to show that this was also the case for all four seasons for many regions worldwide. By carrying out an optimal detection analysis directly on the probability of exceeding very warm regional temperatures they showed that the observed rapid increases in frequencies of very warm temperatures seen in many regions could be directly attributed to human influence. This study serves as an example of a single-step attribution analysis (see Hegerl et al. (2010)), in contrast with multi-step attribution studies that indirectly attribute the changes in probabilities of temperatures exceeding extreme thresholds based on attribution of mean temperatures (e.g., Stott et al. (2004b); see 10.6.2).

Qualitative comparison of observed and modeled trends in indices of extreme temperatures shows good agreement. Alexander and Arblaster (2009) compared trends in observed and 9 GCMs modeled temperature extremes over Australia. They found that trends in 'warm nights' could only be reproduced by a coupled model that included anthropogenic forcings. Meehl et al. (2007a), compared observed changes in the number of frost days, the length of growing season, the number of warm nights, and the heatwave intensity for the 2nd half of the 20th century over the U.S. with those simulated in a nine member multi-model ensemble simulation. They showed that changes in those temperature indices are consistent with model expected changes. The decrease of frost days, an increase in growing season length, and an increase in heatwave intensity all show similar changes in 20th century experiments that combine anthropogenic and natural forcings, although the relative contributions of each are unclear. Results from two global coupled climate models (PCM and CCSM3) with separate anthropogenic and natural forcing runs indicate that the observed changes are simulated with anthropogenic forcings, but not with natural forcings (even though there are some differences in the details of the forcings).

Quantitative detection and attribution studies have also shown evidence for anthropogenic influence on temperature extremes, at both global and regional scales. Previous detection of an anthropogenic influence on extremely warm nights globally (Christidis et al., 2005), based on analysis of a single climate model and a daily temperature dataset (Caesar et al., 2006) of the warmest daily minimum temperature of the year, is now supported by simulations using other models (Christidis et al., 2011b; Zwiers et al., 2011). Morak et al. (2011) analysed the sub-continental scale regions over land defined by Giorgi et al. (2001) and found that over many of these regions (but not all) the number of warm nights (as defined by the TN90 index, number of days exceeding the 90th percentile of daily minimum temperatures; Alexander et al., 2006) show detectable changes over the second half of the 20th century that are consistent with the expected changes due to greenhouse gas increases. They also found changes consistent with anthropogenic greenhouse gas increases when the data were analysed over the globe as a whole. As the trend in TN90 can be well predicted based on the correlation of its variability with mean temperature variability, Morak et al. (2011) conclude that the detectable changes are probably in part due to greenhouse gas increases.

An analysis of extremely cold days and nights (TN10, TX10) has detected a human influence on these indices (Christidis et al., 2005) although with evidence that the model used in that study underestimates observed changes. However this study did not detect human influence on extremely hot days and at the time of AR4 the evidence was lacking for the anthropogenic fingerprint of human influence having emerged significantly in the observed record of extremely warm days.

Since AR4, new studies, using extreme value theory to better estimate changes in the extreme tails of distributions have been carried out. Zwiers et al. (2011) compare observed annual temperature extremes including annual maximum daily maximum and minimum temperatures, and annual minimum daily maximum and minimum temperatures with those simulated responses to anthropogenic (ANT) forcing or anthropogenic and natural external forcings combined (ALL) by seven GCMs. They fit probability distributions to the observed extreme temperatures with location parameters as linear functions of signals obtained from the model simulation, and found that both anthropogenic influence and combined influence of anthropogenic and natural forcing can be detected in all four extreme temperature variables at the global scale over the land, and also regionally over many large land areas (Figure 10.19).

[INSERT FIGURE 10.19 HERE]

Figure 10.19: Scaling factors and their 90% confidence intervals for annual extreme temperatures for ALL and ANT forcings for period 1961–2000. Red, green, blue, pink error bars are for TNn, TXn, TNx, and TXx respectively. Detection is claimed at the 10% significance level if the 90% confidence interval of a scaling factor is above zero line (Zwiers et al., 2011).

New evidence that human influence on extremes is detected not just for warm night and cold days and nights but also for hot days is additionally supported by an optimal detection analysis on the HadGHCND daily temperature dataset (Caesar et al., 2006) and the HadCM3 model by Christidis et al. (2011a) who analyse the time-varying location parameter introduced by (Brown et al., 2008), computing its values at each grid point by fitting point-process extreme value distributions to anomalies of daily maximum temperature. They find that the effects of anthropogenic forcings on extremely warm daily temperatures are detected both in a single fingerprint analysis and when the effects of natural forcings are also included in a two fingerprint analysis. Christidis et al. (2011a) find that their measure of extremes, which uses all daily maxima in a year to estimate the extreme tails of the distribution of daily maxima, has a higher signal to noise ratio than the simple index of the hottest maximum temperature of the year, which, with only one datapoint a year, is relatively poorly sampled.

10.6.1.2 Precipitation

The observed changes in heavy precipitation appear to be consistent with the expected response to anthropogenic forcing as a result of an enhanced moisture content in the atmosphere but a direct cause-and-effect relationship between changes in external forcing and extreme precipitation had not been established at the time of the AR4. As a result, the AR4 concluded only that it is more likely than not that anthropogenic influence had contributed to a global trend towards increases in the frequency of heavy precipitation events over the second half of the 20th century (Hegerl et al., 2007).

New research since the AR4 provides more evidence of anthropogenic influence on various aspects of the global hydrological cycle (Stott et al., 2010; see also Section 10.3.2), which is directly relevant to extreme precipitation changes. An anthropogenic influence on atmospheric moisture content has been detected (see Section 10.3.2). A higher moisture content in the atmosphere may lead to stronger extreme precipitation. Observational analysis shows that winter season maximum daily precipitation in North America has statistically significant positive corrections with atmospheric moisture (Wang and Zhang, 2008). Model projections of extreme winter precipitation under global warming show similar behaviour (Gutowski et al., 2008).The thermodynamic constraint based on Clausius-Clapeyron relation is now better understood. The thermodynamic constraint is a good predictor for extreme precipitation changes in a warmer world in regions where the circulation changes little (Pall et al., 2007) but it may not be a good predictor in regions with circulation changes such as mid- to higher-latitudes (Meehl et al., 2005a) and the tropics (Emori and Brown, 2005). The rate of changes in precipitation extremes with temperature also depends on other factors such as changes in the moist-adiabatic temperature lapse rate, in the upward velocity, and in the temperature when precipitation extremes occur (O'Gorman and Schneider, 2009a, 2009b; Sugiyama et al., 2010). In parts of the tropics, increases in precipitation extremes could exceed moisture content increases due to changes in vertical motion (Shiogama et al., 2010). Elsewhere, dynamical changes could lead to precipitation extremes less than expected from simple thermodynamics arguments which may explain why there have not been increases in precipitation extremes everywhere, although a low signal to noise ratio may also play a role. Analysis of daily precipitation from the Special Sensor Microwave Imager (SSM/I) over the tropical oceans shows a direct link between rainfall extremes and temperature: heavy rainfall events increase during warm periods (El Niño) and decrease during cold periods (Allan and Soden, 2008). However, the observed amplification of rainfall extremes is larger than that predicted by climate models (Allan and Soden, 2008), due possibly to widely varying changes in upward velocities associated with precipitation extremes (O'Gorman and Schneider, 2008). Evidence from measurements in the Netherlands seems to suggest that hourly precipitation extremes may in some cases increase more strongly with temperature (twice as fast) than would be expected from the Clausius-Clapeyron relationship alone (Lenderink and Van Meijgaard, 2008), though this is still under debate (Haerter and Berg, 2009; Lenderink and Van Meijgaard, 2009).

Quantitative detection and attribution studies have also shown evidence for anthropogenic influence on extreme precipitation. Min et al. (2011) used an optimal detection method to compare observed and multi-model simulated extreme precipitation. They found that the human-induced increase in greenhouse gases has contributed to the observed intensification of heavy precipitation events over large Northern Hemispheric land areas during the latter half of the 20th century (see Figure 10.20). Detection of anthropogenic influence at smaller spatial scale is more difficult due to increased noise level. Fowler and Wilby (2010) suggested that there may only be 50% chance of detecting anthropogenic influence on UK extreme precipitation in winter by now, but a very small likelihood to detect it in other seasons now. An event attribution analysis suggested that anthropogenic influence has increased the likelihood of the 2000 August floods in UK (Pall et al., 2011; see also Section 10.6.2)

[INSERT FIGURE 10.20 HERE]
Figure 10.20: Time series of five-year mean area-averaged extreme precipitation indices anomalies for 1-day (RX1D, left) and 5-day (RX5D, right) precipitation amounts over Northern Hemisphere land during 1951–1999. Model simulations with anthropogenic (ANT, upper) forcing; model simulations with anthropogenic plus natural (ALL, lower) forcing. Black solid lines are observations and dashed lines represent multi-model means. Coloured lines indicate results for individual model averages (see Supplementary Table 1 of Min et al. (2011) for the list of climate model simulations and Supplementary Figure 2 of Min et al. (2011) for time series of individual simulations). Annual extremes of 1-day and 5-day accumulations were fitted to the Generalized Extreme Value distribution which was then inverted to map the extremes onto a 0–100% probability scale. Each time series is represented as anomalies with respect to its 1951–1999 mean (Min et al. 2011).

10.6.1.3 Drought

The AR4 (Hegerl et al., 2007b) concluded that it is *more likely than not* that anthropogenic influence has contributed to the increase in the droughts observed in the second half of the 20th century. This assessment was based on multiple lines of evidence including a detection study which identified an anthropogenic fingerprint in a global PDSI data set with high significance (Burke et al., 2006).The IPCC-SREX (Nicholls et al., 2011) gives essentially the same assessment stating that there is *medium confidence* (see also Section 3.1.5) that anthropogenic influence has contributed to the increase in the droughts observed in the second half of the 20th century.

There is now a better understanding of the potential role of land-atmosphere feedbacks versus SST forcing for droughts (Schubert et al., 2008) as well as of potential impacts of land use changes (Deo et al., 2009), but large uncertainties remain in the field of land surface modeling and land-atmosphere interactions, in part due to lack of observations (Seneviratne et al., 2010) and inter-model discrepancies (e.g., Pitman, 2009). Modelling studies show that U.S. drought response to SST variability is consistent with observations

(Schubert, 2009). Trends in drought are also consistent with trends in global precipitation and temperature, and the latter two are consistent with expected responses to anthropogenic forcing (Hegerl et al., 2007b; Zhang et al., 2007b). The change in the pattern of global precipitation in the observations and in model simulations are also consistent with theoretical understanding of hydrological response to global warming that wet regions become wetter and dry regions drier in a warming world (Held and Soden, 2006b). For soil moisture and streamflow drought it has been suggested that the stomatal "antitranspirant" responses of plants to rising atmospheric CO_2 may lead to a decrease in evapotranspiration (Gedney et al., 2006). This could mean that increasing CO_2 levels alleviate soil moisture and streamflow drought, but this result is still debated. These studies were assessed by the IPCC SREX report (Nicholls et al., 2011, in preparation) who concluded that though these new studies have improved the understanding of the mechanisms leading to drought, there is still not enough evidence to alter the AR4 assessment, in particular given the associated observational data issues (Section 3.2.1), that there is *medium confidence* (see also Section 3.1.5) that anthropogenic influence has contributed to the increase in the droughts observed in the second half of the 20th century.

10.6.1.4 Storms

The storm tracks in the northern and southern hemispheres have been observed to shift poleward. The AR4 concluded that such changes that are associated with changes in the Northern and Southern Annular Modes, sea level pressure decreases over the poles but increases at mid latitudes, are likely related in part to human activity. However, an anthropogenic influence on extratropical cyclones was not formally detected, owing to large internal variability and problems due to changes in observing systems (Hegerl et al., 2007b).

Anthropogenic influence on the sea level pressure distribution has been detected in individual seasons (Giannini et al., 2003; Gillett and Stott, 2009; Gillett et al., 2005; Wang et al., 2009b) (Wang et al., 2009b) detected influence of anthropogenic and natural forcings in the atmospheric storminess represented by geostrophic wind energy and ocean wave heights, with the effect of external forcings being strongest in the winter hemisphere. However, they also found that the climate models generally simulate smaller changes than observed and also appear to under-estimate the internal variability, reducing the robustness of their detection results. New idealized studies have found that storm track changes are closely related to changes in SST. An uniform increase in SST may lead to reduced cyclone intensity or number of cyclones and a poleward shift in the stormtrack. Strengthened SST gradients near the subtropical jet may lead to a meridional shift in the stormtrack either towards the poles or the equator depending on the location of the SST gradient change (Brayshaw et al., 2008; Kodama and Iwasaki, 2009; Semmler et al., 2008). The average global cyclone activity is expected to change little under moderate greenhouse gas forcing (Bengtsson and Hodges, 2009; O'Gorman and Schneider, 2008).

10.6.1.5 Tropic Cyclones

The AR4 concluded that "it is more likely than not that anthropogenic influence has contributed to increases in the frequency of the most intense tropical cyclones" (Hegerl et al., 2007b), but it noted significant deficiencies in theoretical understanding of tropical cyclones, their modelling and their long-term monitoring. Contributing to evidence that support the AR4 assessment was the strong correlation between the Power Dissipation Index (PDI, an index of the destructiveness of tropical cyclones) and tropical Atlantic SSTs (Elsner, 2006; Emanuel, 2005) and the association between Atlantic warming and the increase in global temperatures (Mann and Emanuel, 2006; Trenberth and Shea, 2006). While the US CCSP (Kunkel et al., 2008) supported the view that there was a link between anthropogenic influence and increases in the frequency of the most intense tropical cyclones some recent evidence casts doubt on such a link (Knutson, 2010) (Nicholls et al., 2011, in preparation).

SSTs in the tropics have increased and a significant part of this increase has been attributed to anthropogenic emissions of greenhouse gases (Gillett et al., 2008a; Karoly and Wu, 2005; Knutson et al., 2006; Santer, 2006). As SST plays a significant role in many aspects of tropical cyclones such as their formation, tracks, and intensity, an anthropogenic induced SST increase may be expected to also lead to changes in tropical cyclone activities. However, the mechanisms linking anthropogenic induced tropical SST increase and changes in tropical cyclone activities are still poorly understood. For example, there is a growing body of evidence that the minimum SST threshold for tropical cyclogenesis increases at about the same rate as the

SST increase due solely to greenhouse gases forcing (Bengtsson et al., 2007; Dutton et al., 2000; Johnson and Xie, 2010; Knutson et al., 2008; Ryan et al., 1992; Yoshimura et al., 2006), which suggests that anthropogenic SST increase, by itself, may not necessarily lead to increased tropical cyclone frequency. GCM simulations seem to support this as tropical cyclone frequency is not projected to increase into the future. Similarly, there is a theoretical expectation that increases in potential intensity will lead to stronger tropical cyclones (Elsner et al., 2008; Emanuel, 2000; Wing et al., 2007) and observations demonstrate a strong positive correlation between SST and the potential intensity. However, there is a growing body of research suggesting that regional potential intensity is controlled by the difference between regional SSTs and spatially averaged SSTs in the tropics (Ramsay and Sobel, 2011; Vecchi and Soden, 2007; Xie et al., 2010) rather than simply the SSTs underlying tropical cyclones. Since anthropogenic forcing is not expected to lead to increasingly large SST gradients (Xie et al., 2010), the implication of recent research is that there is not a clearly understood physical link between anthropogenic induced SST increases and the potential formation of increasingly strong tropical cyclones.

Given such uncertainties in the relationships between tropical cyclones and internal climate variability, including factors related to the SST distribution, such as vertical wind shear, Knutson et al. (2010) concluded that these uncertainties "reduce our ability to confidently attribute observed intensity changes to greenhouse warming". The IPCC SREX report (Nicholls et al., 2011, in preparation) concluded that there is low confidence for the attribution of any detectable changes in tropical cyclone activity to anthropogenic influences.

10.6.2 Attribution of Observed Weather and Climate Events

Since many of the impacts of climate change are likely to manifest themselves through extreme weather, there is increasing interest in quantifying the role of human and other external influences on climate in specific weather events. This presents particular challenges for both science and the communication of results to policy-makers and the public. It has so far been attempted for a relatively small number of specific events, including the UK floods of autumn 2000 (Kay et al., 2011; Pall et al., 2011), the European summer heat-wave of 2003 (Feudale and Shukla, 2007; Fischer et al., 2007; Schär et al., 2004; Stott et al., 2004a; Sutton and Hodson, 2005), the cooling over North America in 2008 (Perlwitz et al., 2009) and the Russian heat-wave of 2010 (Dole et al., 2011).

Many of the most extreme and damaging weather events occur because a self-reinforcing process amplifies an initial weather anomaly. This has two important implications. First, predicting the statistics of such extreme weather events by extrapolating the statistics of less extreme events requires caution, since the governing physical processes may change in these most extreme cases. Second, it is generally impossible in principle to say how much smaller an event would have been in the absence of human influence. Instead, it is necessary to consider the event as a single, self-reinforcing whole, and ask how external drivers contributed to the probability of that event occurring (Allen, 2003; Christidis et al., 2011b; Pall et al., 2011; Stone et al., 2009; Stone and Allen, 2005b; Stott et al., 2004b).

Much of the informal discussion of the role of human influence in specific extreme weather events focuses on the question of whether an event may have a precedent in the early instrumental or paleo-climate record before a substantial human influence on climate occurred. This is generally beside the point, because no regional weather event has yet been reported for which there was only a negligible chance of it occurring in the absence of human influence. Schär et al. (2004) assigned an extremely long return-time to the temperatures observed in summer 2003 under pre-industrial conditions, but also noted that this result was sensitive to assumption of a Gaussian distribution of summer temperatures. Fischer et al. (2007) show how, in a regional climate modeling study, warm temperatures in central Europe in the summer of 2003 were amplified by dry soil-moisture conditions. This is an example of a self-reinforcing process which makes estimated return-times based on the distribution of normal summer temperatures irrelevant.

Quantifying the absolute probability of an event occurring in a hypothetical world without human influence on climate is necessarily very uncertain: hence studies focus on quantifying relative probabilities, or specifically the Fraction Attributable Risk (FAR), where $FAR=1-P0/P1$, $P0$ being the probability of an event occurring in the absence of human influence on climate, and $P1$ the corresponding probability in a world in which human influence is included.

For events that occur relatively frequently, or events for which statistics can be aggregated over a large number of independent locations, it may be possible to identify trends in occurrence-frequency that are attributable to human influence on climate through a single-step procedure, comparing observed and modeled changes in occurrence-frequency. This is the approach taken, for example, by Min et al. (2011) and Stott et al. (2011) and discussed in the Section 10.6.1.

For events with return-times of the same order as the time-scale over which the signal of human influence is emerging (30–50 years, meaning cases in which P0 and P1 are of the order of a few percent or less in any given year), single-step attribution is impossible in principle: it is impossible to observe a change in return-time taking place over a time-scale that is comparable to the return-time itself. For these events, attribution is necessarily a multi-step procedure. Either a trend in occurrence-frequency of more frequent events may be attributed to human influence and a statistical extrapolation model then used to assess the implications for the extreme event in question; or an attributable trend is identified in some other variable entirely, such as surface temperature, and a physically-based weather model is used to assess the implications. Neither approach is free of assumptions: no weather model is perfect, but statistical extrapolation may also be misleading for reasons given above.

Pall et al. (2011) provide a demonstration of multi-step attribution using a physically-based model, applied to the floods that occurred in the UK in the autumn of 2000. The immediate cause of these floods was exceptional precipitation, this being the wettest autumn to have occurred in England and Wales since records began. To assess the contribution of the anthropogenic increase in greenhouse gases to the risk of these floods, the period April 2000 to March 2001 was simulated several thousand times using a seasonal-forecast-resolution atmospheric model with realistic atmospheric composition, sea surface temperature and sea ice boundary conditions imposed. This ensemble was then repeated with both composition and surface temperatures modified to simulate conditions that would have occurred had there been no anthropogenic increase in greenhouse gases since 1900. The change in surface temperatures was estimated using a conventional detection and attribution analysis using response-patterns predicted by four different coupled models, constrained by observations over the 20th century, allowing for uncertainty in response amplitude. Simulated daily precipitation from these two ensembles was fed into an empirical rainfall-runoff model and severe daily England and Wales runoff used as a proxy for flood risk.

Results are shown in Figure 10.21 Panel a, which shows the distribution of simulated runoff events in the realistic autumn 2000 ensemble in blue, and in the range of possible “climates that might have been” in other colours. Including the influence of anthropogenic greenhouse warming increases flood risk at the threshold relevant to autumn 2000 by around a factor of two in the majority of cases, but with a broad range of uncertainty: in 10% of cases the increase in risk is less than 20%.

Pall et al.’s conclusions pertained to the particular flood diagnostic they considered. Kay et al. (2011), analysing the same ensembles but using a more sophisticated hydrological model with explicit representation of individual catchments found that greenhouse gas increase has more likely than not increase flood risk in the October to December period, with best-estimate increases also around a factor of two for daily runoff. The increased noise resulting from smaller catchments and the impact of re-evaporation of rainfall, however, increased uncertainty to the extent that the null-hypothesis of no attributable increase in risk could no longer be rejected at the 10% level for any individual catchment.

More significantly, Kay et al. also showed that the change in flood risk over the entire October to March period was substantially lower, due to a reduction in the risk of snow-melt-induced flooding in spring, such as occurred in 1947, compensating for the increased risk of precipitation-induced flooding in autumn (see Figure 10.21, Panel b). This illustrates an important general point: even if a particular flood event may have been made more likely by human influence on climate, there is no certainty that all kinds of flood events have been made more likely.

Dole et al. (2011) take a different approach to event attribution, analysing causal factors underlying the Russian heatwave of 2010 through a combination of observational analysis and modeling, and find no evidence for a substantial role for human influence in that event. First, the observations show no evidence of any trend in occurrence-frequency of hot summers in central Russia, with mean summer temperatures in that region actually displaying a (statistically insignificant) cooling trend, in contrast to the case for central and southern European summer temperatures (Fischer and Schär, 2010; Stott et al., 2004a). Members of the CMIP3 multi-model ensemble likewise show no evidence of a trend towards warming summers in central Russia.

In common with many mid-latitude heatwaves, the 2010 Russian event was associated with a strong blocking atmospheric flow anomaly. Dole et al. find atmospheric models are capable of reproducing this blocking, albeit with somewhat weaker amplitude than observed, but only when initialised with late June conditions when the blocking pattern was already established: even the complete 2010 boundary conditions are insufficient to increase the probability of a prolonged blocking event in central Russia, in contrast again to the situation in Europe in 2003 (Feudale and Shukla, 2010).

Atmospheric flow anomalies, notably the Scandinavia pattern, also played a substantial role in the autumn 2000 floods in the UK (Blackburn and Hoskins, 2011, in preparation), although Pall et al. (2011) argue thermodynamic mechanisms were primarily responsible for the increase in risk between their ensembles. Evidence of a causal link between rising greenhouse gases and the occurrence or persistence of atmospheric flow anomalies would have a very substantial impact on any event attribution claims, since anomalous atmospheric flow is often the principal immediate cause of extreme weather (Perlwitz et al., 2009).

The science of event attribution is still confined to isolated case studies, often using a single model, but our ability to quantify the role of human influence in individual events is improving. Rising greenhouse gases may have contributed substantially to an increased risk of some events, such as precipitation-induced flooding in autumn 2000 in the UK and the European summer heat wave of 2003. They may also have decreased the risk of others, such as snow-melt-induced spring UK floods or the North American cold events such as occurred in 2008, while current evidence suggests that many other events, such as the Russian heat-wave of 2010, have not been affected either way. The comparison of the risk assessments of the European heatwave of 2003 and the Russian heatwave of 2010 illustrate that a regional attribution resulting from one region is not necessarily portable to another region even when the two regions are relatively close geographically.

[INSERT FIGURE 10.21 HERE]
Figure 10.21: Return times for precipitation-induced floods aggregated over England and Wales for conditions corresponding to October to December 2000 with boundary conditions as observed (blue) and under a range of simulations of the conditions that would have obtained in the absence of anthropogenic greenhouse warming over the 20th century – colours correspond to different AOGCMs used to define the greenhouse signal, black horizontal line to the threshold exceeded in autumn 2000 – from Pall et al. (2011). [This figure will also include a Panel b: corresponding figure for precipitation- and snow-melt-induced floods in 4 catchments across the UK for conditions corresponding to January to March 2001, from Kay et al., 2011 (in preparation). This would probably look similar to the above, but with most of the non-industrial distributions above the industrial one.]

10.7 Millennia to [Multi]Century Perspective

[PLACEHOLDER FOR FIRST ORDER DRAFT]

10.7.1 Relevance of and Challenges in Detection and Attribution Studies Prior to the Late 20th Century

Evaluating the causes of change in climate before the middle of the 20th century is important for attributing recent change as it tests understanding of the role of internal and forced natural variability at a time when the anthropogenic perturbation was probably small. Since CMIP5 simulations of the last millennium, LGM and Mid-Holocene are performed with the same or closely related climate models as those used for projections, detection and attribution of changes in the more distant past to assesses the ability of climate models to simulate past changes and the level of natural variability (Tett et al., 2007). These two periods are also a useful test of all relevant processes are included and reasonably well simulated in the models. The residual unexplained variability in records provide a very useful constraint on climate model internal variability estimates.

However, uncertainties, particularly over the period covered by indirect, or proxy, data are larger than over the instrumental period (see Chapter 5). The recording system is more spotty, and often limited to few sites that respond (indirectly) to the variable of interest, such as temperature or precipitation. (see Chapter 5). Also, it is not clear to what extent proxy data record the full extent of past variability (see Chapter 5), which is an important caveat in evaluating climate variability. Records of past radiative influences on climate are also uncertain. For example, for the last millennium solar, volcanic, greenhouse gas and land use change are potentially important (Chapter 5?). Estimates of solar forcing, particularly the solar forcing's low-frequency component over the last millennium have been revised downward compared to early estimates and the relationship of proxies such as sunspot numbers and cosmogenic isotopes is uncertain (Beer et al., 2009; Grey et al., 2010), although uncertainties remain large and there are recent larger forcing estimates (Shapiro et al., 2011). Estimates of past volcanism from ice core records from both Northern and Southern Hemispheres are relatively well established in their timing, but the magnitude of the radiative forcing of individual events is quite uncertain. It is possible that large eruptions that deposited large amounts of sulfates in ice cores had a moderated climate effect due to faster fallout associated with larger particle size (Timmreck et al., 2009), or injected water vapour (Joshi and Jones, 2009). For eruptions which cannot be identified in historical records, the location and with it the spatial pattern of forcing is uncertain. A further large uncertainty is associated with past reconstructions of land use change (Pongratz et al., 2009; Kaplan, 2011). Greenhouse gas forcing shows subtle variations that can be used to attempt to relate past CO_2 fluctuations to temperature (Frank et al., 2010). For periods further in the past, such as the Last Glacial Maximum or the Mid-Holocene, uncertainties in forcing and data are even larger.

However, uncertainties and noise in records of past forcing and climate are generally expected to be uncorrelated and thus detectable signals in response to forcing estimates, particularly at timescales that are covered by substantial samples, are unlikely to be spuriously detected. In other words, the probability of detection will be properly reflected in the uncertainty level and if the assumption of id independence between uncertainties in forcings and climate records. The most reliable detection and attribution results for the longer time horizon originate from studies that consider all relevant forcings, since despite the longer time horizon, fictitious correlations between external forcings can occur. Examples are a period of possibly elevated solar forcing that coincides with a hiatus in volcanism in the mid 18th century, and the Maunder Minimum period coinciding with extensive volcanism. In such an example, misleading results can be obtained if proper account is not taken of the range of possible forcing factors and uncertainty in records and analysis methods (Legras et al., 2010).

10.7.2 Causes of Change in Large-Scale Temperature over the past Millennium

Reconstructions of temperature changes over the past millennium are uncertain due to data limitations as well as due to uncertainties in reconstruction methods. Uncertainties in reconstruction methods can be tested by perfect model studies (Hegerl et al., 2007a; von Storch et al., 2004) , but it is quite difficult to quantify and reduce uncertainties due to data limitations except by obtaining independent records of past change, such as from boreholes, glacier based reconstructions or tree rings.

Despite the uncertainties in reconstructions of Hemispheric mean temperatures in the past, there are well-defined climatic periods in the last Millennium that are quite robust to reconstruction method and data (see Chapter 5): The early millennium started relatively warm (although the level of warmth of the medieval warm period is highly uncertain), followed by a gradual cooling peaking in the cold conditions in the late 17th and early 19th century, after which warming occurred (see Figure 5.X). This general evolution is captured by most climate model simulations of the last millennium (figure in Chapter 5?) and can be quantitatively reproduced by ensembles of climate models for relevant reconstructions from proxy data (Figure 10.22).

[INSERT FIGURE 10.22 HERE]

Figure 10.22: [REVIEWERS NOTE THAT ALL FIGURES WILL BE REDONE USING THE CMIP5 ARCHIVE AND MORE COMPLETE DATA] Role of external forcing for hemispheric (a,b) and European (c) temperature variability. **a)** Reconstructed changes in NH mean temperature (30-90N) reconstructed by Moberg et al. (2005), black compared to best fit simulation from OAGCM [NOT YET SHOWN] and an Energy Balance Model Simulation (red; highly significantly detectable). Middle panel: estimated contribution from volcanic (blue, detectable based on EBM and OAGCM), solar (detectable for EBM) and

greenhouse gas forcing (detectable based on OAGCM). The fingerprints are based on EBM simulations [SHOWN] and GCM simulations [NOT YET SHOWN]. Bottom shows the unexplained residual; figure after Hegerl et al., 2007b. **b)** shows an analysis focusing on the Northern Hemispheric temperature difference between the coldest 30-year period during the Little Ice Age 1550–1750 and the warmest 30-year period during the Medieval Warm Period (900–1300) from reconstructions (green symbols, see Jansen et al., 2007) compared to climate model simulations without forcing (black), all forcings included using present best estimate solar forcing (red) and the same using high solar forcing estimates (blue; from Jungclaus et al., 2010). Panel **c)** shows a reconstruction of European mean winter temperature (Luterbacher et al., 2004) compared to a best estimate of the fingerprint for all forcings combined (detectable at the 10% level, uncertainty range shown grey) from OAGCMs, and the detectable contribution to the long-term evolution by greenhouse gas plus aerosol forcing from an Energy Balance Model (red). From Hegerl et al. (2011).

The AR4 concluded that 'a substantial fraction of the reconstructed Northern Hemispheric inter-decadal temperature is very likely attributable to natural external forcing'. The literature since the AR4, and the availability of more simulations of the last millennium with more complete forcing and more sophisticated models support these conclusions. Since the AR4, AOGCM simulations with individual forcing with coupled climate models are available. Results from new modelling studies (Jungclaus et al., 2010; Schurer et al., 2011, in preparation) support results from prior work (Hegerl et al., 2007a; Tett et al., 2007; Yoshimori and Broccoli, 2008; Yoshimori et al., 2006) that found that external forcing plays a key role over the last millennium. (Jungclaus et al., 2010) demonstrate that low-frequency variability is significantly stronger in simulations of the last millennium than in control simulations for a large fraction of the millennium. Volcanic forcing plays an important role in explaining past cool episodes, for example, in the late 17th and early 19th century in their model simulations, consistent with detection and attribution studies, and is key to reproducing the reconstructed temperature evolution (Jungclaus et al., 2010; Schurer et al., 2011, in preparation). Jungclaus et al. (2009) compare different reconstructions of cooling from the Medieval Warm Period into the Little Ice Age (Figure 10.22) and find that their model can reproduce the changes between both periods within data and forcing uncertainty. Higher than present best estimate solar forcing is needed to explain the change between both periods for reconstructions with larger variance. Both model simulations (Frank et al., 2010; Jungclaus et al., 2010) and detection and attribution studies (Hegerl et al., 2007a) suggest that the small drop in CO_2 during the little ice age may have contributed to the cool conditions during the 16th and 17th century.

Since the AR4, more estimates of land use forcing as well as discussion of its importance is available. Goosse et al. (2010) estimates that while the total external forcing between the cold conditions in the so-called Little Ice Age and the recent past has been strongly positive, that total forcing between the Medieval warm period and the recent past in European summer has been quite a bit smaller, due to some cancellation between negative forcing from land use changes associated with the transition from forest to agricultural land and aerosols (which is larger in summer), and positive greenhouse gas forcing. This is consistent with the much smaller change over time in European summer temperatures compared to winter (Hegerl et al., 2011; Luterbacher et al., 2004).

A recent data assimilation study confirms the important role of external forcing to explain temperatures of the last millennium, which reproduces regional records very closely (Goosse et al., 2010). All these results support and strengthen the conclusion that external forcing combined with internal variability as estimated by climate models provides a convincing explanation for Northern Hemispheric temperature variability of the last millennium.

10.7.3 Changes of Past Regional Temperature

Several reconstructions of past regional past temperature variability are available. Luterbacher et al. (2004) reconstructed temperature variability in Europe from 1500 on over all four seasons, with the reconstructions dominated by documentary evidence throughout and by instrumental data from the late 17th century on. This reduces uncertainty compared to regions where only proxy data are available. Bengtsson et al. (2006) concluded that preindustrial European climate captured in the reconstruction is 'fundamentally a consequence of internal fluctuations of the climate system'. This conclusion is based on the consistent variability found for short timescales in an OAGCM control simulation and the reconstruction. However, Hegerl et al. (2011) analyzed 5-year averaged European seasonal temperatures and find detectable response to external forcing in summer temperatures in the period prior to 1900, and detectable signals throughout the record in the other seasons (clearest in winter, weakest in fall). The authors use a multi-model fingerprint of temperature change over time that is derived from three model simulations with slightly different combinations of external forcings (notably, land use change is used in only one of three simulations, aerosols are missing in one simulation and different estimates and implementations of solar and volcanic forcing are chosen in the three model simulations). Despite the forcing uncertainties, the fingerprint for external forcing shows coherent time evolution between models and reconstruction over the entire period analysed (both before and after 1900), and suggests that the cold winter conditions in the late 17th and early 19th century were externally driven, as was the warming between the two peak cold conditions. An epoch analysis of years immediately following volcanic eruptions shows that European summers following volcanic eruptions are detectably colder than average years, while winters show a response of warming in Northern Europe and cooling in Southern Europe. However, multiple eruptions need to be combined in order to be able to detect, particularly, the winter response from climate variability. The winter pattern is most detectable if the analysis is restricted to those volcanic eruptions whose timing in the seasonal cycle is such as to cause strong tropical stratospheric warming affecting the Northern hemisphere in the following winter. The only forcing factor to be individually detected was anthropogenic forcing in winter, although there was some suggestive evidence for a role of solar forcing in summer.

Since the AR4 there has been an increased emphasis laid on the importance of modes of climate variability in explaining regional changes over the last millennium and relating it to large-scale temperature change patterns. There is evidence that the NAO/AO underwent substantial low-frequency variability in the past (Trouet et al., 2009), which may explain some of the large-scale temperature changes that have been reconstructed (Mann et al., 2009). The extent to which these variations in circulation are themselves affected by external forcing is unclear at present, although there is suggestive evidence for ENSO responding to volcanism (Adams et al., 2003; Zanchettin et al., 2011, in preparation). Note that comparisons between spatial patterns in models and data are inconclusive unless the probability of an agreement by chance and the quantitative ability of the model to explain reconstructed changes is assessed. However, Palastanga (2011) show, with a modeling study using data assimilation techniques, that neither a slowdown of the thermohaline circulation nor a persistently negative NAO alone can explain the reconstructed temperature evolution over Europe during the Little Ice Age (periods 1675–1715 and 1790–1820). This is consistent with detection and attribution studies that found detectable influences from external forcing on European temperatures (Hegerl et al., 2011).

10.7.4 Changes in Regional Precipitation, Drought and Circulation

Reconstructions of past regional precipitation and drought (see Chapter 5) suggest substantial regional drought in the past, for example, in Western North America (Cook et al., 2007) (see Chapter 5), which often exceeded droughts recorded in the 20th century. Research suggests a role of tropical Pacific variability in these large droughts. Seager et al. (2008) show that if forced with SSTs reconstructed from corals, a large ensemble of atmospheric model produces droughts that match mega droughts in North America in the 14th and 15th century that have been recorded from treering records, although the ensemble failed to reproduce the wetter period between these two dry periods. The dry conditions in that case are associated by extended La-Nina like states. Herweijer and Seager (2008) show that dry conditions in western North America in the 19th and early 20th century coincided with dry conditions in Europe, southern South American and western Australia, and coincide with cool conditions of the Eastern Tropical Pacific.

10.7.5 Causes or Contributors to Change in Specific Periods

[PLACEHOLDER FOR FIRST ORDER DRAFT]

10.7.5.1 The Early 20th Century Warming

The instrumental surface air temperature (SAT) record shows two phases of warming during the past century: the present warming largely attributed to increasing anthropogenic forcing and an earlier climate fluctuation that appeared from about 1920 and persisted into the mid-20th century. The emergence of the early 20th century warming (ETCW) episode was noted at the time (Kincer, 1933; Scherhag, 1937) and it has been studied repeatedly over the past 80 years (Ahlmann, 1948; Bengtsson et al., 2004; Lysgaard, 1949; Mitchell, 1963; Rodgers, 1985; Willett, 1950).

The AR4 concluded that 'the early 20-th century warming is very likely in part due to external forcing (Hegerl et al., 2007a), and that it is 'likely' that anthropogenic forcing contributed to this warming. Results since then have been consistent with that assessment. The assessment was based on detection and attribution results from analyses of the 20th century (Shiogama et al., 2006; Stott et al., 2003) indicating a detectable contribution to early 20th century global warming by natural forcing, and by detection and attribution assessments based on palaeoclimatic reconstructions that cover the early 20th century (Hegerl et al., 2007a). As discussed in AR4, results vary on the exact contribution to that warming by an increase in solar radiation at the time, and by a warming in response to an almost complete hiatus in volcanism during the early 20th century, following eruptions early in the century in Kamchutka (1907) and the Caribbean (1912) (Robock, 2000; Shindell and Faluvegi, 2009) Shiogama et al. (2006) find an approximately equal contribution by solar and volcanic forcing to observed warming to 1949, and a quite small unexplained residual. In contrast, the residual warming found in a study of Northern Hemispheric records was substantial (Hegerl et al., 2007a; Hegerl et al., 2007b), pointing at a contribution by internal variability, consistent with other publications (Delworth and Knutson, 2000). Since the AR4, an inhomogeneity in sea surface temperature data has been found that affected the middle of the century (Thompson et al., 2008) and may reduce some of the unexplained variance at the very end of the early 20th century warming. However, a distinguishing feature of the early 20th century is its pattern (Bronnimann, 2009) which shows most pronounced warming in the Arctic cold season, followed by North American (warm season), the North Atlantic Ocean and the tropics. In contrast, there was no unusual warming in Australia and Asia (see AR4). Such a pronounced pattern points at a role of circulation change as a contributing factor to the regional anomalies contributing to this warming. Some studies suggested the warming is a response to a quasi-periodic oscillation in the overturning circulation North Atlantic ocean or some other governing aspect of the climate system (Knight et al., 2006; Polyakov et al., 2005; Schlesinger and Ramankutty, 1994), or a large but random expression of internal variability (Bengtsson et al., 2006; Wood and Overland, 2010). The contribution by internal variability is highlighted by the pattern of warming, with the largest positive anomalies occurring in the high latitude North Atlantic between western Greenland and northern Russia, while no anomalous temperatures were seen at Barrow, Alaska. The anomalies were associated with fluctuations in the atmospheric circulation in the region (Peterssen, 1949) and concurrent with positive sea-surface temperature anomalies in the mid-latitude western Atlantic (Bjerknes, 1959). Knight et al. (2009) diagnose a shift from the negative to the positive phase of the AMO from 1910 to 1940, a mode of circulation that is estimated to contribute approximately 0.1°C, trough to peak, to global temperatures (Knight et al., 2005).

The peak and later part of the early 20th century warming coincided with substantial drought in the US midwest, the so-called 'dust bowl' years. Modelling studies suggest that the dry conditions can be explained by the state of the tropical Pacific ocean at the time, and may have been exacerbated by dust forcing due to land use change and erosion (Cook et al., 2008).

10.7.5.2 The so-called Little Ice Age

The Little Ice Age is a period of relatively cool conditions from 1550–1750 and again about 1880–1920 (see Chapter 5, will be synchronized). Radiative forcing into the little ice age on long time scales is dominated by solar and greenhouse gas forcing (Chapter 5), although the late 17th and early 19th century were also subject to short lived, but substantial pulses of volcanism, including the powerful eruption of Mount Tambora in 1815, which can lead in models to long-term cooling despite the short lived nature of the forcing (see discussion by Gregory et al., 2011). The overall level of cooling between the present and the peak cold periods in the late 17th and early 19th century varies between reconstructions. Modelling studies reproduce this cooling if forced with a combination of solar, volcanic, and greenhouse gas forcing (Ammann et al., 2007; Jungclaus et al., 2010; Tett et al., 2007). Detection and attribution results are usually based on longer time periods including the LIA, and confirm a role of volcanic and greenhouse gas forcing, with a more uncertain contribution from solar forcing (Hegerl et al., 2007a), consistent with modelling studies (Goosse et al., 2010; Jungclaus et al., 2010; Schurer et al., 2011, in preparation). Records also suggest a shift Southward of the ITCZ during the Little Ice Age (see Chapter 5?), which in a model simulation can be explained by a small cooling of the low-latitude Atlantic (Saenger et al., 2009), but not by high-latitude cooling even if the latter is large, indicating a substantial role for low-latitude ocean temperatures in tropical precipitation variability.

10.7.5.3 The Medieval Warm Period

Conditions in the early centuries of the last millennium were generally warmer than at present (Chapter 5, see also Buentgen et al., 2011 for Europe), and were substantially warmer than the so-called Little Ice Age. However, warm conditions around the early millennium occurred at different times for different locations, leading to less unusual warmth for the Northern Hemisphere as a whole compared to individual regions (see Briffa et al. 2002). Conditions in Europe in summer were similar to the late 20th century, although most recent summer temperatures increases are highly unusual (Hegerl et al., 2011; Luterbacher et al., 2004). Goosse(2006) estimates that the radiative forcing for the medieval warm period, particularly for European summer, was quite similar to the recent past, since, they argue, recent aerosol cooling and land use change effects due to changes in albedo during the transition from a more forested stage early in the millennium to more agricultural land in the present day (Ruddiman and Ellis, 2009) have cancelled out a substantial part of the greenhouse gas forcing. Solar forcing estimates in the MWP are uncertain, although results suggest an overall slightly elevated solar forcing (see Chapter 5). In contrast to the LIA, the elevated temperatures caused little CO_2 change in that period (Frank et al., 2008). Detection and attribution analyses of the entire millennium suggest that small volcanic forcing and small positive solar forcing explain the estimated warmth in many, but not all records during the MWP. (The size of the 1258 eruption, which shows a large aerosol spike in ice cores, may be overestimated due to particle conglomeration, (Timmreck et al., 2009). The residual unexplained variability is not unusual after about 1300 (Hegerl et al., 2007a).)

10.7.5.4 The Mid-Holocene

It is presently unclear if climate models are able to reproduce apparent changes in the strength and frequency of El Nino over the Holocene (see Chapter 5), and uncertainty in the connection between indirect proxy evidence and the state of the tropical Pacific contribute to this uncertainty. Comparisons between models and reconstructions suggest some difficulty in reproducing the full extent of wettening in North Africa during the Mid Holocene that is suggested by records. (Chapter 5).

10.7.6 Estimates of Unforced Internal Climate Variability

The residual variability in past climate that is not explained by changes in radiative forcing provides an estimate of unforced internal variability of the climate system that is independent from that over the 20th century instrumental period. This is important as questions remain to what extent climate models fully capture the climate systems internal variability and if they contain all the processes needed to reproduce changes recorded in the past. As the level of internal variability is the background against which forced signals are detected, such an estimate of internal climate variability that is largely independent from climate modelling is invaluable. The removal of the forced signal from estimates of pre-industrial climate variability is a remaining model dependency, but incomplete removal will tend to increase estimates of past variability and therefore provide a harder test of climate models' ability to simulate internal variability.

The interdecadal and longer-term variability in large-scale temperatures in climate model simulations with and without past external forcing is quite different (Jungclaus et al., 2010; Tett et al., 2007), suggesting that a large fraction of temperature variance in the last millennium has been externally driven (>50% on decadal and hemispheric scales), even over the pre-instrumental period. This is in agreement with detection and attribution studies, where the residual, unexplained variability in reconstructions is quite small compared to the overall variability (Hegerl et al., 2007a; Jungclaus et al., 2010) and similar or smaller than climate model variability (see figure, refs). For drought, precipitation and circulation changes, the evidence is less clear, as it is presently unknown to what extent simulations of the last millennium quantitatively reproduce long-term severe drought present in reconstructions.

10.7.7 Information on Longer Timescales and for Individual Forcings

As discussed in Chapter 5 there is substantial evidence for correlations between proxies for solar radiation changes, e.g., cosmogenic isotopes 10Be and 14C (Beer, 2006; Lockwood and Frohlich, 2007), and indicators for past climate, including, for example, ice rafted debris (Bond et al., 2001) or proxies for the location of the intertropical convergence zone (Wang et al., 2005). The cyclicity of solar forcing seems to correspond significantly to peaks in power spectra of reconstructed records, but present techniques and data do not allow to estimate the magnitude of past solar responses on long timescales, and the significance of individual peaks is difficult to establish due to long-memory processes in the climate system leading to variability on all timescales.

10.7.8 Summary: Lessons from the Past

Reconstructions and long records of past climate support a significant role of external forcing on climate variability and change, particularly on hemispheric scales. Climate model simulations forced with realistic estimates of past natural and anthropogenic forcings can convincingly reproduce climate variability over the last millennium, both free-running and with the help of data assimilation. Detection and attribution studies can show that this agreement is not spurious, and that the time evolution of forcings points at particularly volcanic forcing and CO_2 forcing being important to explain past changes in Northern Hemispheric temperatures. The role of forcing extends to regional records, for example, European seasonal temperatures, where the response to all forcings combined is detected prior to 1900 in summer, and prior to 1950 in winter. The reconstructions do not suggest that climate models underestimate internal variability of temperature on large spatial scales, but raise tentative questions about the magnitude of past precipitation changes, although uncertainties are large. There are also results on the role of external forcings on longer-term records. Changes in circulation may have shaped regional climate variability, although there are large uncertainties in reconstructions of modes of climate variability in the past.

10.8 Whole System Attribution

Much of the literature that applies formal detection and attribution methodologies (such methodologies having been described in Section 10.2) have dealt with a particular component of the climate system in isolation, often by examining one individual climate variable, such as, air temperature, surface precipitation, ocean salinity, or sea ice extent. This section examines what additional information is provided by formal attribution studies that consider multiple climate variables in a single analysis.

Given that different aspects of the climate system are related through the interplay of physical processes, it could be that formal detection and attribution studies that consider multiple climate variables could better identify fingerprints of anthropogenic and natural forcings in the observations. If climate variables change together more coherently as a result of forcings than they do as a result of internal variability, the signal to noise of the combined multi-variable fingerprint could be higher than for the individual variables.

The first application of such an approach was made by (Barnett et al., 2008),who applied a multi-variable approach in analysing changes in the hydrology of the Western United States (see also Section 10.3). They constructed a multi-variable fingerprint, consisting of snow pack (measured as snow water equivalent), the timing of runoff into the major rivers in the region, and average January to March daily minimum temperature over the region. Observed changes were compared with the output of a regional hydrologic model forced by the PCM and MIROC climate models (Figure 10.23). They derived a multi-variable fingerprint of anthropogenic changes from the two climate models and found that the observations, when projected onto this fingerprint, show a positive signal strength consistent with the climate model simulations. This observed signal falls outside the range expected from natural internal variability as estimated from 1,600 years of downscaled climate model data. The expected response to solar and natural forcing estimated from the PCM model has a signal with the opposite sign to that observed. They conclude that there is a detectable and attributable signature of human effects on the hydrology of this region with up to 60% of the observed trend in their diagnostic being attributable to human influence.

[INSERT FIGURE 10.23 HERE]

Figure 10.23: Observed time series of selected variables (expressed as unit normal deviates) used in the multivariate detection and attribution analysis. Taken in isolation, seven of nine SWE/P, seven of nine JFM Tmin, and one of the three river flow variables have statistically significant trends (Barnett et al., 2008).

While their analysis shows clearly that the three variables are changing coherently in a systematic fashion, how much additional information is provided by snow mass and timing of river flows in addition to temperature? (Barnett et al., 2008) examine signal to noise ratios and find that the signal to noise ratio of their multi-variable fingerprint is higher than for each of the individual three components, confirming that the multi-variable fingerprint has higher detectability.

The potential for a multi-variable analysis to have greater power to discriminate between forced changes and internal variability was also demonstrated by (Stott and Jones, 2009), in this case for a different combination of climate variables. They showed that a multi-variable fingerprint consisting of the responses of global mean temperature and sub-tropical Atlantic salinity has a higher signal to noise than the fingerprints of each variable separately. Previous work using the HadCM3 model had shown detection of increases of Atlantic salinity between 20-50N (Stott et al., 2008b). Stott and Jones (2009) calculated trends from the HadCM3 model for increasing trend lengths ending in 2006 and estimated theoretical detection times as the shortest trend length for which the trend exceeds the 95 percentiles of trends expected from internal variability, as estimated by the HadCM3 control simulation. To detect trends of global mean temperature and sub-tropical Atlantic salinity requires at least 13 and 18 years respectively, whereas they found it is possible to detect a change in the combined trend fingerprint after only 8 years. This reduced detection time was found to result from low correlations between the two variables in the control simulation although the detection result depends on the ability of the models to represent the co-variability of the variables concerned.

More recently Ma et al. (2011) have conducted a multi-variable optimal detection analysis on North American and Eurasian continental winter and spring snow cover extent and surface mean temperature. While in many locations, snow cover variability may be expected to be strongly related to temperature variability, it can also be related to variability in precipitation. Ma et al. (2011) analysed monthly satellite based snow cover extents (Robinson et al., 1993) and monthly air temp anomalies from CRUTEM3V (Brohan et al., 2006). Consistent with previous studies showing an increase in signal to noise ratios of multi-variable fingerprints compared to uni-variate fingerprints (as discussed above) Ma et al. (2011) show that uncertainties in estimates of attributable changes are reduced when calculated using their multi-variate approach, providing that the covariance structure is well estimated. In analysing the extent to which modelled changes are consistent with observed changes, multi-variable attribution studies potentially provide a stronger test of climate models than single variable attribution studies. However, when several variables are convolved into one analysis, it is not necessarily clear where inconsistencies come from. Therefore it could be argued that single variable attribution studies are more informative for identifying model errors. In addition, multi-variable studies may provide little additional information if additional variables are correlated with each other.Perhaps as a result of such concerns, there are currently rather few formal detection and attribution studies that consider multiple variables simultaneously.

10.9 Implications for Projections

Detection and Attribution results not only provide information on the causes of past climate change, but the estimates of the magnitude of the externally driven component of these changes can be used to constrain predictions of future changes and provide uncertainty ranges for these predictions that are anchored in already observed climate change. The value and strength of the constraint on future changes depends on how relevant observable climate changes are for the prediction in question. This constraint works particularly well for signals with high signal-to-noise ratios, such as large-scale temperature change. Those constraints yield estimates of future warming under a particular emissions scenario, equilibrium climate sensitivity, or transient climate response, a measure of the magnitude of transient warming while the system is not in equilibrium, which is particularly relevant for near-term temperature changes (Section 10.9.1.). Comparisons of simulated and observed precipitation changes, provide evidence that climate models underestimate recent changes in mean and intense precipitation, suggesting that they may also underestimate projected future changes (Section 10.9.2). Also, directly relevant for the near-term are the implications of the reversal in Ozone forcing (10.9.3). The Equilibrium Climate Sensitivity (ECS; Section 10.9.4) is relevant to determining the CO_2 concentration levels that keep global warming below particular thresholds in the long term. Constraints on estimates of longer-term climate change and equilibrium climate change from recent warming hinge on the rate at which the ocean has taken up heat, and for both transient and equilibrium changes, the amount of recent warming prevented by aerosol forcing is relevant. Therefore, attempts to estimate climate sensitivity (transient or equilibrium) often also estimate the total aerosol forcing and the rate of ocean heat uptake (10.9.5).

The AR4 had for the first time a detailed discussion on estimating these quantities relevant for predictions, including equilibrium climate sensitivity and transient climate response, and included an appendix with relevant methods. We build on the AR4, repeating information and discussion given there only if necessary to provide context.

10.9.1 Near Term Near-Surface Temperature Change

Scaling factors derived from a comparison of the simulated and observed responses to greenhouse gas changes and aerosol changes over the historical period may be used to scale projections of the future response to these forcings (Allen et al., 2000; Kettleborough et al., 2007; Meehl et al., 2007b; Stott and Kettleborough, 2002; Stott and Forest, 2007; Stott et al., 2008a; Stott et al., 2006b). Based on energy balance models, Allen et al. (2000) and Kettleborough et al. (2007) demonstrate a close to linear relationship between 20th century warming and warming by the mid-21st century, as EBM parameters are varied, justifying this approach. Such studies use estimates of the uncertainties in these scaling factors, derived from detection and attribution analyses, together with estimates of natural variability, to make observationally-constrained projections of 21st century warming. Such projections (Stott et al., 2006b) were presented in the AR4 (Meehl et al., 2007b). Stott et al. (2008a) demonstrate that an optimal detection analysis of 20th century temperature changes applied using HadCM3 is able to rule out both very high and very low temperature responses to aerosols, or equivalently aerosol forcings, and therefore that projected 21st century warming may be more closely constained than if the full range of aerosol forcings is assumed (Andreae et al., 2005). Stott and Forest (2007) demonstrate that projections obtained from such an approach, are similar to those obtained by constraining EBM parameters from observations.

The AR4 discussed for the first time estimates of the transient climate response, or TCR, which was originally defined as the warming at the time of CO_2 doubling (i.e., after 70 years) in a 1%y^{-1} increasing CO_2 experiment. Like ECS, TCR can also be thought of (Frame et al., 2006; Held et al., 2010) as a generic property of the climate system that determines the transient response to any gradual increase in radiative forcing taking place over a similar timescale. Held et al. (2010) use the simple two-box model of Gregory et al. (2000) in which TCR is determined by the heat capacity of ocean mixed layer, a radiative damping term corresponding to the ‘fast’ climate sensitivity, and the rate of heat uptake by the deep ocean. To the extent that deep ocean heat uptake is simply proportional to the temperature difference between the mixed layer and deep ocean, it affects the surface temperature response as if it were an enhanced radiative damping: hence the difficulty of placing an upper bound on climate sensitivity from the observed surface warming alone (Forest et al., 2002; Frame et al., 2005). Heating of the deep ocean introduces a slow, or ‘recalcitrant’, component of the response, which Held et al. note could not be reversed for many decades even if it were possible to return radiative forcing to pre-industrial values. To the extent that the fast response is linear, Held’s ‘transient climate sensitivity ‘(TCS) as well as TCR is independent of the actual percent-per-year rate of CO_2 increase, and hence can be estimated from the response to any transient forcing operating over a similar timescale. This is similar in motivation to the ‘normalised TCR’ (NTCR), defined by Frame et al. (2006) as the rate of warming in degrees per year divided by the fractional rate of CO_2 increase per year over a 70-year period: both TCS and NTCR were introduced to avoid the apparent scenario-dependence of the traditional definition of TCR. Since, however, both are just multiples of TCR itself ($TCS=TCR/F_{2x}$; NTCR=TCR/0.7), it may be simpler to avoid introducing any new notation and, following (2007b), to recognise that TCR as well as ECS describe general emergent properties of a climate model or the climate system itself rather than outcomes of specific climate model experiments. Since TCR focuses on the short term response, constraining it is a key step in constraining future global temperature change under scenarios in which forcing continues to increase and also those in which forcing peaks (Frame et al., 2006) until the point at which concentrations stabilize. At that point, the Equilibrium climate sensitivity becomes relevant.

The AR4 concluded that, based on observational constraints, the TCR is very likely to be larger than 1°C and very unlikely to be greater than 3.5°C (Hegerl et al., 2007b). This supported the overall assessment that the transient climate response is very unlikely greater than 3°C and very likely greater than 1°C (Meehl et al., 2007a). Meanwhile, several new estimates of the TCR are now available (Knutti and Tomassini, 2008), which show a PDF shifted slightly towards lower values with a 5–95% percent range of 1.11–2.34K. Several of the estimates of TCR cited by Hegerl et al. (2007b) used estimates of 20th century radiative forcing due to well-mixed greenhouse gases that may have underestimated the efficacies of non-CO_2 gases relative to the estimates in Forster et al. (2007): since observationally constrained estimates of TCR are based on the ratio between past attributable warming and past forcing, this would account for a high bias in AR4 upper bound.

Held et al. (2010) show that their two-box model, distinguishing the fast and recalcitrant responses, fits both historical simulations and instantaneous doubled CO_2 simulations of the GFDL coupled model CM2.1, where the fast response has a relaxation time of 3–5 years, and where the 20th century response is almost completely described by the fast component of warming. Padilla et al. (2011) use this simple model to derive an observationally-constrained estimate of the TCR of 1.3–2.6K, similar to other recent estimates.

10.9.2 Precipitation Change

As discussed in Section 10.3.2.3, since the publication of the AR4 anthropogenic influence on precipitation has been detected globally (Zhang et al., 2007b) and over the Arctic (Min et al., 2008a). The simulated and observed pattern of mean precipitation change consists of increases in the high latitudes, decreases in the NH subtropics and an increase in the SH tropics (Hegerl et al., 2007b; Zhang et al., 2007b). Zhang et al. (2007b) found that the best estimate of the regression coefficient of precipitation changes observed at land stations onto the simulated anthropogenic response was about 5, with a 90% uncertainty range of about 2–8, based on an analysis of zonal mean precipitation trends over the 1950–1999 period, indicating that the multimodel zonal mean trend pattern needs to be enhanced by a factor of at least two to reproduce the observed trend. A response to natural forcings was also detected with a best-estimate regression coefficient of about 8, consistent with previous studies (Gillett et al., 2004). Zhang et al. (2007b) caution that individual models do in some cases show simulated zonal mean precipitation changes as large as those observed, but that regions of increase and decrease are not in the same place in different models, and therefore the multi-model mean contains smaller amplitude changes than most individual models. Min et al. (2008a) derived a similarly high regression coefficient for the anthropogenic response over the Arctic alone.

Wentz et al. (2007) find that ocean-mean precipitation in SSM/I data shows an increase per unit changes in temperature (hydrological sensitivity) of close to 7%K^{-1} over the period 1987–2006, which is larger than the 1-3%K^{-1} predicted by climate models. Other studies find that moistening of the wet regions of the tropics and drying in the dry regions is also underestimated in atmospheric models forced with observed SST (Allan and Soden, 2007; Allan et al., 2010). Liepert et al. (2009) find that this discrepancy may be explainable by internal variability, and that some 20-year sections of model simulation show a similar hydrological sensitivity to the observations. They also show that the simulated hydrological sensitivity is higher for aerosol forcing than it is for greenhouse gases, consistent with earlier studies arguing that precipitation is more sensitive to shortwave forcings than longwave forcing (Hegerl et al., 2007b). This means that the apparent hydrological sensitivity will depend on the relative size of changes in aerosol and GHG forcing, and that the hydrological sensitivity calculated for a period in the past in which greenhouse gas and aerosol forcings were both increasing may be smaller than that for a future period, where aerosol forcing is decreasing while GHG forcing continues to increase. (Liepert and Previdi (2009) do not find a systematic difference between median simulated hydrological sensitivity in the 20th and 21st centuries, based on an analysis of trends in overlapping 20-year periods, but their analysis includes a number of periods in the 20th century with near-zero or negative 20-year temperature trends which would tend to be associated with large positive hydrological sensitivity). This also implies that scaling the projected future changes in precipitation by a regression coefficient of the observed to simulated combined anthropogenic response during the 20th century would only be a valid approach if the simulated precipitation responses to greenhouse gases and sulphate aerosol are under- or overestimated by the same factor. So far regression coefficients for these two forcings have not been separately evaluated from observations.

An apparent underestimate of observed precipitation trends in models is also found in precipitation extremes. Min et al. (2011) find a detectable anthropogenic response in two measures of precipitation extremes over the Northern Hemisphere, with a best-estimate regression coefficient of 2–3 and an uncertainty range that includes one. The authors diagnose the location in the cumulative extreme value distribution function for extremes for models and data separately, which yields model and data comparible and find that the more rare events are becoming more frequent faster for the observations than in the models. An underestimation of changes in extreme precipitation in models with prescribed SSTs has also been found in the tropics (Allan and Soden, 2008; Allan et al., 2010).

To date, no studies have used attribution results for precipitation to scale projected future changes, as hasbeen done for temperature (Section 10.9.1). Nonetheless, several authors have concluded that projected future changes in mean precipitation (Zhang et al., 2007b), and extreme precipitation (Min et al., 2011) (IPCC, 2012, in preparation) are likely to be underestimated by GCM's. We thus conclude that it is that projected future changes in mean and extreme precipitation could be underestimated by GCMs, possibly by a substantial factor, but the magnitude of any underestimation has yet to be quantified, and is subject to considerable uncertainty.

10.9.3 Ozone Forcing Reversal

After about 20 years of increasing depletion from the late 1970s to late 1990s, the stratospheric ozone concentration has broadly stabilized over the past decade, consistent with the observed decline in ozone depleting substances (ODSs) that peaked in the middle 1990s (Weatherhead and Andersen, 2006; WMO, 2011). Coupled chemistry-climate model (CCM) simulations, with projected 21st century stratospheric chlorine loading, predict that global stratospheric ozone will return to pre-1980 levels around 2050. However, the return to pre-1980 levels will not occur at the same time in all regions, due to changes in stratospheric circulation and temperatures resulting form increasing greenhouse gas concentrations. Ozone abundances may increase to above pre-1980 levels by 2100 in some regions like the Arctic and mid-latitudes while other regions like the tropical lower stratosphere will never return to pre-1980 levels (WMO, 2011).

There is increasing evidence from simulations with climate models and CCMs that over the last 30 years the Antarctic ozone hole has affected Southern Hemisphere climate from the Antarctic continent to subtropics mostly during austral summer (Section 10.3.3). Stratospheric ozone depletion causes stratospheric polar cooling in late winter/early spring and delays the breakup of the stratospheric polar vortex (McLandress et al., 2010). Simulations show that these stratospheric changes cause a shift of the SAM towards its positive polarity related to a poleward shift of the mid-latitude jet, a poleward expansion of the Hadley cell, anomalous cooling of the Antarctic interior, warming of the Antarctic Peninsula and a poleward shift of precipitation patterns (Gillett and Thompson, 2003; McLandress et al., 2011; Polvani et al., 2010; Son et al., 2009; Son et al., 2008; Son et al., 2010; Thompson and Solomon, 2002). Model simulations also suggest that the increase of greenhouse gas concentrations have a similar effect on tropospheric circulation and precipitation patterns (McLandress et al., 2011; Perlwitz et al., 2008; Sigmond et al., 2011; Son et al., 2009; Son et al., 2008; WMO, 2011).

While the recovery from Antarctic ozone depletion will tend to drive a reversal in summer of the shift in the southern hemisphere mid-latitude jet observed in recent decades, increasing greenhouse gas concentrations are expected to drive a continuing poleward shift. Thus, overall, while the poleward shift in the jet is likely to continue in most seasons, in summer the jet location trend is likely to be small over the coming decades. Some models simulate a small equatorward trend in this season, while others indicate a small poleward trend, or no significant trend (McLandress et al., 2011; Perlwitz et al., 2008; Polvani et al., 2011; Son et al., 2008; Son et al., 2010; WMO, 2011). Overall projected Southern Hemisphere circulation changes do not appear to be strongly sensitive to the projected rate of ozone recovery (Karpechko et al., 2010). Since stratospheric ozone abundances in the stratosphere have reached a turning point in most regions during the past decade, this should be accounted for in studies which attempt to constrain future regional Southern Hemisphere climate changes based on observed trends over recent decades. The potential effects of super recovery of Arctic ozone on the Northern Annular Mode are uncertain, but super recovery may contribute a modest negative NAM trend during spring (Morgenstern et al., 2010).

10.9.4 Constraints on Long Term Climate Change and the Equilibrium Climate Sensitivity

The equilibrium climate sensitivity (ECS) is defined as the warming in response to a sustained doubling of carbon dioxide in the atmosphere relative to preindustrial levels (see AR4). This is generally assumed to be an equilibrium involving the ocean-atmosphere system, which does not include long-term melting of ice sheets and ice caps. The latter would lead to continued warming for a longer time before a warmer equilibrium is reached (Hansen et al., 2005). Estimates of climate sensitivity can be based on estimating, with uncertainties, past warming per unit forcing changing, and then adapting this sensitivity parameter by multiplying it with the forcing associated with CO_2 doubling, or by fitting simple energy balance models to observed temperature evolution. While such energy balance calculations are beautiful in their simplicity, they often need to be simplified to such an extent that affects uncertainties: for example, they might need to assume a single response timescale rather than the multiple response timescales that are observed, and cannot account for nonlinearities in the climate system that lead, for example, to generally larger responses for negative forcings (Hegerl et al., 2007b). Therefore, this section is mainly based on estimates that use climate model ensembles with varying parameters, and evaluate the ability of these models to reproduce a particular observed change. The estimates are often based on an approach where the probability of observed data is evaluated for a range of climate models with varying parameters. From this, the probability of the different model versions being correct is inferred. Such estimates are inherently based on Bayesian statistics and therefore, even if it is not explicitly obvious, usually involve using prior information or prior beliefs. This prior information shapes the sampling distribution of the models (e.g., Frame et al., 2005; Hegerl et al., 2007b). Analyses that make a more complete effort to estimate all uncertainties affecting the model-data comparison lead to more trustworthy results, but are often more uncertain than methods that apply more assumptions (Knutti and Hegerl, 2008).

The AR4 concluded overall that the ‘likely’ range of ECS is 2-4.5, but that higher values cannot be excluded, and that ECS is very likely to be larger than 1.5°C. This assessment was based on modelling studies varying uncertain model parameters, on estimates of feedbacks and on estimates of observed and reconstructed climate change in response to past forcing. The latter line of evidence is re-assessed in this section. Readers should refer to the AR4 for a more complete explanation of methods and theory.

10.9.4.1 Estimates from Recent Surface Temperature Change

Many estimates of the equilibrium climate sensitivity in AR4 were based on climate change that has been observed over the instrumental period (Hegerl et al., 2007b), and their ranges are given in Figure 10.24 for comparison with new estimates. However, the distribution of ECS estimates are wide and cannot exclude high sensitivities, particularly when the forcing uncertainty is considered fully (Tanaka et al., 2009). Since the AR4, Forest et al. (2008) have updated their study using a newer version of the MIT model used in earlier studies (see Figure 10.24). The main reason for a wide estimate based on 20th century warming is that based on surface temperature alone, and even based on surface temperature data combined with ocean warming data the possibility cannot be excluded, within data uncertainties, that a strong aerosol forcing or a large ocean heat uptake might have masked a strong greenhouse warming. This is consistent with the finding that a set of models with a larger range of ECS and aerosol forcing than the ranges spanned in the CMIP3 ensemble could be consistent with the observed warming (Kiehl, 2007). .However, application of fingerprint methods can often yield substantially more information than results based on simple global mean diagnostics (Hegerl et al., 2007b; Stott and Kettleborough, 2002). Note that the transient warming is far from an equilibrium state (Hansen et al., 2005), which is why the 20th century temperature record lends itself better to estimating the transient warming. However, the advantage of the 20th century for estimating the ECS compared to other periods is that it focuses on a state of the climate similar to today, and uses similar timescales of observations as the projections we are interested in, thus providing constraints on the overall feedbacks operating currently. A recent estimate of the uncertainty in climate sensitivity and aerosol forcing combined (Schwartz et al., 2010) postulates that based on global temperature alone, aerosol forcing needs to be constrained in order to enable estimates of future warming. This postulate is inconsistent with estimates that make more complete use of the available space-time pattern of aerosol and greenhouse gas forcing (Stott et al., 2006a).

10.9.4.2 Estimates Based on Top-of the Atmosphere (TOA) Radiative Balance

Since the satellite era, measurements are available of the energy budget of the planet, which can directly quantify the radiative imbalance of incoming shortwave and outgoing longwave radiation. Such measurements could in theory provide tight constraints on the sensitivity of the atmosphere to radiative forcing changes by providing very direct estimates of the climate feedback parameter as the regression coefficient of radiative forcing against global mean temperature , which is inversely proportional to the ECS (see AR4; Forster and Gregory, 2006). Due to the heat uptake by the ocean, a radiative imbalance is expected (Hansen et al., 2005), which relates to ocean warming. Most estimates use a simple energy balance relationship of the form $N = F - \lambda\Delta T + \varepsilon$ (Murphy et al., 2009), where N is the net energy flow towards the Earth (which will decay to zero as the equilibrium is reached), F is the net forcing, λ is the climate feedback parameter and ε is an uncertainty term due to noise and measurement uncertainty. However, the overall trend in shortwave outgoing radiation and with it net radiation budget is affected by uncertainties in measurements, for example, related to the de-seasonalization of the satellite records which can reduce an ERBE-measured decrease in reflected shortwave radiation over time to an almost flat curve (Harries and Belotti, 2010). Lin et al.(2010) find, assuming a (Hansen et al., 2005) model-estimated TOA imbalance of 0.85W/m^2 a climate feedback coefficient ranging from -1.3 to -1.0 W/(m^2 K). However, accounting for the uncertainty in the estimated imbalance, would result in a larger uncertainty range. Lindzen and Choi (2009) used data from the radiative budget and simple energy balance models over the tropics to investigate if the feedbacks shown in climate models are realistic. The authors point out that based on their comparison, climate models overestimate the outgoing shortwave radiation compared to ERBE data, leading to an overall mis-estimation of the radiative budget. However, the ERBE decrease in outgoing shortwave radiation is highly uncertain as discussed in Harries and Belotti (2010). Also, the result of Lindzen and Choi (2009) is derived from temperatures of the tropics (20N-20S) only, which tends to lead to substantially underestimated uncertainties (Chung et al., 2010; Trenberth et al., 2010) and a possible change in feedback slope, as high latitude feedbacks can be substantial (Murphy et al., 2009). Spencer and Braswell (2008) point at a systematic bias in analysis methods for feedbacks, which would bias estimates of feedback to low values, and with it estimates of sensitivity to high values if variability noise in radiative balance correlates with temperature. However, Murphy and Forster (2010) show that Spencer and Braswell's estimate relaxes to values more consistent with climate models if assuming a more realistic timescale of the response (i.e., ocean effective mixed layer depth), more realistic OLR error estimates and more comparable values for models and observations (Murphy and Forster, 2010). Murphy et al. (2009) caveat that their estimate of λ is not suitable to estimate its inverse, the ECS, since multiple timescales are involved in feedbacks that contribute to climate sensitivity (Knutti and Hegerl, 2008; Lin et al., 2010) and thus a simple relationship as above will yield misleading and non-robust estimates for ECS as long as N is non-zero. In conclusion, some recent estimates of high feedback/low sensitivities based on aspects of the observed radiative budget appear not to be robust to data and method uncertainties. Consequently present TOA radiation budgets appear consistent with other estimates of climate sensitivity but are unable to further robustly constrain these sensitivity estimates (Bender, 2008).

10.9.4.3 Estimates Based on Response to Volcanism or Internal Variability

Some recent analyses have used the well observed forcing and response to major volcanic eruptions during the 20th century, notably the eruption of Mt. Pinatubo. The constraint is fairly weak since the peak response to short-term volcanic forcing has a nonlinear dependence on equilibrium sensitivity, yielding only slightly enhanced peak cooling for higher values of S (Boer et al., 2007; Wigley et al., 2005). Nevertheless, models with climate sensitivity in the range of 1.5 to 4.5 degrees generally perform well in simulating individual volcanic eruptions and provide an opportunity to test the fast feedbacks in climate models (Hegerl et al., 2007b). Recently, Bender at al. (2010) re-evaluated the constraint and cite a best estimate of 1.7–4.1K. Estimates that neglect key uncertainties, such as the role of internal climate variability or the timescale of the climate system can yield substantially different estimates, that are however not robust, as be demonstrated by applying the proposed analysis methods to climate models with known sensitivities (see discussion in AR4, Hegerl et al., 2007b). Several papers also try to relate the ECS to the strength of natural variability using the fluctuation dissipation theorem (Kirk-Davidoff, 2009; Schwartz, 2007) but studies suggest that the observations are too short to support a tight estimate, and that this method tends to underestimate climate sensitivity for a short time period; and that single timescales are too simplistic for the climate system. The latter problem is also identified to yield substantially underestimated uncertainties in that study (Knutti et al., 2008).

10.9.4.4 Paleoclimatic Evidence

Palaeoclimatic evidence is promising for estimating ECS (Edwards et al., 2007). For periods of past climate which were changing more slowly, the radiative imbalance and with it the ocean heat uptake uncertainty is less important. For example, the climate of the Last Glacial Maximum was much closer to equilibrium. However, for periods such as the Last Glacial Maximum the uncertainty in the radiative forcing due to ice sheets, dust, and CO_2 decreases leads to large uncertainty (see Chapter 5), and the possibility of small forcing

having led to the reconstructed change again leads to a long tail in the estimates of ECS. Estimates of the cooling in response to these boundary conditions during the LGM in climate models compared to data are discussed in Chapter 5 (Otto-Bliesner et al., 2009). At the time of the AR4, several studies were reviewed in which parameters in climate models had been perturbed systematically in order to estimate ECS (Hegerl et al., 2007b). The ECS of a perturbed model is estimated by running it to equilibrium with doubled CO_2, and then a model-data comparison, given uncertainties, assesses whether the same model yields realistic simulations of the LGM conditions. This method avoids directly estimating the relationship between forcing and response. Direct estimates are uncertain because they assume that the feedback factor is invariant for this very different climatic state, which is not correct for climate models and which is also questioned by data (see Chapter 5; Otto-Bliesner et al., 2009). Instead, climate models estimate the change in feedbacks with climate state, yielding substantially different estimates which are quite sensitive to model structure and forcings used (Hargreaves et al., 2007; Schneider von Deimling et al., 2006). Recently, new data synthesis products have become available for assessment with climate model simulations of the LGM (Otto-Bliesner et al., 2009). The LGM simulations are broadly consistent with these data, although the data show more structure in their change with regions of warming interspersed into cooling regions and is different from model simulations that show a broadly uniform cooling into the LGM. Recent data analyses support a range of 1.4–5.2K for the sensitivity based on the LGM which somewhat reduces earlier uncertainty. Chylek and Lohmann (2008a) estimate the ECS to be 1.3 to 2.3 based on data for the transition from the LGM to the Holocene, but consider only a small range of uncertainties. The small range of considered uncertainties leads to underestimation of the overall uncertainties and with it an underestimate of the range of sensitivities consistent with data (Chylek and Lohmann, 2008b; Ganopolski and Schneider von Deimling, 2008)
At the time of the AR4, only few estimates based on the relationship between paleoclimate reconstructions from the last millennium and external forcing were available. Because of a weak signal and large uncertainties in reconstructions and forcing data (particularly solar and volcanic forcing) the long time horizon yielded only a weak constraint on ECS. Direct estimates of the equilibrium sensitivity from forcing between the Maunder Minimum period of low solar forcing and the present are also broadly consistent with other estimates, but need to carefully consider all external forcings, including reduced atmospheric CO_2 and heavy volcanism during this period (see Chapter 5; 10.7).

Some studies of other, more distant paleoclimate periods appear to be broadly consistent with the estimates from the more recent past (see chapter). Lunt et al. (2010) estimate the Earth System Sensitivity as 30-50% increased warming relative to the response based on the fast climate components and thus that the true, long-term climate sensitivity is substantially higher than the so-called 'Charney sensitivity' which does not account for large-scale melting and Earth System feedbacks. Substantially enhanced earth system sensitivity is also supported by other studies (Pagani et al., 2009).

Long-term carbon modelling studies over the last 420 million years (Royer, 2008; Royer et al., 2007) supports sensitivities that are larger than 1.5°C, but the upper tail is poorly constrained and uncertainties in the models that are used are significant and difficult to quantify. Chapter 5 discusses evidence for climate sensitivity from deep time, which for many time periods support estimates of the ECS in ranges that are consistent with the other lines of evidence. Koehler et al. (2010) discuss climate and CO_2 changes in the Pleistocene. They find, again, that tight constraints are not supported by the data, but that sensitivities above 6.1°C are difficult to reconcile with the evidence from proxy indicators. The climate of the early-to-middle Paleogene also points at a CO_2 and temperature relationship, however, data in the proxies suggest less warming than the climate models used (Shellito et al., 2003). Findings like this emphasize the need to confront climate models with proxy and observational data to probe their ability to represent spatial details of climate change – although given large uncertainties in our knowledge of past climates, these tests are rarely conclusive.

10.9.4.5 Estimating Earth System Sensitivity

Recent work has also attempted to use observed relationship between CO_2 and temperatures to constrain the carbon cycle feedback, or the amount of additional CO_2 released into the atmosphere from the terrestrial biosphere and ocean per degree of warming. Frank et al. (2010) estimate the range of carbon cycle sensitivities based on a large range of warming between the Medieval Warm Period, the Little Ice Age and the present and possible changes in CO_2 over that time period, by regressing lagged timeseries of atmospheric CO_2 concentration onto temperature timeseries derived from paleodata. Since they apply ordinary least squares regressions, their estimates of carbon cycle sensitivity could be biased low by noise in the temperature reconstruction (Eby et al., 2011; Frank et al., 2010). The value for the carbon cycle sensitivity they derive is lower than earlier estimates (Cox and Jones, 2008).

10.9.4.6 Combining Evidence and Overall Assessment

In summary, most studies find a lower 5% limit for ECS between 1°C and 2°C (see Figure 10.24). The combined evidence thus indicates that the net feedbacks to radiative forcing are significantly positive and emphasizes that the greenhouse warming problem will not be small. Presently, there is no credible individual line of evidence which yields very high or very low climate sensitivity as best estimate. Some recent studies suggest a low climate sensitivity (Chylek et al., 2007; Lindzen and Choi, 2009; Schwartz et al., 2007), which, however, use problematic assumptions, neglect internal variability, underestimate uncertainties in data, use unrealistic climate response times or a combination of these (Knutti et al., 2008; Lin et al., 2010; Murphy and Forster, 2010). In some cases these results have been refuted by testing the method of estimation with a climate model with known sensitivity.

The difficulty in constraining the upper tail of ECS, which is clearly illustrated in Figure 10.24, is due to a variety of reasons. For estimates based on climate feedbacks, for which Roe and Baker (2007) point out that as the ECS is proportional to the inverse of feedbacks, long tails originate from normal uncertainty distributions of feedbacks, and very large values can occur if feedbacks were small. However, the reason that probability density functions for climate sensitivity are long-tailed is different for different lines of evidence. Estimates based on 20th century warming are long-tailed because large climate sensitivity could be reconciled with observations if either a very large aerosol forcing had prevented the large greenhouse gas response from being visible, or if very fast and large ocean heat uptake would lead to a larger part of the heat than presently estimated being absorbed by the ocean, reducing the surface temperature warming (Forest et al., 2002; Frame et al., 2006; Hannart et al., 2009; Roe and Baker, 2007). These uncertainties could be reduced if aerosol forcing and ocean heat uptake were known better (Urban and Keller, 2009).

Several authors (Annan and Hargreaves, 2006, 2010; Hegerl et al., 2006) have proposed combining estimates of climate sensitivity from different lines of evidence. This formalizes the realization that if independent data point at similar values for ECS, the evidence strengthens, and the uncertainties reduce. However, if several climate properties are estimated simultaneously that are not independent, such as ECS and ocean heat uptake, then combining evidence requires combining joint probabilities rather than multiplying marginal posterior PDFs (Hegerl et al., 2006; Henriksson et al., 2010). Neglected uncertainties will become increasingly important as multiple lines of evidence combined reduce other uncertainties, and the assumption that the climate models simulate changes in feedbacks correctly between the different climate states may be too strong, particularly for simpler models. All this may lead to overly confident assessments, a reason why results combining multiple lines of evidence are still treated with caution. It should also be cautioned that ECS, while independent of climate state to first order, does nonetheless vary somewhat with climate state as individual feedbacks become weaker or stronger: whether it increases or decreases with temperature is model dependent (e.g., Boer and Yu, 2003).

[INSERT FIGURE 10.24 HERE]
Figure 10.24: [DRAFT / SKETCH OF FIGURE IN PLAN] Estimates of equilibrium climate sensitivity from observed / reconstructed changes in climate compared to overall assessed range (to be determined; grey). The estimates are generally based on comparisons of model evidence (ranging from 0-D EBMs through OAGCMs) with given sensitivity with data for climate change and are based on instrumental changes including surface temperature; estimates based on changes in top-of-the atmosphere radiative balance (2nd row); climate change over the last millennium; volcanic eruptions; changes in the last glacial maximum (only showing model-based estimates since these more completely account for uncertainty), and deep time studies (see Chapter 5). The boxes on the right hand side indicate if a condition is fullfilled (green), partly fulfilled (yellow) or problematic (red); assessing advantages and shortcomings/uncertainties of different lines of evidence (Knutti and Hegerl, 2008).

10.9.5 Consequences for Aerosol Forcing and Ocean Heat Uptake

Murphy et al. (2009) use correlations between surface temperature and outgoing shortwave and longwave flux to estimate how much of the total recent forcing has been reduced by aerosol total reflection, which they estimate as -1.1 ± 0.4 W/m^2 from 1970 to 2000 (1 standard deviation) after estimating the rate of heat taken up by ocean (using a range of estimates of ocean warming) and earth, thus ruling out very large indirect aerosol effects.

Forest et al. (2008) updated their estimates of the probability density functions (PDF) of climate system properties (climate sensitivity - S_{eff}, rate of deep ocean heat uptake or global mean vertical diffusivity coefficient - K_v, and the strength of net aerosol forcing - F_{aer}) from Forest et al. (2006). They use a newer version of the MIT 2-D model and a collection of AOGCMs from CMIP3. They find that the ocean heat uptake in the majority of the CMIP3 models lies above the median value based on observational constraints, resulting in a positive bias in their ocean heat uptake. They explore the robustness of their results by systematically examining the sensitivity of the PDFs for S_{eff}, F_{aer}, and K_v to various diagnostics (the pattern of upper air, ocean, and surface temperature changes). Whereas the PDFs for S_{eff} and F_{aer} are not affected much, the constraint on K_v is weakened by removal of any of the diagnostics but the mode of the distribution is fairly robust. On the whole, they find a clear indication that the AOGCMs overestimate the rate of deep-ocean heat uptake suggesting that the results are biased low for projected surface temperature changes while biased high for sea level rise due to thermal expansion of sea water.

10.10 Synthesis

[PLACEHOLDER FOR FIRST ORDER DRAFT: this section will provide a synthesis of evidence across the climate system, analogous to what was done in Section 9.7 of the AR4 WGI. For the ZOD we draw together evidence from across the chapter in the Excutive Summary.]

[START FAQ 10.1 HERE]

FAQ 10.1: Climate Is Always Changing. How Do We Determine the Most Likely Causes of the Observed Changes?

One of the great triumphs of 20th century climate science was the quantitative documentation of profound climate changes throughout Earth's history. We now know that climate is never static or stationary, and that climate has undergone dramatic swings in the distant past, including growth and retreat of huge continental ice sheets. Paleoclimate evidence shows that after the termination of the Younger Dryas, during the climatic period known as the Holocene, global changes have been considerably more subtle than ice age fluctuations. Continent-scale ice sheets on Earth have been confined to Greenland and Antarctica, with considerable sea ice across the Arctic Sea and seasonally variable sea ice around Antarctica. Global temperature changes of less than 1°C have occurred on decade-to-century scales during this relatively warm phase during the most recent 10,000 years of Earth history (Chapter 5).

There are several well-known mechanisms that are known to cause climate to change on decadal to centennial time scales during this period, and all of them are significant for Earth's changing climate today. Each of the following climate change mechanisms is considered and included in the climate modeling studies assessed in this report.

Internal climate variability is driven by processes internal to the atmosphere and ocean, and causes *variations in climate on a range of timescales*. Ocean current anomalies move large amounts of heat around the upper ocean, and are the dominant drivers of internal variability in atmospheric temperatures on decadal to centennial timescales. The El Niño-Southern Oscillation cycle in the Pacific Ocean is the best-known mode of oceanic oscillation. During warm El Niño events the tropical Pacific Ocean loses a vast amount of heat to the atmosphere, causing measurable global atmospheric temperature increases for a year or so. Other, longer-term modes of variability have been documented including the Pacific Decadal Oscillation (PDO/IPO) and the Atlantic multidecadal oscillation (AMO) which can produce sustained temperature anomalies in some regions over many decades, with characteristic spatial patterns. These naturally occurring fluctuations occur without any external forcing at all.

Solar variability occurs on a range of timescales. Solar brightness varies periodically over 11-year cycles, which can be tracked by monitoring sunspots. More recently, instruments on satellites measure solar radiation fluctuations directly. From these measurements, and from records of sunspot counts extending back to the invention of the telescope, we can estimate changes in solar brightness in the past, although there are still substantial uncertainties.

Aerosols in the atmosphere block some sunlight from reaching the surface, and increase the greenhouse effect**.** Overall, increased aerosols generally force cooling of the surface temperature, although some aerosols also absorb radiation and can lead to warming. Fluctuations in aerosol concentrations occur both naturally and anthropogenically. ***Volcanic eruptions*** can disrupt global climate for several years following a major explosive event that injects aerosols into the stratosphere. ***Human emissions*** of sulphur dioxide, soot and other aerosol precursors lead to large-scale clouds of aerosols in the troposphere.

Land surface anomalies affect the exchange of heat and water between the continents and the overlying atmosphere. Land surface changes, such as deforestation, can affect local climate very strongly (see FAQ 10.2).

Enhancement of the Greenhouse Effect due to anthropogenic Greenhouse Gas emissions — primarily fossil fuel burning and disruption of the natural carbon cycle due to land use changes — has provided a significant, and ever-increasing, global forcing since the Industrial Revolution, as documented in Chapter 8.

Determining the most likely causes of observed changes involves first assessing whether a change in climate is different, in a statistical sense, from climate fluctuations due to internal variability of the climate system (which includes processes such as the El Niño-Southern Oscillation). A threshold that is often chosen for this likelihood is <5%. In this case an observed change would only be regarded as significant if there is less than a 5% chance that natural internal processes can explain it.

Once a change has been detected, attribution attempts to determine the most likely causes of the observed change. Attribution relies on a comparison of observed changes with the patterns of change associated with different climate forcing factors, and determines the most likely explanation for the observed change. With longer records of observed climate change, plus better estimates of the climate forcing associated with the mechanisms above, and improved dynamical models, there are multiple ways to compare forcing mechanisms with climate change, in order to attribute the observed changes to constituent causes.

For robust attribution of an observed change, the spatial pattern and/or time evolution of an observed change is compared with a variety of explanations for that change, often based on climate models. Climate models can simulate what would happen in response to the various forcing factors described above, both in isolation and in combination with each other. Detection and attribution methods determine which combinations of the response to forcings match the observed change, and when those responses need to be scaled up or down to best match the observations. For example, attribution methods may be used to assess whether temperature changes over the past century are consistent with a response to solar and volcanic forcings variations alone, or whether human-induced forcings also need to be considered. As climate variability is inherently random and not predictable on timescales relevant here, detection and attribution methods need to allow for climate variability masking the response to forcings.

Such attribution studies can be carried out using coupled atmosphere-ocean models, which allows both spatial and temporal aspects of the observed changes to be considered. They may also be carried out by directly comparing for example global mean temperature evolution directly with estimates of the evolution of the various radiative forcings, or with the response to those forcings predicted with simple models, such as energy balance models. Robust conclusions can be drawn when many different approaches, examining a variety of different datasets and using different models point at the same explanation.

Examining the various forcings that can affect climate shows that that current estimates of average climate forcing since the Industrial Revolution suggest that the net effect of increases in well mixed greenhouse gas concentrations is considerably larger than the other known forcing agents during that 260-year period. This assumes though that the climate responds to radiative forcing, something that detection and attribution studies evaluate rather than assume.

Analysing timeseries of global surface temperatures and forcings can point to possible links between forcings and global temperature. Correlations between a range of possible forcing mechanisms and global surface temperatures show that anthropogenic forcings dominate warming over the last 100 years with solar forcings contributing negligible long term warming since 1980. However care needs to be taken in interpreting such analyses since they make simple assumptions about the climate response to forcing, and all relevant external influences need to be considered otherwise results can be misleading.

The most sophisticated approach is to controlled dynamical model experiments to test the climatic response to each of these forcings independently and collectively. This approach has the advantage that the response of the climate system to particular forcings is characterized more comprehensively. For example, controlled model experiments can be designed to examine the difference in simulated climate variations with, and without, the inclusion of changing greenhouse gas concentrations. If observed climate variations exhibit changes that are only consistent with greenhouse gas-forced simulated climate, this provides evidence that observed change can be attributed, at least in part, to greenhouse gas forcing. This chapter assesses the results of many such studies that have been carried out recently with coupled ocean-atmosphere models.

Detection and attribution analyses, which analyse the outputs of coupled climate models and which quantify the contributions of anthropogenic and natural forcings to observed surface temperature changes, show that the dominant contributor to the overall warming trend since the early and mid 20th century is greenhouse gases. The changes observed in surface temperature (including greater warming at high latitudes and over land areas), in the free atmosphere (cooling in the stratosphere and warming in the troposphere) and in the ocean (warming spreading from the surface to depth) are consistent with the distinctive fingerprints of climate response expected from human influence and different in character from the dominant modes of decadal variability (including the AMO and the PDO) and the expected response to natural forcings from changes in solar output and from explosive volcanic eruptions. A further wealth of evidence from across the climate system, including changes in the water cycle, ocean properties and the cryosphere, points the same way: to the dominant role played by well mixed greenhouse gases on warming observed over recent decades.

Other forcings, including variability in tropospheric and stratospheric aerosols, stratospheric water, and solar output, as well as internal modes of variability, have contributed to the year to year and decade to decade variability of the climate system. In some regions of the world they are likely to have played a larger role in the evolution of local temperatures (See FAQ 10.2). At such scales, further progress in detection and attribution can be expected in the future as climate evolves and long-term climate change signals strengthen, and as models improve by having higher resolution and incorporation of more forcings and processes.

[INSERT FAQ 10.1, FIGURE 1 HERE]

FAQ 10.1, Figure 1: Top part: Comparison between trends over 1979–2010 as observed (top row) and as averaged over the CMIP3 and available CMIP5 datasets when they include anthropogenic and natural forcings (middle row) and when they include only natural forcings (bottom row). Data shown only where observational data are available in the HadCRUT3 dataset. Boxes in 2nd and 3rd rows show where 5 to 95 percentile of model range lies above or below observational value at that grid box. Bottom: Observed pattern of temperature response associated with PDO/IPO (top row) and AMO (bottom row) and their associated timeseries. After (Parker et al., 2007).

[END FAQ 10.1 HERE]

[START FAQ 10.2 HERE]

FAQ 10.2: When Will Human Influences on Climate be Obvious on Local Scales?

Some human influences on local climate have already been detected, and are readily attributed to human causes. For example, anthropogenic (human-caused) land surface changes can have profound local effects on climate. The best-known such climate perturbations are associated with large cities, which have local climates quite distinct from the surrounding countryside. In large industrialized cities, such as London and

Tokyo, temperature in downtown areas can be routinely warmer than the surrounding rural countryside by 1°C or more.

The particulate air pollution generated in large cities, and by large coal-burning power plants, has also clearly affected local climates. Clean air regulations have been proven to effectively reduce particulate air pollution in the countries that have implemented them, notably in North America and Europe. However the increasing depth and spatial extent of large-scale pollution plumes during the past century has been so pronounced that anthropogenic aerosol forcing is now considered to have a very significant effect on the global surface energy budget (Chapter 8), partly cancelling the effects of increasing greenhouse gases.

Other human-caused land surface changes can also have large local effects. Diverting the inflow into the Aral Sea for irrigation in the late 20th Century resulted in severe contraction of the extent of water covered surface. This has led to pronounced environmental effects and a significantly changed climate in the vicinity of the Aral Sea: warmer summers, colder winters, and lower humidity, all consistent with the replacement of a large water-covered surface with bare soil in a mid-continental location.

But what about anthropogenic climate change associated with increased greenhouse gas concentrations? This is generally harder to detect on local scales compared to global scales. Unlike the local forcing mechanisms discussed above, GHGs quickly become well-mixed in the atmosphere and the climate "signal" associated with greenhouse gas increases tends to be large in scale while the "noise" in the climate record due to individual weather events is more pronounced on local scales compared to global scales.

Specifically, *temperature advection* is the cause of most local temperature variability. Cold advection occurs when winds blow from a cold region toward a warmer region, thereby colder temperature downwind; warm advection is the opposite. Outside the tropics, this means that a large fraction of temperature variability is simply associated with shifting winds: when winds blow equatorward the temperature is colder, and when winds shift toward the pole then temperatures become warmer. Such shifts can occur from year to year as large-scale ridges and troughs change position or amplitude. The effects of advection, which are so pronounced in many areas, are reduced substantially if temperatures are averaged over the entire Earth.

Therefore, the climatic effects of global influences on climate, such as increasing greenhouse gases are most readily detected on global scales. Nevertheless the warming signal from human influences is sufficiently strong that it would be expected to have emerged above the noise of natural internal variability in many places. There are a number of ways of representing the natural internal variability that is experienced in a locality and comparing it to systematic long term changes. One is to determine whether observed or simulated long term trends are unusual compared to estimates of the 30- or 50-year warming trends that could result from natural internal variability at that locality (as is done in standard detection and attribution studies). Such analyses show that about many individual 5 x 5 degree grid boxes show significant warming trends already.

[Update this analysis to 2010; do an analysis which demonstrates when trends expected to emerge.]

Another measure of unusual warming at a locality is to determine whether long term warming trends or changes are outside the normal range of expected year to year variability. This measure determines whether the expected temperature, averaged over a number of years in a locality, is now unusual compared to previous non-industrial climate. Such an analysis over land areas shows that a local warming signal that exceeds past year to year variability has already emerged or will emerge in the next two decades in tropical regions. The local warming signal emerges first in the tropics, because the natural variability is less there than in other parts of the globe.

Local warming signals are expected to emerge later at higher latitudes, where climate varies substantially more than in the tropics, and for high northern latitudes not until the middle of the 21st century (Mahlstein et al., 2011).

While a warming signal might be expected to have emerged in some places above the noise of natural variability already and in the next few decades in others, attribution of the observed changes at local scales to different drivers is complicated by the greater role played by dynamical factors (circulation changes) and the effects of external climate drivers, which do not dominate at global scales, but which can be much more important in particular regions. Examples include land use changes and the effects of sulphate and carbonaceous aerosols.

Therefore, despite an expectation that climate change has already manifested itself at many localities around the world, attributing the changes at a specific location, and determining with high confidence that a large proportion of the particularities of the climate evolution in one location can be confidently ascribed to observed greenhouse gas increases, is in many cases still not possible. It is analgous to a prognosis that the health of a high proportion of heavy smokers has been adversely affected, and therefore that heavy smoking can have significant adverse effects on individuals. Yet confidently attributing one particular smoker's ill health to heavy smoking could be complicated by a multitude of other causal factors and the random effects of the expression of risk in the evolution of one individual's health.

Climate change is expected to lead to more frequent hot extremes, heat waves and heavy precipitation events in many areas. Individual extreme weather events cannot be unambiguously ascribed to climate change since such events could have happened in an unchanged climate. However, the odds of such events could have changed significantly at a particular location, "loading the weather dice", as it were. Statistical modelling may be required to infer from observational data series how the extremes of the distribution are changing, or dynamical modelling to simulate climate states with and without anthropogenic drivers (see FAQ 10.1 for a discussion of attribution techniques). There is evidence that human-induced increases in greenhouse gases may have contributed substantially to the probability of some heatwaves and may have contributed to the observed intensification of heavy precipitation events found over large data-covered parts of the northern hemisphere. The probability of other events, including some cold spells, may have reduced while the probability of many other extreme weather events may not have changed substantially.

A full answer to the question as to when human influence on climate — as a result of anthropogenic increases in greenhouse gas concentrations — will be obvious on local scales depends on a consideration of what strength of evidence is required to render something obvious to someone. But the most convincing scientific evidence for the effect of climate change on local scales comes from analysing the global picture, and the wealth of evidence from across the climate system linking observed changes to human influence.

[INSERT FIGURE FAQ 10.2, FIGURE 1 HERE]

FAQ 10.2, Figure 1: The map shows the global temperature increase (^{o}C) needed for a single location to undergo a statistical significant change in average summer seasonal surface temperature, aggregated on a country level. The black line near the colorbar denotes the committed global average warming if all atmospheric consistuents were fixed at 2000 levels. The small panels show the interannual summer-season variability during the base period (1900–1929) (±2 standard deviations shaded in gray) and the multi model summer surface temperature (red line) of one arbitrarily chosen grid cell within the specific country. The shading in red indicates the 5% and 95% quantiles across all model realizations. From Mahlstein et al. (2011, submitted to PNAS).

[END FAQ 10.2 HERE]

References

AchutaRao, K. M., B. D. Santer, P. J. Gleckler, K. E. Taylor, D. W. Pierce, T. P. Barnett, and T. M. L. Wigley, 2006: Variability of ocean heat uptake: Reconciling observations and models. *Journal of Geophysical Research*, **111,** C05019.

AchutaRao, K. M., et al., 2007: Simulated and observed variability in ocean temperature and heat content. *Proceedings of the National Academy of Sciences*, **104,** 10768-10773.

Adams, J., M. Mann, and C. Ammann, 2003: Proxy evidence for an El Nino-like response to volcanic forcing. *Nature*, 274-278.

Ahlmann, H. W., 1948: The present climate fluctuation. 165-195.

Alekseev, G., A. Danilov, V. Kattsov, S. Kuz'mina, and N. Ivanov, 2009: Changes in the climate and sea ice of the Northern Hemisphere in the 20th and 21st centuries from data of observations and modeling. *Izvestiya Atmospheric and Oceanic Physics*, 675-686.

Alexander, L. V., and J. M. Arblaster, 2009: Assessing trends in observed and modelled climate extremes over Australia in relation to future projections. *International Journal of Climatology*, **29,** 417-435.

Alexander, L. V., et al., 2006: Global observed changes in daily climate extremes of temperature and precipitation. *Journal of Geophysical Research*, **111**.

Allan, R., and B. Soden, 2007: Large discrepancy between observed and simulated precipitation trends in the ascending and descending branches of the tropical circulation. *Geophysical Research Letters*, -.

——, 2008: Atmospheric warming and the amplification of precipitation extremes. *Science*, 1481-1484.

Allan, R., B. Soden, V. John, W. Ingram, and P. Good, 2010: Current changes in tropical precipitation. *Environmental Research Letters*, -.

Allen, M., 2007: Scientific challenges in the attribution of harm. *University of Pennsylvania Law Review*, **155,** 1353-1400.

Allen, M., and W. Ingram, 2002: Constraints on future changes in climate and the hydrologic cycle. *Nature*, 224-+.

Allen, M., P. Stott, J. Mitchell, R. Schnur, and T. Delworth, 2000: Quantifying the uncertainty in forecasts of anthropogenic climate change. *Nature*, 617-620.

Allen, M. R., 2003: Liability for climate change. 891-892.

Allen, R. J., and S. C. Sherwood, 2008: Warming maximum in the tropical upper troposphere deduced from thermal winds. *Nature Geoscience*, **1,** 399-403.

Ammann, C. M., F. Joos, D. S. Schimel, B. L. Otto-Bliesner, and R. A. Tomas, 2007: Solar influence on climate during the past millennium: Results from transient simulations with the NCAR Climate System Model. *Proceedings of the National Academy of Sciences of the United States of America*, **104,** 3713-3718.

Anderson, B. T., 2004: Investigation of a large-scale mode of ocean-atmosphere variability and its relation to tropical Pacific sea surface temperature anomalies. *Journal of Climate*, **17,** 4089-4098.

Andreae, M., C. Jones, and P. Cox, 2005: Strong present-day aerosol cooling implies a hot future. *Nature*, 1187-1190.

Annan, J., and J. Hargreaves, 2006: Using multiple observationally-based constraints to estimate climate sensitivity. *Geophysical Research Letters*, -.

——, 2010: Reliability of the CMIP3 ensemble. *Geophysical Research Letters*, -.

Aoki, S., N. Bindoff, and J. Church, 2005: Interdecadal water mass changes in the Southern Ocean between 30 degrees E and 160 degrees E. *Geophysical Research Letters*, -.

Arzhanov, M. M., A. V. Eliseev, P. F. Demchenko, and I. I. Mokhov, 2007: Modeling of changes in temperature and hydrological regimes of subsurface permafrost, using the climate data (reanalysis). *Kriosfera Zemli (Earth Cryosphere)*, **11,** 65-69.

Ashok, K., and T. Yamagata, 2009: CLIMATE CHANGE The El Nino with a difference. *Nature*, **461,** 481-+.

Barnett, T., D. Pierce, K. Achutarao, P. Gleckler, B. Santer, J. Gregory, and W. Washington, 2005: Penetration of Human-Induced Warming into the World's Oceans. *Science*, **309,** 284-287.

Barnett, T. P., et al., 2008: Human-induced changes in the hydrology of the western United States. *Science*, **319,** 1080-1083.

Beer, J., 2006: Solar variability and climate change. *Solar Variability and Earth's Climate*, 751-754.

Beer, J., J. Abreu, and F. Steinhilber, 2009: Sun and planets from a climate point of view. *Universal Heliophysical Processes*, 29-43.

Bender, F., 2008: A note on the effect of GCM tuning on climate sensitivity. *Environmental Research Letters*, -.

Bender, F., A. Ekman, and H. Rodhe, 2010: Response to the eruption of Mount Pinatubo in relation to climate sensitivity in the CMIP3 models. *Climate Dynamics*, 875-886.

Benestad, R. E., and G. A. Schmidt, 2009: Solar trends and global warming. *Journal of Geophysical Research-Atmospheres*, **114**.

Bengtsson, L., and K. I. Hodges, 2009: On the evaluation of temperature trends in the tropical troposphere. *Clim. Dyn.*

Bengtsson, L., V. Semenov, and O. Johannessen, 2004: The early twentieth-century warming in the Arctic - A possible mechanism. *Journal of Climate*, 4045-4057.

Bengtsson, L., K. I. Hodges, E. Roeckner, and R. Brokopf, 2006: On the natural variability of the pre-industrial European climate. *Clim Dyn*, **27,** 17.

Bengtsson, L., K. I. Hodges, M. Esch, N. Keenlyside, L. Kornblueh, J. J. Luo, and T. Yamagata, 2007: How may tropical cyclones change in a warmer climate? *Tellus.Series A: Dynamic Meteorology and Oceanography*, **59(4),** 539-561.
Berliner, L., R. Levine, and D. Shea, 2000: Bayesian climate change assessment. *Journal of Climate***,** 3805-3820.
Bhend, J., and H. von Storch, 2008: Consistency of observed winter precipitation trends in northern Europe with regional climate change projections. *Climate Dynamics*, **31,** 17-28.
Bindoff, N., and T. McDougall, 2000: Decadal changes along an Indian ocean section at 32 degrees S and their interpretation. *Journal of Physical Oceanography***,** 1207-1222.
Bindoff, N. L., et al., 2007: Observations: Oceanic Climate Change and Sea Level. *Climate Change 2007: The Physical Science Basis. Contribution of Working Group I to the Fourth Assessment Report of the Intergovernmental Panel on Climate Change*, Cambridge University Press.
Bjerknes, J., 1959: The recent warming of the North Atlantic. The Rockefeller Institute Press, New York.
Blackburn, M., and B. J. Hoskins, in preparation: Atmospheric variability and extreme autumn rainfall in the UK.
Boe, J., A. Hall, and X. Qu, 2009: September sea-ice cover in the Arctic Ocean projected to vanish by 2100. *Nature Geoscience***,** 341-343.
Boer, G., M. Stowasser, and K. Hamilton, 2007: Inferring climate sensitivity from volcanic events. *Climate Dynamics***,** 481-502.
Bond, G., et al., 2001: Persistent solar influence on north Atlantic climate during the Holocene. *Science***,** 2130-2136.
Bonfils, C., P. B. Duffy, B. D. Santer, T. M. L. Wigley, D. B. Lobell, T. J. Phillips, and C. Doutriaux, 2008: Identification of external influences on temperatures in California. *Climatic Change*, **87,** S43-S55.
Boyer, T., S. Levitus, J. Antonov, R. Locarnini, and H. Garcia, 2005: Linear trends in salinity for the World Ocean, 1955-1998. *Geophysical Research Letters***,** -.
Brayshaw, D. J., B. Hoskins, and M. Blackburn, 2008: he Storm-Track Response to Idealized SST Perturbations in an Aquaplanet GCM. *Journal of Atmospheric Sciences*, **65,** 2842–2860.
Brohan, P., J. J. Kennedy, I. Harris, S. F. B. Tett, and P. D. Jones, 2006: Uncertainty estimates in regional and global observed temperature changes: A new data set from 1850. *Journal of Geophysical Research-Atmospheres*, **111**.
Bronnimann, S., 2009: Early twentieth-century warming. *Nature Geoscience***,** 735-736.
Brown, R., and P. Mote, 2009: The Response of Northern Hemisphere Snow Cover to a Changing Climate. *Journal of Climate***,** 2124-2145.
Brown, S. J., J. Caesar, and C. A. T. Ferro, 2008: Global changes in extreme daily temperature since 1950. *Journal of Geophysical Research-Atmospheres*, **113**.
Budikova, D., 2009: Role of Arctic sea ice in global atmospheric circulation: A review. *Global and Planetary Change***,** 149-163.
Burke, E. J., S. J. Brown, and N. Christidis, 2006: Modeling the recent evolution of global drought and projections for the twenty-first century with the Hadley Centre climate model. *Journal of Hydrometeorology*, **7(5),** 1113-1125.
Caesar, J., L. Alexander, and R. Vose, 2006: Large-scale changes in observed daily maximum and minimum temperatures: Creation and analysis of a new gridded data set. *Journal of Geophysical Research*, **111**.
Cai, W., T. Cowan, and A. Sullivan, 2009: Recent unprecedented skewness towards positive Indian Ocean Dipole occurrences and its impact on Australian rainfall. *Geophysical Research Letters*, **36**.
Cattiaux, J., R. Vautard, C. Cassou, P. Yiou, V. Masson-Delmotte, and F. Codron, 2010: Winter 2010 in Europe: A cold extreme in a warming climate. *Geophysical Research Letters***,** -.
Chang, P., et al., 2007: Pacific meridional mode and El Nino-southern oscillation. *Geophysical Research Letters*, **34**.
Chapman, W., and J. Walsh, 2007: Simulations of Arctic temperature and pressure by global coupled models. *Journal of Climate***,** 609-632.
Cheng, G., and T. Wu, 2007: Responses of permafrost to climate change and their environmental significance, Qinghai-Tibet Plateau. *Journal of Geophysical Research*, **112**.
Chinn, T., S. Winkler, M. Salinger, and N. Haakensen, 2005: Srecent glacier advances in Norway and New Zealand: A comparison of their glaciological and meteorological causes. *Geografiska Annaler Series a-Physical Geography***,** 141-157.
Choi, G., D. Robinson, and S. Kang, 2010: Changing Northern Hemisphere Snow Seasons. *Journal of Climate***,** 5305-5310.
Christidis, N., P. A. Stott, and S. J. Brown, 2011a: The role of human activity in the recent warming of extremely warm daytime temperatures.
Christidis, N., P. A. Stott, S. Brown, G. Hegerl, and J. Caesar, 2005: Detection of changes in temperature extremes during the second half of the 20th century. *Geophysical Research Letters*, **32**.
Christidis, N., P. A. Stott, F. W. Zwiers, H. Shiogama, and T. Nozawa, 2010: Probabilistic estimates of recent changes in temperature: a multi-scale attribution analysis. *Climate Dynamics*, **34,** 1139-1156.
Christidis, N., P. A. Stott, G. S. Jones, H. Shiogama, T. Nozawa, and J. Luterbacher, 2011b: Human activity and anomalously warm seasons in Europe. *International Journal of Climatology*.
Christy, J. R., et al., 2010: What do observational datasets say about modeled tropospheric temperature trends since 1979? *Remote Sens.*, **2,** 2148-2169.
Chung, E., B. Soden, and B. Sohn, 2010: Revisiting the determination of climate sensitivity from relationships between surface temperature and radiative fluxes. *Geophysical Research Letters***,** -.

Church, J., N. White, and J. Arblaster, 2005: Significant decadal-scale impact of volcanic eruptions on sea level and ocean heat content. *Nature*, **438,** 74-77.
Chylek, P., and U. Lohmann, 2008a: Aerosol radiative forcing and climate sensitivity deduced from the last glacial maximum to Holocene transition. *Geophysical Research Letters*, -.
——, 2008b: Reply to comment by Andrey Ganopolski and Thomas Schneider von Deimling on "Aerosol radiative forcing and climate sensitivity deduced from the Last Glacial Maximum to Holocene transition". *Geophysical Research Letters*, -.
Chylek, P., U. Lohmann, M. Dubey, M. Mishchenko, R. Kahn, and A. Ohmura, 2007: Limits on climate sensitivity derived from recent satellite and surface observations. *Journal of Geophysical Research-Atmospheres*, **112**.
Comiso, J., and F. Nishio, 2008: Trends in the sea ice cover using enhanced and compatible AMSR-E, SSM/I, and SMMR data. *Journal of Geophysical Research-Oceans*, -.
Cook, B. I., R. L. Miller, and R. Seager, 2008: Dust and sea surface temperature forcing of the 1930s "Dust Bowl" drought. *Geophysical Research Letters*, **35,** 5.
Cook, E., R. Seager, M. Cane, and D. Stahle, 2007: North American drought: Reconstructions, causes, and consequences. *Earth-Science Reviews*, 93-134.
Cox, P., and C. Jones, 2008: Climate change - Illuminating the modern dance of climate and CO_2. *Science*, 1642-1644.
Curry, R., B. Dickson, and I. Yashayaev, 2003: A change in the freshwater balance of the Atlantic Ocean over the past four decades. *Nature*, 826-829.
Dean, S. M., and P. A. Stott, 2009: The Effect of Local Circulation Variability on the Detection and Attribution of New Zealand Temperature Trends. *Journal of Climate*, **22,** 6217-6229.
Delworth, T., V. Ramaswamy, and G. Stenchikov, 2005: The impact of aerosols on simulated ocean temperature and heat content in the 20th century. *Geophysical Research Letters*, **32,** L24709.
Delworth, T. L., and T. R. Knutson, 2000: Simulation of Early 20th Century Global Warming. *Science*, **287,** 5.
Deo, R. C., J. I. Syktus, C. A. McAlpine, P. J. Lawrence, H. A. McGowan, and S. R. Phinn, 2009: Impact of historical land cover change on daily indices of climate extremes including droughts in eastern <country-region>Australia</country-region>. *Geophysical Research Letters*, **36(L08705)**.
Dery, S. J., and R. D. Brown, 2007: Recent Northern Hemisphere snow cover extenet trends and implications for the snow-albedo feedback. *Geophysical Research Letters*, **34,** 6.
Deser, C., and H. Teng, 2008: Evolution of Arctic sea ice concentration trends and the role of atmospheric circulation forcing, 1979-2007. *Geophysical Research Letters*, -.
Deser, C., A. S. Phillips, and M. A. Alexander, 2010a: Twentieth century tropical sea surface temperature trends revisited. *Geophysical Research Letters*, **37**.
Deser, C., R. Tomas, M. Alexander, and D. Lawrence, 2010b: The Seasonal Atmospheric Response to Projected Arctic Sea Ice Loss in the Late Twenty-First Century. *Journal of Climate*, 333-351.
Deutsch, C., S. Emerson, and L. Thompson, 2005: Fingerprints of climate change in North Pacific oxygen (vol 32, art no L16604, 2005). *Geophysical Research Letters*, -.
Dickson, R., et al., 2000: The Arctic Ocean response to the North Atlantic oscillation. *Journal of Climate*, 2671-2696.
Doherty, S., et al., 2009: LESSONS LEARNED FROM IPCC AR4 Scientific Developments Needed To Understand, Predict, And Respond To Climate Change. *Bulletin of the American Meteorological Society*, 497-+.
Dole, R., et al., 2011: Was there a basis for anticipating the 2010 Russian heat wave? *Geophys. Res. Lett.,*.
Domingues, C., J. Church, N. White, P. Gleckler, S. Wijffels, P. Barker, and J. Dunn, 2008: Improved estimates of upper-ocean warming and multi-decadal sea-level rise. *Nature*, **453,** 1090-1093.
Doscher, R., K. Wyser, H. Meier, M. Qian, and R. Redler, 2010: Quantifying Arctic contributions to climate predictability in a regional coupled ocean-ice-atmosphere model. *Climate Dynamics*, 1157-1176.
Douglass, D., E. Blackman, and R. Knox, 2004: Temperature response of Earth to the annual solar irradiance cycle (vol 323, pg 315, 2004). *Physics Letters a*, 175-176.
Douglass, D. H., J. R. Christy, B. D. Pearson, and S. F. Singer, 2008: A comparison of tropical temperature trends with model predictions. *International Journal of Climatology*, **28,** 1693-1701.
Downes, S., N. Bindoff, and S. Rintoul, 2009: Impacts of Climate Change on the Subduction of Mode and Intermediate Water Masses in the Southern Ocean. *Journal of Climate*, 3289-3302.
——, 2010: Changes in the Subduction of Southern Ocean Water Masses at the End of the Twenty-First Century in Eight IPCC Models. *Journal of Climate*, 6526-6541.
Durack, P., and S. Wijffels, 2010: Fifty-Year Trends in Global Ocean Salinities and Their Relationship to Broad-Scale Warming. *Journal of Climate*, 4342-4362.
Dutton, J. F., C. J. Poulsen, and J. L. Evans, 2000: The effect of global climate change on the regions of tropical convection in CSM1. *Geophysical Research Letters*, **27(19),** 3049-3052.
Easterling, D. R., and M. F. Wehner, 2009: Is the climate warming or cooling? *Geophysical Research Letters*, **36**.
Eby, M., A. Weaver, N. Gillett, and K. Zickfeld, 2011: Carbon feedbacks: Perils in looking back. *Geophysical Research Letters*, **in preparation**.
Edwards, T., M. Crucifix, and S. Harrison, 2007: Using the past to constrain the future: how the palaeorecord can improve estimates of global warming. *Progress in Physical Geography*, 481-500.

Eliseev, A. V., M. M. Arzhanov, P. E. Demchenko, and I. I. Mokhov, 2009: 2009: Changes in climatic characteristics of Northern Hemisphere extratropical land in the 21st century: Assessments with the IAP RAS climate model. *Izvestiya, Atmos. Ocean. Phys.*, **45,** 271-283.

Elsner, J. B., 2006: Evidence in support of the climate change–Atlantic hurricane hypothesis. *Geophysical Research Letters*.

Elsner, J. B., J. P. Kossin, and T. H. Jagger, 2008: The increasing intensity of the strongest tropical cyclones. *Nature*, **455(7209)**.

Emanuel, K., 2000: A statistical analysis of tropical cyclone intensity. *Monthly Weather Review*, **128(4),** 1139-1152.

——, 2005: Increasing destructiveness of tropical cyclones over the past 30 years. *Nature*, **436,** 686-688.

Emerson, S., Y. Watanabe, T. Ono, and S. Mecking, 2004: Temporal trends in apparent oxygen utilization in the upper pycnocline of the North Pacific: 1980-2000. *Journal of Oceanography*, 139-147.

Emori, S., and S. J. Brown, 2005: Dynamic and thermodynamic changes in mean and extreme precipitation under changed climate. *Geophysical Research Letters*, **32(L17706)**.

Eyring, V., T. G. Shepherd, and D. W. Waugh, 2010: SPARC Report on the Evaluation of Chemistry-Climate Models,. WCRP-132, WMO/TD-No. 1526.

Feldstein, S., 2002: The recent trend and variance increase of the annular mode. *Journal of Climate***,** 88-94.

Feng, S., R. J. Oglesby, C. M. Rowe, D. B. Loope, and Q. Hu, 2008: Atlantic and Pacific SST influences on Medieval drought in North America simulated by the Community Atmospheric Model. *Journal of Geophysical Research-Atmospheres*, **113**.

Fettweis, X., G. Mabille, M. Erpicum, S. Nicolay, and M. Van den Broeke, 2011: The 1958-2009 Greenland ice sheet surface melt and the mid-tropospheric atmospheric circulation. *Climate Dynamics***,** 139-159.

Feudale, L., and J. Shukla, 2007: Role of Mediterranean SST in enhancing the European heat wave of summer 2003. *Geophysical Research Letters*, **34**.

——, 2010: Influence of sea surface temperature on the European heat wave
of 2003 summer. Part I: an observational study. *Clim. Dyn.*

Fischer, E. M., and C. Schär 2010: Consistent geographical patterns of changes in high-impact European heatwaves. *Nature Geoscience*, **3,** 398-403.

Fischer, E. M., S. I. Seneviratne, P. L. Vidale, D. Luthi, and C. Schar, 2007: Soil moisture - Atmosphere interactions during the 2003 European summer heat wave. *Journal of Climate*, **20,** 5081-5099.

Fogt, R., J. Perlwitz, A. Monaghan, D. Bromwich, J. Jones, and G. Marshall, 2009: Historical SAM Variability. Part II: Twentieth-Century Variability and Trends from Reconstructions, Observations, and the IPCC AR4 Models. *Journal of Climate***,** 5346-5365.

Forest, C., P. Stone, and A. Sokolov, 2006: Estimated PDFs of climate system properties including natural and anthropogenic forcings. *Geophysical Research Letters***,** -.

——, 2008: Constraining climate model parameters from observed 20th century changes. *Tellus Series a-Dynamic Meteorology and Oceanography***,** 911-920.

Forest, C., P. Stone, A. Sokolov, M. Allen, and M. Webster, 2002: Quantifying uncertainties in climate system properties with the use of recent climate observations. *Science***,** 113-117.

Forster, P., and J. Gregory, 2006: The climate sensitivity and its components diagnosed from Earth Radiation Budget data. *Journal of Climate***,** 39-52.

Forster, P. M., et al., 2011: Stratospheric changes and climate, Chapter 4 in *Scientific Assessment of Ozone Depletion: 2010. Global Ozone Research and Monitoring Project-Report No. 52 (in press)*, P. M. Forster, et al., Ed., World Meteorological Organization.

Fowler, H. J., and R. L. Wilby, 2010: Detecting changes in seasonal precipitation extremes using regional climate model projections: Implications for managing fluvial flood risk. *Water Resources Research*, **46(W0525)**.

Frame, D., D. Stone, P. Stott, and M. Allen, 2006: Alternatives to stabilization scenarios. *Geophysical Research Letters***,** -.

Frame, D., B. Booth, J. Kettleborough, D. Stainforth, J. Gregory, M. Collins, and M. Allen, 2005: Constraining climate forecasts: The role of prior assumptions. *Geophysical Research Letters***,** -.

Frank, D. C., J. Esper, C. C. Raible, U. Buntgen, V. Trouet, B. Stocker, and F. Joos, 2010: Ensemble reconstruction constraints on the global carbon cycle sensitivity to climate, **463,** 6.

Franzke, C., 2010: Long-Range Dependence and Climate Noise Characteristics of Antarctic Temperature Data. *Journal of Climate***,** 6074-6081.

Frierson, D., J. Lu, and G. Chen, 2007: Width of the Hadley cell in simple and comprehensive general circulation models. *Geophysical Research Letters***,** -.

Frierson, D. M. W., 2006: Robust increases in midlatitude static stability in simulations of global warming. *Geophysical Research Letters*, **33**.

Fu, Q., C. M. Johanson, J. M. Wallace, and T. Reichler, 2006: Enhanced mid-latitude tropospheric warming in satellite measurements. *Science*, **312,** 1179-1179.

Fyfe, J. C., and B. Merryfield, 2011: Do dedadal forecasts capture the recent pause in global warming? , in preparation.

Fyfe, J. C., N. P. Gillett, and D. W. J. Thompson, 2010: Comparing variability and trends in observed and modelled global-mean surface temperature. *Geophysical Research Letters*, **37**.

Ganopolski, A., and T. Schneider von Deimling, 2008: Comment on "Aerosol radiative forcing and climate sensitivity deduced from the Last Glacial Maximum to Holocene transition" by Petr Chylek and Ulrike Lohmann. *Geophysical Research Letters*, -.
Gascard, J. C., and e. al, 2008: Exploring Arcitc transpolar drift during dramatic sea ice retreat. *EOS*, **89,** 3.
Gedney, N., P. M. Cox, R. A. Betts, O. Boucher, C. Huntingford, and P. A. Stott, 2006: Detection of a direct carbon dioxide effect in continental river runoff records. *Nature*, **439,** 835-838.
Giannini, A., R. Saravanan, and P. Chang, 2003: Oceanic forcing of Sahel rainfall on interannual to interdecadal time scales. *Science*, **302,** 1027-1030.
Giles, K., S. Laxon, and A. Ridout, 2008: Circumpolar thinning of Arctic sea ice following the 2007 record ice extent minimum. *Geophysical Research Letters*, -.
Gillett, N., 2005: Climate modelling - Northern Hemisphere circulation. *Nature*, 496-496.
Gillett, N., and D. Thompson, 2003: Simulation of recent Southern Hemisphere climate change. *Science*, 273-275.
Gillett, N., and P. Stott, 2009: Attribution of anthropogenic influence on seasonal sea level pressure. *Geophysical Research Letters*, -.
Gillett, N., A. Weaver, F. Zwiers, and M. Wehner, 2004: Detection of volcanic influence on global precipitation. *Geophysical Research Letters*, -.
Gillett, N. P., R. J. Allan, and T. J. Ansell, 2005: Detection of external influence on sea level pressure with a multi-model ensemble. *Geophysical Research Letters*, **32(L19714)**.
Gillett, N. P., P. A. Stott, and B. D. Santer, 2008a: Attribution of cyclogenesis region sea surface temperature change to anthropogenic influence. *Geophysical Research Letters*, **35**.
Gillett, N. P., G. C. Hegerl, M. R. Allen, and P. A. Stott, 2000: Implications of changes in the Northern Hemisphere circulation for the detection of anthropogenic climate change. *Geophysical Research Letters*, **27,** 993-996.
Gillett, N. P., et al., 2008b: Attribution of polar warming to human influence. *Nature Geoscience*, **1,** 750-754.
——, 2011: Attribution of observed changes in stratospheric ozone and temperature. *Atmos. Chem. Phys*, 599-609.
Giorgi, F., et al., 2001: Emerging patterns of simulated regional climatic changes for the 21st century due to anthropogenic forcings. *Geophysical Research Letters*, 3317-3320.
Gleckler, P. J., K. Achutarao, J. M. Gregory, B. D. Santer, K. E. Taylor, and T. M. L. Wigley, 2006a: Krakatoa lives: The effect of volcanic eruptions on ocean heat content and thermal expansion. *Geophysical Research Letters*, **33,** L17702.
Gleckler, P. J., T. M. L. Wigley, B. D. Santer, J. M. Gregory, K. AchutaRao, and K. E. Taylor, 2006b: Volcanoes and climate: Krakatoa's signature persists in the ocean. *Nature*, **439,** 675-675.
Goosse, H., W. Lefebvre, A. de Montety, E. Crespin, and A. Orsi, 2009: Consistent past half-century trends in the atmosphere, the sea ice and the ocean at high southern latitudes. *Climate Dynamics*, 999-1016.
Goosse, H., E. Crespin, A. de Montety, M. Mann, H. Renssen, and A. Timmermann, 2010: Reconstructing surface temperature changes over the past 600 years using climate model simulations with data assimilation. *Journal of Geophysical Research-Atmospheres*, -.
Goosse, H., et al., 2006: The origin of the European "Medieval Warm Period". *Climate of the Past*, 99-113.
Goswami, B. N., M. S. Madhusoodanan, C. P. Neema, and D. Sengupta, 2006: A physical mechanism for North Atlantic SST influence on the Indian summer monsoon. *Geophysical Research Letters*, **33**.
Gouretski, V., and K. Koltermann, 2007: How much is the ocean really warming? *Geophysical Research Letters*, **34,** L01610.
Graversen, R., and M. Wang, 2009: Polar amplification in a coupled climate model with locked albedo. *Climate Dynamics*, 629-643.
Gregory, J., 2000: Vertical heat transports in the ocean and their effect an time-dependent climate change. *Climate Dynamics*, 501-515.
Gregory, J. M., H. T. Banks, P. A. Stott, J. A. Lowe, and M. D. Palmer, 2004: Simulated and observed decadal variability in ocean heat content. *Geophysical Research Letters*, **31,** L15312.
Gregory, J. M., et al., 2001: Comparison of results from several AOGCMs for global and regional sea-level change 1900–2100. *Climate Dynamics*, **18,** 225-240.
Guilyardi, E., 2006: El Nino-mean state-seasonal cycle interactions in a multi-model ensemble. *Climate Dynamics*, **26,** 329-348.
Gutowski, W. J., et al., 2008: Causes of Observed Changes in Extremes and Projections of Future Changes. *Weather and Climate Extremes in a Changing Climate. Regions of Focus: North America, Hawaii, Caribbean, and U.S. Pacific Islands*, T. R. Karl, et al., Ed., A Report by the U.S. Climate Change Science Program and the Subcommittee on Global Change Research.
Haerter, J. O., and P. Berg, 2009: Unexpected rise in extreme precipitation caused by a shift in rain type? *Nature Geoscience*, **2(6),** 372-373.
Han, W., et al., 2010: Patterns of Indian Ocean sea-level change in a warming climate. *Nature Geoscience*, **3,** 546-550.
Hannart, A., J. Dufresne, and P. Naveau, 2009: Why climate sensitivity may not be so unpredictable. *Geophysical Research Letters*, -.
HANSEN, J., and S. LEBEDEFF, 1987: GLOBAL TRENDS OF MEASURED SURFACE AIR-TEMPERATURE. *Journal of Geophysical Research-Atmospheres*, 13345-13372.

Hansen, J., R. Ruedy, M. Sato, and K. Lo, 2010: GLOBAL SURFACE TEMPERATURE CHANGE. *Reviews of Geophysics*, **48**.
Hansen, J., et al., 2001: A closer look at United States and global surface temperature change. *Journal of Geophysical Research-Atmospheres*, **106,** 23947-23963.
——, 2005: Earth's energy imbalance: Confirmation and implications. *Science***,** 1431-1435.
HANSEN, J., et al., 2007: Climate simulations for 1880-2003 with GISS modelE. *CLIMATE DYNAMICS*, **29,** 661-696.
Hargreaves, J., A. Abe-Ouchi, and J. Annan, 2007: Linking glacial and future climates through an ensemble of GCM simulations. *Climate of the Past***,** 77-87.
Harries, J., and C. Belotti, 2010: On the Variability of the Global Net Radiative Energy Balance of the Nonequilibrium Earth. *Journal of Climate***,** 1277-1290.
Hasselmann, K., 1997: Multi-pattern fingerprint method for detection and attribution of climate change. *Climate Dynamics***,** 601-611.
Hawkins, E., and R. Sutton, 2009: THE POTENTIAL TO NARROW UNCERTAINTY IN REGIONAL CLIMATE PREDICTIONS. *Bulletin of the American Meteorological Society***,** 1095-+.
Hegerl, G., and F. Zwiers, 2011: Use of models in detection and attribution of climate change. Wiley.
Hegerl, G., T. Crowley, W. Hyde, and D. Frame, 2006: Climate sensitivity constrained by temperature reconstructions over the past seven centuries. *Nature***,** 1029-1032.
Hegerl, G., J. Luterbacher, F. Gonzalez-Rouco, S. F. B. Tett, T. Crowley, and E. Xoplaki, 2011: Influence of human and natural forcing on European seasonal temperatures. *Nature Geoscience*, published online 16 January 2011, 5.
Hegerl, G., T. Crowley, M. Allen, W. Hyde, H. Pollack, J. Smerdon, and E. Zorita, 2007a: Detection of human influence on a new, validated 1500-year temperature reconstruction. *Journal of Climate***,** 650-666.
Hegerl, G. C., et al., 2010: Good Practice Guidance Paper on Detection and Attribution Related to Anthropogenic Climate Change.
——, 2007b: Understanding and Attributing Climate Change. *Climate Change 2007: The Physical Science Basis. Contribution of Working Group I to the Fourth Assessment Report of the Intergovernmental Panel on Climate Change*, Cambridge University Press.
Held, I., and B. Soden, 2006a: Robust responses of the hydrological cycle to global warming. *Journal of Climate***,** 5686-5699.
Held, I., M. Winton, K. Takahashi, T. Delworth, F. Zeng, and G. Vallis, 2010: Probing the Fast and Slow Components of Global Warming by Returning Abruptly to Preindustrial Forcing. *Journal of Climate***,** 2418-2427.
Held, I. M., 2000: The general circulation of the atmosphere, 70 pp.
Held, I. M., and B. J. Soden, 2006b: Robust responses of the hydrological cycle to global warming. *Journal of Climate*, **19,** 5686-5699.
Helm, K., N. Bindoff, and J. Church, 2010: Changes in the global hydrological-cycle inferred from ocean salinity. *Geophysical Research Letters***,** -.
Henriksson, S., E. Arjas, M. Laine, J. Tamminen, and A. Laaksonen, 2010: Comment on 'Using multiple observationally-based constraints to estimate climate sensitivity' by J. D. Annan and J. C. Hargreaves, Geophys. Res. Lett., 2006. *Climate of the Past***,** 411-414.
Herweijer, C., and R. Seager, 2008: The global footprint of persistent extra-tropical drought in the instrumental era. *International Journal of Climatology*, **28,** 14.
Hidalgo, H. G., et al., 2009: Detection and Attribution of Streamflow Timing Changes to Climate Change in the Western United States. *Journal of Climate*, **22,** 3838-3855.
Hodge, S., D. Trabant, R. Krimmel, T. Heinrichs, R. March, and E. Josberger, 1998: Climate variations and changes in mass of three glaciers in western North America. *Journal of Climate***,** 2161-2179.
Hoerling, M., and A. Kumar, 2003: The perfect ocean for drought. *Science*, **299,** 691-694.
Hoerling, M., *D. Easterling*, *J.* P*erlwitz*, *J. E*ischeid, *P. Pegi*on, and *D. Murray*, 2011: An Assessment of 2010 North American Temperatures. *In: State of the climate in 2008*, submitted.
Hofmann, D., J. Barnes, M. O'Neill, M. Trudeau, and R. Neely, 2009: Increase in background stratospheric aerosol observed with lidar at Mauna Loa Observatory and Boulder, Colorado. *Geophysical Research Letters*, **36**.
Holland, D., R. Thomas, B. De Young, M. Ribergaard, and B. Lyberth, 2008: Acceleration of Jakobshavn Isbrae triggered by warm subsurface ocean waters. *Nature Geoscience***,** 659-664.
Holland, M., M. Serreze, and J. Stroeve, 2010: The sea ice mass budget of the Arctic and its future change as simulated by coupled climate models. *Climate Dynamics***,** 185-200.
Hosoda, S., T. Suga, N. Shikama, and K. Mizuno, 2009: Global Surface Layer Salinity Change Detected by Argo and Its Implication for Hydrological Cycle Intensification. *Journal of Oceanography***,** 579-586.
Hu, Y., and Q. Fu, 2007: Observed poleward expansion of the Hadley circulation since 1979. *Atmospheric Chemistry and Physics*, **7,** 5229-5236.
——, 2009: Stratospheric warming in Southern Hemisphere high latitudes since 1979. *Atmospheric Chemistry and Physics*, **9,** 4329-4340.
Hu, Y. Y., C. Zhou, and J. P. Liu, 2011: Observational Evidence for Poleward Expansion of the Hadley Circulation. *Advances in Atmospheric Sciences*, **28,** 33-44.

Hudson, R. D., M. F. Andrade, M. B. Follette, and A. D. Frolov, 2006: The total ozone field separated into meteorological regimes - Part II: Northern Hemisphere mid-latitude total ozone trends. *Atmospheric Chemistry and Physics*, **6,** 5183-5191.
Huntington, T. G., 2006: Evidence for intensification of the global water cycle: Review and synthesis. *Journal of Hydrology*, **319,** 83-95.
Huss, M., R. Hock, A. Bauder, and M. Funk, 2010: 100-year mass changes in the Swiss Alps linked to the Atlantic Multidecadal Oscillation. *Geophysical Research Letters*, -.
Huybers, P., 2010: Compensation between Model Feedbacks and Curtailment of Climate Sensitivity. *Journal of Climate*, **23,** 3009-3018.
Ihara, C., Y. Kushnir, and M. A. Cane, 2008: Warming trend of the Indian Ocean SST and Indian Ocean dipole from 1880 to 2004. *Journal of Climate*, **21,** 2035-2046.
Ingram, and William, 2006: Detection and attribution of climate change and understanding of solar influence on climate. *Space Science Reviews*, **125,** 199-211.
Izumo, T., et al., 2010: Influence of the state of the Indian Ocean Dipole on the following year's El Nino. *Nature Geoscience*, **3,** 168-172.
Jackson, J., E. Carmack, F. McLaughlin, S. Allen, and R. Ingram, 2010: Identification, characterization, and change of the near-surface temperature maximum in the Canada Basin, 1993-2008. *Journal of Geophysical Research-Oceans*, -.
Johannessen, O., et al., 2004: Arctic climate change: observed and modelled temperature and sea-ice variability (vol 56A, pg 328, 2004). *Tellus Series a-Dynamic Meteorology and Oceanography*, 559-560.
Johanson, C. M., and Q. Fu, 2009: Hadley Cell Widening: Model Simulations versus Observations. *Journal of Climate*, **22,** 2713-2725.
Johnson, G., and A. Orsi, 1997: Southwest Pacific Ocean water-mass changes between 1968/69 and 1990/91. *Journal of Climate*, 306-316.
Johnson, N. C., and S.-P. Xie, 2010: Changes in the sea surface temperature threshold for tropical convection. *Nature Geoscience*, **3(12),** 842-845.
Jones, G. S., P. A. Stott, and N. Christidis, 2008: Human contribution to rapidly increasing frequency of very warm Northern Hemisphere summers. *Journal of Geophysical Research-Atmospheres*, **113**.
Jones, G. S., N. Christidis, and P. A. Stott, 2010: Detecting the influence of fossil fuel and bio-fuel black carbon aerosols on near surface temperature changes. *Atmos. Chem. Phys. Discuss.*, 20921-20974.
Joshi, M., and G. Jones, 2009: The climatic effects of the direct injection of water vapour into the stratosphere by large volcanic eruptions. *Atmospheric Chemistry and Physics*, 6109-6118.
Jung, M., et al., 2010: Recent decline in the global land evapotranspiration trend due to limited moisture supply. *Nature*, **467,** 951-954.
Jungclaus, J., 2009: Lessons from the past millennium. *Nature Geoscience*, 468-470.
Jungclaus, J., et al., 2010: Climate and carbon-cycle variability over the last millennium. *Climate of the Past*, 723-737.
Karl, T. R., S. J. Hassol, C. Miller, D., and W. L. Murray, 2006: Temperature Trends in the Lower Atmosphere: Steps for Understanding and Reconciling Differences. A Report by the Climate Change Science Program and Subcommittee on Global Change Research, 180pp pp.
Karoly, D. J., and Q. G. Wu, 2005: Detection of regional surface temperature trends. *Journal of Climate*, **18,** 4337-4343.
Karoly, D. J., and P. A. Stott, 2006: Anthropogenic warming of central England temperature. *Atmos. Sci. Let.*, 81-85.
Karpechko, A., N. Gillett, L. Gray, and M. Dall'Amico, 2010: Influence of ozone recovery and greenhouse gas increases on Southern Hemisphere circulation. *Journal of Geophysical Research-Atmospheres*, -.
Karpechko, A. Y., N. P. Gillett, G. J. Marshall, and A. A. Scaife, 2008: Stratospheric influence on circulation changes in the Southern Hemisphere troposphere in coupled climate models. *Geophysical Research Letters*, **35**.
Kay, A. L., S. M. Crooks, P. Pall, and D. A. Stone, 2011: Attribution of Autumn 2000 flood risk in England to anthropogenic climate change. submitted.
Keeling, R., and H. Garcia, 2002: The change in oceanic O-2 inventory associated with recent global warming. *Proceedings of the National Academy of Sciences of the United States of America*, 7848-7853.
Kennedy, J. J., N. A. Rayner, R. O. Smith, M. Saunby, and D. E. Parker, 2011a: Reassessing biases and other uncertainties in sea-surface temperature observations since 1850 part 2: biases and homogenisation. *J. Geophys. Res.*, in revision.
——, 2011b: Reassessing biases and other uncertainties in sea-surface temperature observations since 1850 part 1: measurement and sampling errors. *J. Geophys. Res.*, in revision.
Kettleborough, J., B. Booth, P. Stott, and M. Allen, 2007: Estimates of uncertainty in predictions of global mean surface temperature. *Journal of Climate*, 843-855.
Kiehl, J. T., 2007: Twentieth century climate model response and climate sensitivity. *Geophysical Research Letters*, **34,** 4.
Kim, H. M., P. J. Webster, and J. A. Curry, 2009: Impact of Shifting Patterns of Pacific Ocean Warming on North Atlantic Tropical Cyclones. *Science*, **325,** 77-80.
Kim, H. M., C. D. Hoyos, P. J. Webster, and I. S. Kang, 2010: Ocean-atmosphere coupling and the boreal winter MJO. *Climate Dynamics*, **35,** 771-784.

Kincer, J., 1933: Is our climate changing ? , 251-259.
Kirk-Davidoff, D., 2009: On the diagnosis of climate sensitivity using observations of fluctuations. *Atmospheric Chemistry and Physics***,** 813-822.
Kitaev, L. M., and A. V. Kislov, 2008: Regional differences of snow accumulation - contemporary and future changes (on the example of Northern Europe and northern part of West Siberia). *Kriosfera Zemly (Earth Cryosphere)*, **12,** 98-104.
Kitaev, L. M., T. B. Titkova, and E. A. Cherenkova, 2007: Snow accumulation tendencies in Northern Eurasia , Vol.11, No.3, 71-77. *Kriosfera Zemly (Earth Cryosphere)*, **11,** 71-77.
Klotzbach, P. J., R. A. Pielke, J. R. Christy, and R. T. McNider, 2009: An alternative explanation for differential temperature trends at the surface and in the lower troposphere. *Journal of Geophysical Research-Atmospheres*, **114,** 8.
Knight, J., et al., 2009: Do global temperature trends over the last decade falsify climate predictions? *In: State of the climate in 2008*, Bull. Amer. Meteor. Soc., S22-S23.
Knight, J. R., C. K. Folland, and A. A. Scaife, 2006: Climate impacts of the Atlantic Multidecadal Oscillation. *Geophysical Research Letters*, **33**.
Knight, J. R., R. J. Allan, C. K. Folland, M. Vellinga, and M. E. Mann, 2005: A signature of persistent natural thermohaline circulation cycles in observed climate. *Geophysical Research Letters*, **32**.
Knutson, T., J. Sirutis, S. Garner, G. Vecchi, and I. Held, 2008: Simulated reduction in Atlantic hurricane frequency under twenty-first-century warming conditions. *Nature Geoscience***,** 359-364.
Knutson, T. R., et al., 2006: Assessment of twentieth-century regional surface temperature trends using the GFDL CM2 coupled models. *Journal of Climate*, **19(9),** 1624-1651.
Knutson, T. R., et al., 2010: Tropical cyclones and climate change. *Nature Geoscience*, ***3*****,** *1*57-163.
Knutti, R., 2008: Why are climate models reproducing the observed global surface warming so well? *Geophysical Research Letters***,** -.
Knutti, R., and G. Hegerl, 2008: The equilibrium sensitivity of the Earth's temperature to radiation changes. *Nature Geoscience***,** 735-743.
Knutti, R., and L. Tomassini, 2008: Constraints on the transient climate response from observed global temperature and ocean heat uptake. *Geophysical Research Letters***,** -.
Knutti, R., et al., 2008: A review of uncertainties in global temperature projections over the twenty-first century. *Journal of Climate*, **21,** 2651-2663.
Kodama, C., and T. Iwasaki, 2009: Influence of the SST Rise on Baroclinic Instability Wave Activity under an Aquaplanet Condition. *J. Atmos. Sci.*, **66,** 2272–2287.
Kohler, P., R. Bintanja, H. Fischer, F. Joos, R. Knutti, G. Lohmann, and V. Masson-Delmotte, 2010: What caused Earth's temperature variations during the last 800,000 years? Data-based evidence on radiative forcing and constraints on climate sensitivity. *Quaternary Science Reviews*, 129-145.
Korhonen, H., K. S. Carslaw, P. M. Forster, S. Mikkonen, N. D. Gordon, and H. Kokkola, 2010: Aerosol climate feedback due to decadal increases in Southern Hemisphere wind speeds. *Geophysical Research Letters*, **37**.
Kucharski, F., A. Bracco, R. Barimalala, and J. Yoo, 2010: Contribution of the east–west thermal heating contrast to the South Asian Monsoon and consequences for its variability. *Climate Dynamics***,** 1-15-15.
Kumar, A., et al., 2010: Contribution of sea ice loss to Arctic amplification. *Geophysical Research Letters***,** -.
Kunkel, K. E., et al., 2008: Observed Changes in Weather and Climate Extremes. *Weather and Climate Extremes in a Changing Climate. Regions of Focus: North America, Hawaii, Caribbean, and U.S. Pacific Islands*, G. A. M. T. R. Karl, C. D. Miller, S. J. Hassol, A. M. Waple, and W. L. Murray, Ed., A Report by the U.S. Climate Change Science Program and the Subcommittee on Global Change Research.
Kwok, R., G. Cunningham, M. Wensnahan, I. Rigor, H. Zwally, and D. Yi, 2009: Thinning and volume loss of the Arctic Ocean sea ice cover: 2003-2008. *Journal of Geophysical Research-Oceans***,** -.
L'Heureux, M., A. Butler, B. Jha, A. Kumar, and W. Wang, 2010: Unusual extremes in the negative phase of the Arctic Oscillation during 2009. *Geophysical Research Letters***,** -.
Lambert, F., P. Stott, M. Allen, and M. Palmer, 2004: Detection and attribution of changes in 20th century land precipitation. *Geophysical Research Letters***,** -.
Lambert, F. H., and M. R. Allen, 2009: Are Changes in Global Precipitation Constrained by the Tropospheric Energy Budget? *Journal of Climate*, **22,** 499-517.
Langen, P., and V. Alexeev, 2007: Polar amplification as a preferred response in an idealized aquaplanet GCM. *Climate Dynamics***,** 305-317.
Latif, M., M. Collins, H. Pohlmann, and N. Keenlyside, 2006: A review of predictability studies of Atlantic sector climate on decadal time scales. *Journal of Climate*, **19,** 5971-5987.
Lau, N. C., A. Leetmaa, and M. J. Nath, 2006: Attribution of atmospheric variations in the 1997-2003 period to SST anomalies in the Pacific and Indian ocean basins. *Journal of Climate*, **19,** 3607-3628.
Lau, N. C., A. Leetmaa, M. J. Nath, and H. L. Wang, 2005: Influences of ENSO-induced Indo-Western Pacific SST anomalies on extratropical atmospheric variability during the boreal summer. *Journal of Climate*, **18,** 2922-2942.
Lean, J., 2006: Comment on "Estimated solar contribution to the global surface warming using the ACRIM TSI satellite composite" by N. Scafetta and B. J. West. *Geophysical Research Letters***,** -.

Lean, J., and D. Rind, 2008: How natural and anthropogenic influences alter global and regional surface temperatures: 1889 to 2006. *Geophysical Research Letters*, -.
Lean, J. L., and D. H. Rind, 2009: How will Earth's surface temperature change in future decades? *Geophysical Research Letters*, **36**.
Ledoit, O., and M. Wolf, 2004: A well-conditioned estimator for large-dimensional covariance matrices. *Journal of Multivariate Analysis*, 365-411.
Lee, T., and M. J. McPhaden, 2010: Increasing intensity of El Nino in the central-equatorial Pacific. *Geophysical Research Letters*, **37**.
Legras, B., O. Mestre, E. Bard, and P. Yiou, 2010: A critical look at solar-climate relationships from long temperature series. *Climate of the Past*, **6,** 745-758.
Lenderink, G., and E. Van Meijgaard, 2008: Increase in hourly precipitation extremes beyond expectations from temperature changes. *Nature Geoscience*, **1(8),** 511-514.
——, 2009: Unexpected rise in extreme precipitation caused by a shift in rain type? *Nature Geoscience*, **2(6),** 373-373.
Li, S. L., J. Perlwitz, X. W. Quan, and M. P. Hoerling, 2008: Modelling the influence of North Atlantic multidecadal warmth on the Indian summer rainfall. *Geophysical Research Letters*, **35**.
Liebmann, B., R. M. Dole, C. Jones, I. Blade, and D. Allured, 2010: INFLUENCE OF CHOICE OF TIME PERIOD ON GLOBAL SURFACE TEMPERATURE TREND ESTIMATES. *Bulletin of the American Meteorological Society*, **91,** 1485-U1471.
Liepert, B. G., and M. Previdi, 2009: Do Models and Observations Disagree on the Rainfall Response to Global Warming? *Journal of Climate*, **22,** 3156-3166.
Lin, P., Q. A. Fu, S. Solomon, and J. M. Wallace, 2010: Temperature Trend Patterns in Southern Hemisphere High Latitudes: Novel Indicators of Stratospheric Change (vol 22, pg 6325, 2009). *Journal of Climate*, **23,** 4263-4280.
Lindzen, R., and Y. Choi, 2009: On the determination of climate feedbacks from ERBE data. *Geophysical Research Letters*, -.
Lockwood, J. G., 1999: Is potential evapotranspiration and its relationship with actual evapotranspiration sensitive to elevated atmospheric CO_2 levels? *Climatic Change*, **41,** 193-212.
Lockwood, M., 2008: Recent changes in solar outputs and the global mean surface temperature. III. Analysis of contributions to global mean air surface temperature rise. *Proceedings of the Royal Society a-Mathematical Physical and Engineering Sciences*, **464,** 1387-1404.
Lockwood, M., and C. Frohlich, 2007: Recent oppositely directed trends in solar climate forcings and the global mean surface air temperature. *Proceedings of the Royal Society a-Mathematical Physical and Engineering Sciences*, 2447-2460.
Lu, J., G. A. Vecchi, and T. Reichler, 2007: Expansion of the Hadley cell under global warming. *Geophysical Research Letters*, **34**.
Lu, J., G. Chen, and D. M. W. Frierson, 2008: Response of the Zonal Mean Atmospheric Circulation to El Nino versus Global Warming. *Journal of Climate*, **21,** 5835-5851.
Lu, J., C. Deser, and T. Reichler, 2009: Cause of the widening of the tropical belt since 1958. *Geophysical Research Letters*, **36**.
Lunt, D., A. Haywood, G. Schmidt, U. Salzmann, P. Valdes, and H. Dowsett, 2010: Earth system sensitivity inferred from Pliocene modelling and data. *Nature Geoscience*, 60-64.
Luterbacher, J., D. Dietrich, E. Xoplaki, M. Grosjean, and H. Wanner, 2004: European Seasonal and Annual Temperature Variability, Trend, and Extremes Since 1500. *Science*, **303,** 5.
Lysgaard, L., 1949: Recent climate fluctuations.
Ma, T., X. Zhang, H. Massam, F. W. Zwiers, G. Monette, and D. Robinson, 2011: Bayesian hierarchical models for climate change detection and attribution.
Mann, M., et al., 2009: Global Signatures and Dynamical Origins of the Little Ice Age and Medieval Climate Anomaly. *Science*, 1256-1260.
Mann, M. E., and K. A. Emanuel, 2006: Atlantic hurricane trends linked to climate change. *Eos Transactions*, **87(24),** 233-241.
Maslanik, J., C. Fowler, J. Stroeve, S. Drobot, J. Zwally, D. Yi, and W. Emery, 2007: A younger, thinner Arctic ice cover: Increased potential for rapid, extensive sea-ice loss. *Geophysical Research Letters*, -.
Matear, R., and A. Hirst, 2003: Long-term changes in dissolved oxygen concentrations in the ocean caused by protracted global warming. *Global Biogeochemical Cycles*, -.
Matear, R. J., A. C. Hirst, and B. I. McNeil, 2000: Changes in dissolved oxygen in the Southern Ocean with climate change. *Geochemistry, Geophysics, Geosystems.*
An electronic journal of the Earth Sciences, **1,** 12.
McKitrick, R., S. McIntyre, and C. Herman, 2010: Panel and multivariate methods for tests of trend equivalence in climate data series. *Atmospheric Science Letters*, **11,** 270-277.
McLandress, C., A. I. Jonsson, D. A. Plummer, M. C. Reader, J. F. Scinocca, and T. G. Shepherd, 2010: Separating the Dynamical Effects of Climate Change and Ozone Depletion. Part I: Southern Hemisphere Stratosphere. *Journal of Climate*, **23,** 5002-5020.

McLandress, C., T. G. Shepherd, J. F. Scinocca, D. A. Plummer, M. Sigmond, A. I. Jonsson, and R. M. C., 2011: Separating the dynamical effects of climate change and ozone depletion: Part 2. Southern Hemisphere Troposphere. *J. Clim.***,** press.
Mecking, S., M. Warner, and J. Bullister, 2006: Temporal changes in pCFC-12 ages and AOU along two hydrographic sections in the eastern subtropical North Pacific. *Deep-Sea Research Part I-Oceanographic Research Papers***,** 169-187.
Meehl, G. A., J. M. Arblaster, and C. Tebaldi, 2005a: Understanding future patterns of increased precipitation intensity in climate model simulations. *Geophysical Research Letters*, **32(L18719)**.
——, 2007a: Contributions of natural and anthropogenic forcing to changes in temperature extremes over the U.S. *Geophysical Research Letters*, **34**.
Meehl, G. A., C. Covey, B. McAvaney, M. Latif, and R. J. Stouffer, 2005b: Overview of the Coupled Model Intercomparison Project. *Bulletin of the American Meteorological Society*, **86,** 89-+.
Meehl, G. A., et al., 2007b: Global Climate Projections. *Climate Change 2007: The Physical Science Basis. Contribution of Working Group I to the Fourth Assessment Report of the Intergovernmental Panel on Climate Change*, Cambridge University Press.
Mernild, S., G. Liston, C. Hiemstra, K. Steffen, E. Hanna, and J. Christensen, 2009: Greenland Ice Sheet surface mass-balance modelling and freshwater flux for 2007, and in a 1995-2007 perspective. *Hydrological Processes***,** 2470-2484.
Merryfield, W. J., 2006: Changes to ENSO under CO_2 doubling in a multimodel ensemble. *Journal of Climate*, **19,** 4009-4027.
Miller, G., R. Alley, J. Brigham-Grette, J. Fitzpatrick, L. Polyak, M. Serreze, and J. White, 2010: Arctic amplification: can the past constrain the future? *Quaternary Science Reviews***,** 1779-1790.
Milne, G., R. Gehrels, C. Hughes, and M. Tamisiea, 2009: Identifying the causes of sea-level change. *Nature Geosci*, **2,** 471-478.
Min, S.-K., X. Zhang, F. W. Zwiers, and G. C. Hegerl, 2011: Human contribution to more intense precipitation extremes. *Nature*, **470,** 378-381.
Min, S., X. Zhang, and F. Zwiers, 2008a: Human-induced arctic moistening. *Science***,** 518-520.
Min, S., X. Zhang, F. Zwiers, and T. Agnew, 2008b: Human influence on Arctic sea ice detectable from early 1990s onwards. *Geophysical Research Letters***,** -.
Min, S. K., and A. Hense, 2007: A Bayesian assessment of climate change using multimodel ensembles. Part II: Regional and seasonal mean surface temperatures. *Journal of Climate*, **20,** 2769-2790.
Mitchell, J. M., 1963: On the world-wide pattern of secular temperature change. WMO.
Molg, T., and G. Kaser, 2011: Unifying large-scale atmospheric dynamics and glacier scale mass balance without the need for scale bridging. *Geophysical Research*, **13**.
Molg, T., N. Cullen, D. Hardy, M. Winkler, and G. Kaser, 2009: Quantifying Climate Change in the Tropical Midtroposphere over East Africa from Glacier Shrinkage on Kilimanjaro. *Journal of Climate***,** 4162-4181.
Morak, S., G. C. Hegerl, and J. Kenyon, 2011: Detectable regional changes in the number of warm nights. *(submitted)*.
Morgenstern, O., et al., 2010: Anthropogenic forcing of the Northern Annular Mode in CCMVal-2 models. *Journal of Geophysical Research-Atmospheres*, **115**.
Murphy, D., and P. Forster, 2010: On the Accuracy of Deriving Climate Feedback Parameters from Correlations between Surface Temperature and Outgoing Radiation. *Journal of Climate***,** 4983-4988.
Murphy, D., S. Solomon, R. Portmann, K. Rosenlof, P. Forster, and T. Wong, 2009: An observationally based energy balance for the Earth since 1950. *Journal of Geophysical Research-Atmospheres***,** -.
Nakanowatari, T., K. Ohshima, and M. Wakatsuchi, 2007: Warming and oxygen decrease of intermediate water in the northwestern North Pacific, originating from the Sea of Okhotsk, 1955-2004. *Geophysical Research Letters***,** -.
Nesje, A., O. Lie, and S. Dahl, 2000: Is the North Atlantic Oscillation reflected in Scandinavian glacier mass balance records? *Journal of Quaternary Science***,** 587-601.
Nghiem, S., I. Rigor, D. Perovich, P. Clemente-Colon, J. Weatherly, and G. Neumann, 2007: Rapid reduction of Arctic perennial sea ice. *Geophysical Research Letters***,** -.
Nicholls, N., et al., 2011 In Prep: Changes in Climate Extremes and their Impacts on the Natural Physical Environment. *IPCC Special Report: Managing the Risks of Extreme Events and Disasters to Advance Climate Change Adaptation*.
O'Gorman, P. A., and T. Schneider, 2008: Energy of Midlatitude Transient Eddies in Idealized Simulations of Changed Climates. *Journal of Climate*, **21(22),** 5797-5806.
——, 2009a: Scaling of Precipitation Extremes over a Wide Range of Climates Simulated with an Idealized GCM. *Journal of Climate*, **22(21),** 5676-5685.
——, 2009b: The physical basis for increases in precipitation extremes in simulations of 21st-century climate change. *Proceedings of the National Academy of Sciences of the Unied States of America*, **106(35),** 14773-14777.
Oldenborgh, G. J. v., S. Y. Philip, and M. Collins, 2005: El Niño in a changing climate: a multi-model study. Copernicus GmbH on behalf of the European Geosciences Union (EGU).
Ono, T., T. Midorikawa, Y. Watanabe, K. Tadokoro, and T. Saino, 2001: Temporal increases of phosphate and apparent oxygen utilization in the subsurface waters of western subarctic Pacific from 1968 to 1998. *Geophysical Research Letters***,** 3285-3288.

Osterkamp, T. E., 2005: The recent warming of permafrost in Alaska. *Global and Planetary Change*, **49,** 187-202.
Otto-Bliesner, B., et al., 2009: A comparison of PMIP2 model simulations and the MARGO proxy reconstruction for tropical sea surface temperatures at last glacial maximum. *Climate Dynamics***,** 799-815.
Overland, J., 2009: The case for global warming in the Arctic. *Influence of Climate Change on the Changing Arctic and Sub-Arctic Conditions***,** 13-23.
Overland, J., and M. Wang, 2005: The Arctic climate paradox: The recent decrease of the Arctic Oscillation. *Geophysical Research Letters***,** -.
Overland, J., M. Wang, and S. Salo, 2008: The recent Arctic warm period. *Tellus Series a-Dynamic Meteorology and Oceanography***,** 589-597.
Overland, J. E., and M. Wang, 2010: Large-scale atmospheric circulation changes are associated with the recent loss of Arctic sea ice. *Tellus*, **62A,** 9.
Padilla, L., G. Vallis, and C. Rowley, 2011: Probabilistic estimates of transient climate sensitivity subject to uncertainty in forcing and natural variability *Journal of Climate*, **submitted**.
Pagani, M., K. Caldeira, R. Berner, and D. Beerling, 2009: The role of terrestrial plants in limiting atmospheric CO_2 decline over the past 24 million years. *Nature***,** 85-U94.
Palastanga, V., G. van der Schrier, S. L. Weber, T. Kleinen, K. R. Briffa, and T. J. Osborn, 2011: Atmosphere and ocean dynamics: contributors to the Little Ice Age and Medieval Climate Anomaly. 973-987.
Pall, P., A. M. R., and D. A. Stone, 2007: Testing the Clausius-Clapeyron constraint on changes in extreme precipitation under CO_2 warming. *Climate Dynamics*, **28,** 353-361.
Pall, P., et al., 2011: Anthropogenic greenhouse gas contribution to <country-region>UK</country-region> autumn flood risk. *Nature*.
Palmer, M., and K. Haines, 2009: Estimating Oceanic Heat Content Change Using Isotherms. *Journal of Climate*, **22,** 4953-4969.
Palmer, M. D., K. Haines, S. F. B. Tett, and T. J. Ansell, 2007: Isolating the signal of ocean global warming. *Geophysical Research Letters*, **34,** L23610.
Palmer, M. D., S. A. Good, K. Haines, N. A. Rayner, and P. A. Stott, 2009: A new perspective on warming of the global oceans. *Geophysical Research Letters*, **36,** L20709.
Palmer, T., 1999: A nonlinear dynamical perspective on climate prediction. *Journal of Climate***,** 575-591.
Parker, D., C. Folland, A. Scaife, J. Knight, A. Colman, P. Baines, and B. Dong, 2007: Decadal to multidecadal variability and the climate change background. *Journal of Geophysical Research-Atmospheres*.
Parker, D. E., L. V. Alexander, and J. Kennedy, 2004: Global and regional climate in 2003. *Weather,* 59**,** 145-152.
Pavlov, A. V., and V. G. Malkova, 2010: Dynamics of permafrost zone of Russia under changing climate conditions. *Izvestiya, Ser. Geogr.*, **5,** 44-51.
Peel, M. C., and T. A. McMahon, 2006: Continental runoff - A quality-controlled global runoff data set. *Nature*, **444,** E14-E14.
Peltier, W. R., 2004: GLOBAL GLACIAL ISOSTASY AND THE SURFACE OF THE ICE-AGE EARTH: The ICE-5G (VM2) Model and GRACE. *Annual Review of Earth and Planetary Sciences*, **32,** 111-149.
Perlwitz, J., S. Pawson, R. Fogt, J. Nielsen, and W. Neff, 2008: Impact of stratospheric ozone hole recovery on Antarctic climate. *Geophysical Research Letters***,** -.
Perlwitz, J., M. Hoerling, J. Eischeid, T. Xu, and A. Kumar, 2009: A strong bout of natural cooling in 2008. *Geophysical Research Letters*, **36**.
Peterssen, S., 1949: Changes in the general circulation associated with the recent climatic variation. 212-221.
Petoukhov, V., and V. Semenov, 2010: A link between reduced Barents-Kara sea ice and cold winter extremes over northern continents. *Journal of Geophysical Research-Atmospheres***,** -.
Pierce, D., T. Barnett, K. AchutaRao, P. Gleckler, J. Gregory, and W. Washington, 2006: Anthropogenic Warming of the Oceans: Observations and Model Results. *Journal of Climate*, **19,** 1873-1900.
Pierce, D. W., and e. al, 2008: Attribution of declining Western US Snowpack to Human effects. *American Meteorological Society***,** 20.
Pierce, D. W., T. P. Barnett, B. D. Santer, and P. J. Gleckler, 2009: Selecting global climate models for regional climate change studies. *Proceedings of the National Academy of Sciences of the United States of America*, **106,** 8441-8446.
Pitman, A. J., et al., 2009: Uncertainties in climate responses to past land cover change: first results from the LUCID intercomparison study. *Geophysical Research Letters*, **36(L14814)**.
Plattner, G. K., F. Joos, and T. F. Stocker, 2002: Revision of the global carbon budget due to changing air-sea oxygen fluxes. *Global Biogeochemical Cycles*, **16,** 12.
Polvani, L. M., M. Previdi, and C. Deser, 2011: Large cancellation, due to ozone recovery, of future Southern Hemisphere atmospheric circulation trends. *Geophys. Res. Lett.*
Polvani, L. M., D. W. Waugh, G. J. P. Correa, and S.-W. Son, 2010: Stratospheric ozone depletion: the main driver of 20th Century atmospheric circulation changes in the Southern Hemisphere. *Journal of Climate*.
Polyakov, I., U. Bhatt, H. Simmons, D. Walsh, J. Walsh, and X. Zhang, 2005: Multidecadal variability of North Atlantic temperature and salinity during the twentieth century. *Journal of Climate***,** 4562-4581.
Polyakov, I., et al., 2003: Variability and trends of air temperature and pressure in the maritime Arctic, 1875-2000. *Journal of Climate***,** 2067-2077.

Pongratz, J., C. Reick, T. Raddatz, and M. Claussen, 2009: Effects of anthropogenic land cover change on the carbon cycle of the last millennium. *Global Biogeochemical Cycles*, -.
Quadrelli, R., and J. Wallace, 2004: A simplified linear framework for interpreting patterns of Northern Hemisphere wintertime climate variability. *Journal of Climate*, 3728-3744.
Ramsay, H. A., and A. H. Sobel, 2011: The effects of relative and absolute sea surface temperature on tropical cyclone potential intensity using a single column model. *Journal of Climate, (in press)*.
Randel, W. J., F. Wu, H. Vˆmel, G. E. Nedoluha, and P. Forster, 2006: Decreases in stratospheric water vapor after 2001: Links to changes in the tropical tropopause and the Brewer-Dobson circulation. *J. Geophys. Res.*, **111,** D12312.
Randel, W. J., et al., 2009: An update of observed stratospheric temperature trends. *Journal of Geophysical Research-Atmospheres*, **114,** 21.
Reichert, B., L. Bengtsson, and J. Oerlemans, 2002: Recent glacier retreat exceeds internal variability. *Journal of Climate*, 3069-3081.
Ribes, A., J. M. Azais, and S. Planton, 2009: Adaptation of the optimal fingerprint method for climate change detection using a well-conditioned covariance matrix estimate. *Climate Dynamics*, **33,** 707-722.
——, 2010: A method for regional climate change detection using smooth temporal patterns. *Climate Dynamics*, **35,** 391-406.
Robinson, D. A., K. F. Dewey, and R. R. Heim, 1993: GLOBAL SNOW COVER MONITORING - AN UPDATE. *Bulletin of the American Meteorological Society*, **74,** 1689-1696.
Robock, A., 2000: Volcanic eruptions and climate. *Reviews of Geophysics*, 191-219.
Rodgers, J. C., 1985: Atmospheric circulation changes associated with the warming over the Northern North Atlantic in the 1920s. 1303-1310.
Roe, G., and M. Baker, 2007: Why is climate sensitivity so unpredictable? *Science*, 629-632.
Roemmich, D., and J. Gilson, 2009: The 2004-2008 mean and annual cycle of temperature, salinity, and steric height in the global ocean from the Argo Program. *Progress in Oceanography*, 81-100.
Rosenlof, K. H., and G. C. Reid, 2008: Trends in the temperature and water vapor content of the tropical lower stratosphere: Sea surface connection. *Journal of Geophysical Research-Atmospheres*, **113**.
Royer, D., 2008: Linkages between CO_2, climate, and evolution in deep time. *Proceedings of the National Academy of Sciences of the United States of America*, 407-408.
Royer, D., R. Berner, and J. Park, 2007: Climate sensitivity constrained by CO_2 concentrations over the past 420 million years. *Nature*, 530-532.
Ruddiman, W. F., and E. C. Ellis, 2009: Effect of per-capita land use changes on Holocene forest clearance and CO_2 emissions. *Quaternary Science Reviews*, **28,** 3011-3015.
Ryan, B. F., I. G. Watterson, and J. L. Evans, 1992: Tropical Cyclone Frequencies Inferred from Grays Yearly Genesis Parameter - Validation of Gcm Tropical Climates. *Geophysical Research Letters*, **19(18),** 1831-1834.
Santer, B. D., and Coauthors, 2011a: Understanding the causes of differences between modeled and observed temperature trends. in preparation.
——, 2011b: On the timescale-dependence of signal-to noise ratios for atmospheric temperature changes. in preparation.
Santer, B. D., et al., 2009: Incorporating model quality information in climate change detection and attribution studies. *Proceedings of the National Academy of Sciences of the United States of America*, **106,** 14778-14783.
——, 2007: Identification of human-induced changes in atmospheric moisture content. *Proceedings of the National Academy of Sciences of the United States of America*, **104,** 15248-15253.
——, 2008: Consistency of modelled and observed temperature trends in the tropical troposphere. *International Journal of Climatology*, **28,** 1703-1722.
Santer, B. D., et al., 2006: Forced and unforced ocean temperature changes in Atlantic and Pacific tropical cyclogenesis regions. *Proceedings of the National Academy of Sciences*, **103(38),** 13905-13910.
Santer, B. D., et al., 2007: Identification of human-induced changes in atmospheric moisture content. *Proceedings of the National Academy of Sciences of the <country-region>United States of America</country-region>*, **104,** 15248-15253.
Scafetta, N., and B. West, 2007: Phenomenological reconstructions of the solar signature in the Northern Hemisphere surface temperature records since 1600. *Journal of Geophysical Research-Atmospheres*, -.
Schär , C., P. L. Vidale, D. Lüthi, C. Frei, C. Häberl, M. A. Liniger, and C. Appenzeller, 2004: The role of increasing temperature variability in European summer heatwaves. *Nature*, **427,** 332-336.
Scherhag, R., 1937: Die Erwarmung der Arktis. 263-276.
SCHLESINGER, M., and N. RAMANKUTTY, 1994: AN OSCILLATION IN THE GLOBAL CLIMATE SYSTEM OF PERIOD 65-70 YEARS. *Nature*, 723-726.
Schneider von Deimling, T., H. Held, A. Ganopolski, and S. Rahmstorf, 2006: Climate sensitivity estimated from ensemble simulations of glacial climate. *Climate Dynamics*, 149-163.
Schopf, P. S., and R. J. Burgman, 2006: A simple mechanism for ENSO residuals and asymmetry. *Journal of Climate*, **19,** 3167-3179.

Schubert, S., et al., 2009: A <country-region>US</country-region> CLIVAR Project to Assess and Compare the Responses of Global Climate Models to Drought-Related SST Forcing Patterns: Overview and Results. *Journal of Climate*, **22,** 5251-5272.

Schubert, S. D., M. J. Suarez, P. J. Pegion, R. D. Koster, and J. T. Bacmeister, 2008: Potential predictability of long-term drought and pluvial conditions in the US Great Plains. *Journal of Climate*, **21(4),** 802-816.

Schwartz, S., 2007: Heat capacity, time constant, and sensitivity of Earth's climate system. *Journal of Geophysical Research-Atmospheres***,** -.

Schwartz, S., R. Charlson, R. Kahn, J. Ogren, and H. Rodhe, 2010: Why Hasn't Earth Warmed as Much as Expected? *Journal of Climate***,** 2453-2464.

Schwartz, S. E., R. J. Charlson, and H. Rodhe, 2007: Quantifying climate change — too rosy a picture? *Nature Reports Climate Change*, 23-24.

Schwarzkopf, M. D., and V. Ramaswamy, 2008: Evolution of stratospheric temperature in the 20th century. *Geophysical Research Letters*, **35,** 6.

Schweiger, A., R. Lindsay, S. Vavrus, and J. Francis, 2009: Relationships between Arctic Sea ice and clouds during autumn (vol 21, pg 4799, 2008). *Journal of Climate***,** 2793-2793.

Screen, J., and I. Simmonds, 2010: Increasing fall-winter energy loss from the Arctic Ocean and its role in Arctic temperature amplification. *Geophysical Research Letters***,** -.

Seager, R., Y. Kushnir, J. Nakamura, M. Ting, and N. Naik, 2010: Northern Hemisphere winter snow anomalies: ENSO, NAO and the winter of 2009/10. *Geophysical Research Letters***,** -.

Seager, R., R. Burgman, Y. Kushnir, A. Clement, E. Cook, N. Naik, and J. Miller, 2008: Tropical Pacific Forcing of North American Medieval Megadroughts: Testing the Concept with an Atmosphere Model Forced by Coral-Reconstructed SSTs. *Journal of Climate*, **21,** 6175-6190.

Seidel, D. J., and W. J. Randel, 2007: Recent widening of the tropical belt: Evidence from tropopause observations. *Journal of Geophysical Research-Atmospheres*, **112**.

Seidel, D. J., Q. Fu, W. J. Randel, and T. J. Reichler, 2008: Widening of the tropical belt in a changing climate. *Nature Geoscience*, **1,** 21-24.

Seidel, D. J., N. P. Gillett, J. R. Lanzante, K. P. Shine, and P. W. Thorne, 2011: Stratospheric temperature trends: Our evolving understanding. *Wiley Interdisciplinary Reviews: Climate Change***,** submitted.

Seierstad, I. A., and J. Bader, 2009: Impact of a projected future Arcitc Sea Ice reduction on extratropical storminess and the NAO. *Clim Dyn*, **33,** 7.

Semenov, V., 2008: Influence of oceanic inflow to the Barents Sea on climate variability in the Arctic region. *Doklady Earth Sciences***,** 91-94.

Semmler, T., S. Varghese, R. McGrath, P. Nolan, S. L. Wang, P., and C. O'Dowd, 2008: Regional climate model simulations of NorthAtlantic cyclones: frequency and intensity changes. *Climate Research*, **36**.

Seneviratne, S. I., et al., 2010: Investigating soil moisture-climate interactions in a changing climate: A review. *Earth Science Reviews*, 125-161.

Serreze, M., and J. Francis, 2006: The arctic amplification debate. *Climatic Change***,** 241-264.

Serreze, M., M. Holland, and J. Stroeve, 2007: Perspectives on the Arctic's shrinking sea-ice cover. *Science***,** 1533-1536.

Serreze, M., et al., 2000: Observational evidence of recent change in the northern high-latitude environment. *Climatic Change***,** 159-207.

Serreze, M. C., A. P. Barrett, J. C. Stroeve, D. N. Kindig, and M. M. Holland, 2009: The emergence of surface-based Arctic amplification. *The Cryosphere*, **3,** 9.

Shanahan, T. M., et al., 2009: Atlantic Forcing of Persistent Drought in West Africa. *Science*, **324,** 377-380.

Shapiro, A., E. Rozanov, T. Egorova, A. Shapiro, T. Peter, and W. Schmutz, 2011: Sensitivity of the Earth's middle atmosphere to short-term solar variability and its dependence on the choice of solar irradiance data set. *Journal of Atmospheric and Solar-Terrestrial Physics***,** 348-355.

Shellito, C., L. Sloan, and M. Huber, 2003: Climate model sensitivity to atmospheric CO_2 levels in the Early-Middle Paleogene. *Palaeogeography Palaeoclimatology Palaeoecology***,** 113-123.

Shepherd, T. G., and A. I. Jonsson, 2008: On the attribution of stratospheric ozone and temperature changes to changes in ozone-depleting substances and well-mixed greenhouse gases. *Atmospheric Chemistry and Physics*, **8,** 1435-1444.

Shindell, D., and G. Faluvegi, 2009: Climate response to regional radiative forcing during the twentieth century. *Nature Geoscience*, **2,** 294-300.

Shiogama, H., T. Nagashima, T. Yokohata, S. Crooks, and T. Nozawa, 2006: Influence of volcanic activity and changes in solar irradiance on surface air temperatures in the early twentieth century. *Geophysical Research Letters***,** -.

Sigmond, M., and J. Fyfe, 2010: Has the ozone hole contributed to increased Antarctic sea ice extent? *Geophysical Research Letters***,** -.

Sigmond, M., M. C. Reader, J. C. Fyfe, and N. P. Gillett, 2011: Drivers of past and future Southern Ocean change: stratospheric ozone versus greenhouse gas impacts. *Geophys. Res. Lett.*, submitted.

Simmons, A. J., K. M. Willett, P. D. Jones, P. W. Thorne, and D. P. Dee, 2010: Low-frequency variations in surface atmospheric humidity, temperature, and precipitation: Inferences from reanalyses and monthly gridded observational data sets. *Journal of Geophysical Research-Atmospheres*, **115**.

Singarayer, J., J. Bamber, and P. Valdes, 2006: Twenty-first-century climate impacts from a declining Arctic sea ice cover. *Journal of Climate*, 1109-1125.

Smirnov, D., and I. Mokhov, 2009: From Granger causality to long-term causality: Application to climatic data. *Physical Review E*, -.

Sokolova, E., K. Dethloff, A. Rinke, and A. Benkel, 2007: Planetary and synoptic scale adjustment of the Arctic atmosphere to sea ice cover changes. *Geophysical Research Letters*, -.

Solomon, S., K. H. Rosenlof, R. W. Portmann, J. S. Daniel, S. M. Davis, T. J. Sanford, and G. K. Plattner, 2010: Contributions of Stratospheric Water Vapor to Decadal Changes in the Rate of Global Warming. *Science*, **327,** 1219-1223.

Son, S. W., N. F. Tandon, L. M. Polvani, and D. W. Waugh, 2009: Ozone hole and Southern Hemisphere climate change. *Geophysical Research Letters*, **36**.

Son, S. W., et al., 2008: The impact of stratospheric ozone recovery on the Southern Hemisphere westerly jet. *Science*, **320,** 1486-1489.

——, 2010: Impact of stratospheric ozone on Southern Hemisphere circulation change: A multimodel assessment. *Journal of Geophysical Research-Atmospheres*, **115**.

Stainforth, D. A., et al., 2005: Uncertainty in predictions of the climate response to rising levels of greenhouse gases. *Nature*, **433,** 403-406.

Steig, E., D. Schneider, S. Rutherford, M. Mann, J. Comiso, and D. Shindell, 2009: Warming of the Antarctic ice-sheet surface since the 1957 International Geophysical Year (vol 457, pg 459, 2009). *Nature*, 766-766.

Stone, D., and M. Allen, 2005a: Attribution of global surface warming without dynamical models. *Geophysical Research Letters*, -.

Stone, D., M. Allen, P. Stott, P. Pall, S. Min, T. Nozawa, and S. Yukimoto, 2009: The Detection and Attribution of Human Influence on Climate. *Annual Review of Environment and Resources*, 1-16.

Stone, D. A., and M. R. Allen, 2005b: The end-to-end attribution problem: From emissions to impacts. *Climatic Change*, **71,** 303-318.

Stott, P., and J. Kettleborough, 2002: Origins and estimates of uncertainty in predictions of twenty-first century temperature rise (vol 416, pg 723, 2002). *Nature*, 205-205.

Stott, P., and C. Forest, 2007: Ensemble climate predictions using climate models and observational constraints. *Philosophical Transactions of the Royal Society a-Mathematical Physical and Engineering Sciences*, 2029-2052.

Stott, P., G. Jones, and J. Mitchell, 2003: Do models underestimate the solar contribution to recent climate change? *Journal of Climate*, 4079-4093.

Stott, P., D. Stone, and M. Allen, 2004a: Human contribution to the European heatwave of 2003. *Nature*, 610-614.

Stott, P., C. Huntingford, C. Jones, and J. Kettleborough, 2008a: Observed climate change constrains the likelihood of extreme future global warming. *Tellus Series B-Chemical and Physical Meteorology*, 76-81.

Stott, P., J. Mitchell, M. Allen, T. Delworth, J. Gregory, G. Meehl, and B. Santer, 2006a: Observational constraints on past attributable warming and predictions of future global warming. *Journal of Climate*, 3055-3069.

Stott, P. A., and G. S. Jones, 2009: Variability of high latitude amplification of anthropogenic warming. *Geophysical Research Letters*, **36,** 6.

Stott, P. A., D. A. Stone, and M. R. Allen, 2004b: Human contribution to the European heatwave of 2003. *Nature*, **432,** 610-614.

Stott, P. A., R. T. Sutton, and D. M. Smith, 2008b: Detection and attribution of Atlantic salinity changes. *Geophysical Research Letters*, **35,** 5.

Stott, P. A., J. F. B. Mitchell, M. R. Allen, T. L. Delworth, J. M. Gregory, G. A. Meehl, and B. D. Santer, 2006b: Observational constraints on past attributable warming and predictions of future global warming. *Journal of Climate*, **19,** 3055-3069.

Stott, P. A., N. P. Gillett, G. C. Hegerl, D. J. Karoly, D. A. Stone, X. Zhang, and F. Zwiers, 2010: Detection and attribution of climate change: a regional perspective. *Wiley Interdisciplinary Reviews: Climate Change*, **1,** 192-211.

Stott., P. A., G. S. Jones, N. Christidis, F. W. Zwiers, G. Hegerl, and H. Shiogama, 2011: Single-step attribution of increasing frequencies of very warm regional temperatures to human influence.

Stroeve, J., M. Holland, W. Meier, T. Scambos, and M. Serreze, 2007: Arctic sea ice decline: Faster than forecast. *Geophysical Research Letters*, -.

Sugiyama, M., H. Shiogama, and S. Emori, 2010: Precipitation extreme changes exceeding moisture content increases in MIROC and IPCC climate models. *Proceedings of the National Academy of Sciences of the <country-region>United States of America</country-region>*, **107(2),** 571-575.

Sutton, R. T., and D. L. R. Hodson, 2005: Atlantic Ocean forcing of North American and European summer climate. *Science*, **309,** 115-118.

——, 2007: Climate response to basin-scale warming and cooling of the North Atlantic Ocean. *Journal of Climate*, **20,** 891-907.

Tett, S., et al., 2007: The impact of natural and anthropogenic forcings on climate and hydrology since 1550. *Climate Dynamics*, 3-34.

Thompson, D., and S. Solomon, 2002: Interpretation of recent Southern Hemisphere climate change. *Science*, 895-899.

Thompson, D. W. J., J. J. Kennedy, J. M. Wallace, and P. D. Jones, 2008: A large discontinuity in the mid-twentieth century in observed global-mean surface temperature. *Nature*, **453,** 646-U645.
Thorne, P. W., J. R. Lanzante, T. C. Peterson, D. J. Seidel, and S. K. P., 2010: Tropospheric temperature trends: history of an ongoing controversy. *You have free access to this contentWiley Interdisciplinary Reviews: Climate Change*.
Thorne, P. W., et al., 2007: Tropical vertical temperature trends: A real discrepancy? *Geophysical Research Letters*, **34,** 5.
——, 2011: A quantification of the uncertainty in historical tropical tropospheric temperature trends from radiosondes. *J. Geophys. Res.*, in revision.
Timmreck, C., S. Lorenz, T. Crowley, S. Kinne, T. Raddatz, M. Thomas, and J. Jungclaus, 2009: Limited temperature response to the very large AD 1258 volcanic eruption. *Geophysical Research Letters*, -.
Titchner, H. A., P. W. Thorne, M. P. McCarthy, S. F. B. Tett, L. Haimberger, and D. E. Parker, 2009: Critically Reassessing Tropospheric Temperature Trends from Radiosondes Using Realistic Validation Experiments. *Journal of Climate*, **22,** 465-485.
Tourre, Y. M., S. Paz, Y. Kushnir, and W. B. White, 2010: Low-frequency climate variability in the Atlantic basin during the 20th century. *Atmospheric Science Letters*, **11,** 180-185.
Trenberth, K., J. Fasullo, and L. Smith, 2005: Trends and variability in column-integrated atmospheric water vapor. *Climate Dynamics*, **24,** 741-758.
Trenberth, K., J. Fasullo, C. O'Dell, and T. Wong, 2010: Relationships between tropical sea surface temperature and top-of-atmosphere radiation. *Geophysical Research Letters*, -.
Trenberth, K. E., and D. J. Shea, 2006: Atlantic hurricanes and natural variability in 2005. *GEOPHYSICAL RESEARCH LETTERS*, **33**.
Trouet, V., J. Esper, N. Graham, A. Baker, J. D. Scourse, and D. C. Frank, 2009: Persistent Positive North Atlantic Oscillation Mode Dominated the Medieval Climate Anomaly. *Science*, **324,** 3.
Turner, J., and J. Overland, 2009: Contrasting climate change in the two polar regions. *Polar Research*, 146-164.
Turner, J., et al., 2005: Antarctic change during the last 50 years (vol 25, pg 279, 2005). *International Journal of Climatology*, 1147-1148.
——, 2009: Non-annular atmospheric circulation change induced by stratospheric ozone depletion and its role in the recent increase of Antarctic sea ice extent. *Geophysical Research Letters*, -.
Urban, N., and K. Keller, 2009: Complementary observational constraints on climate sensitivity. *Geophysical Research Letters*, -.
Vecchi, G. A., and B. J. Soden, 2007: Global Warming and the Weakening of the Tropical Circulation. *Journal of Climate*, **20,** 4316-4340.
Vimont, D. J., J. M. Wallace, and D. S. Battisti, 2003: The seasonal footprinting mechanism in the Pacific: Implications for ENSO. *Journal of Climate*, **16,** 2668-2675.
von Schuckmann, K., F. Gaillard, and P. Le Traon, 2009: Global hydrographic variability patterns during 2003-2008. *Journal of Geophysical Research-Oceans*, -.
von Storch, H., E. Zorita, J. Jones, Y. Dimitriev, F. Gonzalez-Rouco, and S. Tett, 2004: Reconstructing past climate from noisy data. *Science*, 679-682.
Vorosmarty, C., L. Hinzman, and J. Pundsack, 2008: Introduction to special section on Changes in the Arctic Freshwater System: Identification, Attribution, and Impacts at Local and Global Scales. *Journal of Geophysical Research-Biogeosciences*, -.
Vose, R., 2011: The NOAA Global Temperature Product. *Bull. Amer. Meteor. Soc.*, submitted.
Vuille, M., G. Kaser, and I. Juen, 2008: Glacier mass balance variability in the Cordillera Blanca, Peru and its relationship with climate and the large-scale circulation. *Global and Planetary Change*, 14-28.
Walker, R., T. Dupont, D. Holland, B. Parizek, and R. Alley, 2009: Initial effects of oceanic warming on a coupled ocean-ice shelf-ice stream system. *Earth and Planetary Science Letters*, 483-487.
Wang, J., and X. Zhang, 2008: Downscaling and projection of winter extreme daily precipitation over North America. *Journal of Climate*, **21,** 923-937.
Wang, J., et al., 2009a: Is the Dipole Anomaly a major driver to record lows in Arctic summer sea ice extent? *Geophysical Research Letters*, -.
Wang, M., and J. Overland, 2009: A sea ice free summer Arctic within 30 years? *Geophysical Research Letters*, -.
Wang, X. L., V. R. Swail, F. W. Zwiers, X. Zhang, and Y. Feng, 2009b: Detection of external influence on trends of atmospheric storminess and northern oceans wave heights. *Climate Dynamics*, **32(2-3),** 189-203.
Weatherhead, E., and S. Andersen, 2006: The search for signs of recovery of the ozone layer. *Nature*, 39-45.
Weng, H. Y., S. K. Behera, and T. Yamagata, 2009: Anomalous winter climate conditions in the Pacific rim during recent El NiA +/- o Modoki and El NiA +/- o events. *Climate Dynamics*, **32,** 663-674.
Wentz, F., L. Ricciardulli, K. Hilburn, and C. Mears, 2007: How much more rain will global warming bring? *Science*, 233-235.
Wigley, T., C. Ammann, B. Santer, and K. Taylor, 2005: Comment on "Climate forcing by the volcanic eruption of Mount Pinatubo" by David H. Douglass and Robert S. Knox. *Geophysical Research Letters*, -.
Wijffels, S., et al., 2008: Changing Expendable Bathythermograph Fall Rates and Their Impact on Estimates of Thermosteric Sea Level Rise. *Journal of Climate*, **21,** 5657-5672.

Willett, H. C., 1950: Temperature trends of the last century. Royal Meteorological Society, Oxford.

Willett, K. M., N. P. Gillett, P. D. Jones, and P. W. Thorne, 2007a: Attribution of observed surface humidity changes to human influence. *Nature*, **449,** 710-712.

——, 2007b: Attribution of observed surface humidity changes to human influence. *Nature*, **449,** 710-U716.

Willett, K. M., P. D. Jones, N. P. Gillett, and P. W. Thorne, 2008: Recent Changes in Surface Humidity: Development of the HadCRUH Dataset. *Journal of Climate*, **21,** 5364-5383.

Wing, A. A., A. H. Sobel, and S. J. Camargo, 2007: Relationship between the potential and actual intensities of tropical cyclones on interannual time scales. *Geophysical Research Letters*, **34(L08810)**.

WMO, 2011: (World Meteorological Organization), *Scientific Assessment of Ozone Depletion: 2010*, Global Ozone Research and Monitoring Project–Report, 516pp pp.

Wong, A., N. Bindoff, and J. Church, 1999: Large-scale freshening of intermediate waters in the Pacific and Indian oceans. *Nature***,** 440-443.

Wood, K., and J. Overland, 2010: Early 20th century Arctic warming in retrospect. *International Journal of Climatology***,** 1269-1279.

Woollings, T., 2008: Vertical structure of anthropogenic zonal-mean atmospheric circulation change. *Geophysical Research Letters*, **35**.

Wu, Q. G., and D. J. Karoly, 2007: Implications of changes in the atmospheric circulation on the detection of regional surface air temperature trends. *Geophysical Research Letters*, **34**.

Xie, S.-P., C. Deser, G. A. Vecchi, J. Ma, H. Teng, and A. T. Wittenberg, 2010: Global Warming Pattern Formation: Sea Surface Temperature and Rainfall. *Journal of Climate*, **23(4),** 966-986.

Yeh, S.-W., et al., 2010: Two leading modes of Western-Pacific warm pool SST variability. *J. Climate***,** in press.

Yoshimori, M., and A. J. Broccoli, 2008: Equilibrium response of an atmosphere-mixed layer ocean model to different radiative forcing agents: Global and zonal mean response. *Journal of Climate*, **21,** 4399-4423.

Yoshimori, M., C. Raible, T. Stocker, and M. Renold, 2006: On the interpretation of low-latitude hydrological proxy records based on Maunder Minimum AOGCM simulations. *Climate Dynamics***,** 493-513.

Yoshimura, J., M. Sugi, and A. Noda, 2006: Influence of greenhouse warming on tropical cyclone frequency. *Journal of the Meteorological Society of <country-region>Japan</country-region>*, **84(2),** 405-428.

Zhang, Q., Y. Guan, and H. J. Yang, 2008a: ENSO amplitude change in observation and coupled models. *Advances in Atmospheric Sciences*, **25,** 361-366.

Zhang, R., and T. L. Delworth, 2006: Impact of Atlantic multidecadal oscillations on India/Sahel rainfall and Atlantic hurricanes. *Geophysical Research Letters*, **33**.

Zhang, R., T. L. Delworth, and I. M. Held, 2007a: Can the Atlantic Ocean drive the observed multidecadal variability in Northern Hemisphere mean temperature? *Geophysical Research Letters*, **34**.

Zhang, T., et al., 2005: Spatial and temporal variability of active layer thickness over the Russian Arctic drainage basin. *Journal of Geophysical Research*, **110**.

Zhang, X., A. Sorteberg, J. Zhang, R. Gerdes, and J. Comiso, 2008b: Recent radical shifts of atmospheric circulations and rapid changes in Arctic climate system. *Geophysical Research Letters***,** -.

Zhang, X. B., K. D. Harvey, W. D. Hogg, and T. R. Yuzyk, 2001: Trends in Canadian streamflow. *Water Resources Research*, **37,** 987-998.

Zhang, X. B., et al., 2007b: Detection of human influence on twentieth-century precipitation trends. *Nature*, **448,** 461-U464.

Zheng, X. T., S. P. Xie, G. A. Vecchi, Q. Y. Liu, and J. Hafner, 2010: Indian Ocean Dipole Response to Global Warming: Analysis of Ocean-Atmospheric Feedbacks in a Coupled Model. *Journal of Climate*, **23,** 1240-1253.

Zorita, E., T. Stocker, and H. von Storch, 2008: How unusual is the recent series of warm years? *Geophysical Research Letters***,** -.

Zou, C. Z., M. D. Goldberg, Z. H. Cheng, N. C. Grody, J. T. Sullivan, C. Y. Cao, and D. Tarpley, 2006: Recalibration of microwave sounding unit for climate studies using simultaneous nadir overpasses. *Journal of Geophysical Research-Atmospheres*, **111**.

Zwiers, F. W., X. Zhang, and Y. Feng, 2011: Anthropogenic influence on long return period daily temperature extremes at regional scales. *Journal of Climate*.

Chapter 10: Detection and Attribution of Climate Change: from Global to Regional

Coordinating Lead Authors: Nathaniel Bindoff (Australia), Peter Stott (UK)

Lead Authors: Krishna Mirle AchutaRao (India), Myles Allen (UK), Nathan Gillett (Canada), David Gutzler (USA), Kabumbwe Hansingo (Zambia), Gabriele Hegerl (UK), Yongyun Hu (China), Suman Jain (Zambia), Igor Mokhov (Russia), James Overland (USA), Judith Perlwitz (USA), Rachid Sebbari (Morocco), Xuebin Zhang (Canada)

Contributing Authors: Ping Chang, Paul Durack, Jara Imbers Quintana, Gareth S. Jones, Georg Kaser, Alison Kay, Reto Knutti, James Kossin, Mike Lockwood, Fraser Lott, Jian Lu, Seung-Ki Min, Thomas Moelg, Pardeep Pall, Aurelien Ribes, Peter Thorne, Rong Zhang

Review Editors: Judit Bartholy (Hungary), Robert Vautard (France), Tetsuzo Yasunari (Japan)

Date of Draft: 15 April 2011

Notes: TSU Compiled Version

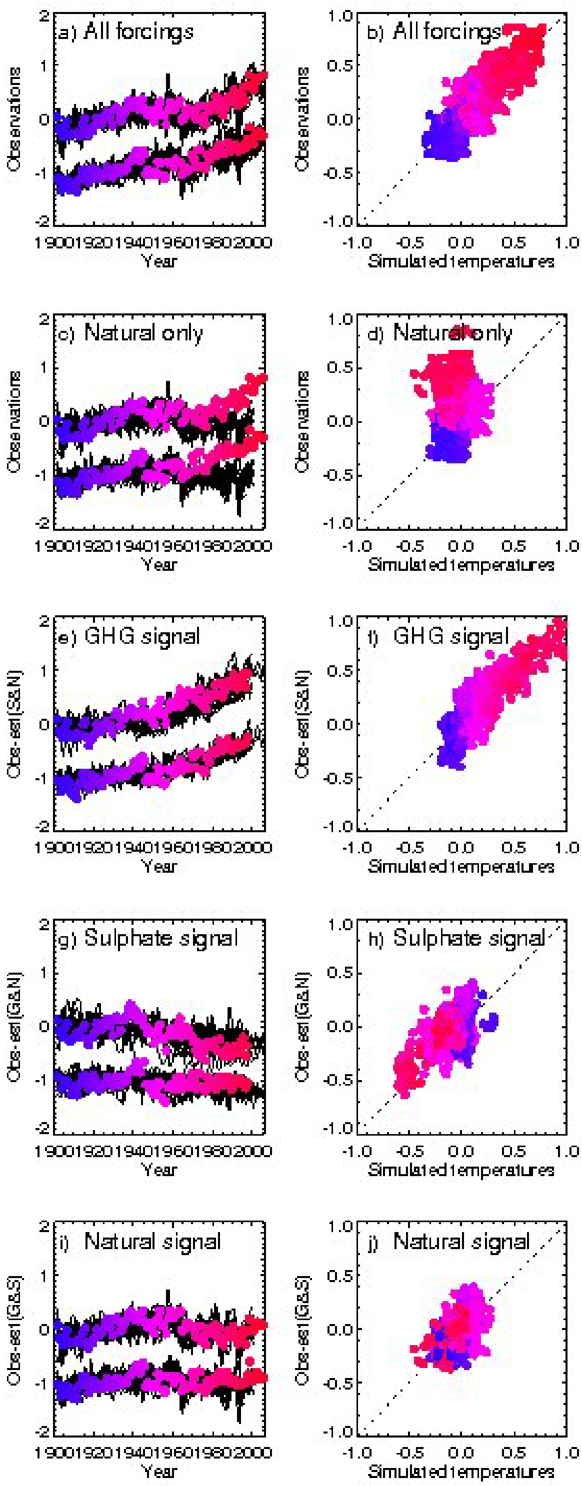

Figure 10.1: Schematic demonstration of optimal detection (Allen et al., 2007; to be updated to CMIP-5 models by Imbers et al., 2011). A simple attribution analysis, comparing model simulations with observed temperature changes over the 20th century. **a)** Observed northern and southern hemisphere area-averaged near-surface temperature anomalies during the period 1901–2005 relative to average temperatures between 1900–1940. Colour scale indicates time, with redder being more recent. Black lines: Corresponding simulated temperatures from six of the models shown in Figure 1 driven by the combination of GHG increase, anthropogenic sulfate aerosols, and natural (solar and volcanic) variability. Southern Hemisphere points are offset by 1^{o}C. **b)** Same data, plotting model simulations (horizontal) against observations (vertical). Colour scale indicates time, as in panel a). **c)** and **d)** show the same but where the models only

include natural forcings. **e)** Observed temperature anomalies after removing the best-fit contribution from sulfate and natural forcing. Best-fit is obtained from a three-way, least-squares multiple linear regression between the observations and model-simulated responses to GHGs, sulfate, and natural forcing, obtained from simulations in which drivers are prescribed separately (ensemble means smoothed with a five-point running mean). Black lines: Simulated temperatures from three models driven by GHGs alone. **f)** Simulated greenhouse response versus observed temperatures after removing best-fit sulfate and natural contributions. Regression fits are obtained for the models separately, hence allowing the models to make different errors in the magnitudes of their responses. Fitted points are plotted separately in panel f) and averaged together before being removed from the observation in panel e). **g)** and **h)**: same as in e) and f), but showing the response to anthropogenic sulfates. **i)** and **j)**: the response to natural (solar and volcanic) variability. Formal uncertainty analysis of regression slopes requires a more sophisticated treatment. The fact that the dots in panel f) lie along the leading diagonal indicates that these models are neither overestimating nor underestimating the response to GHG increase (Allen, 2007).

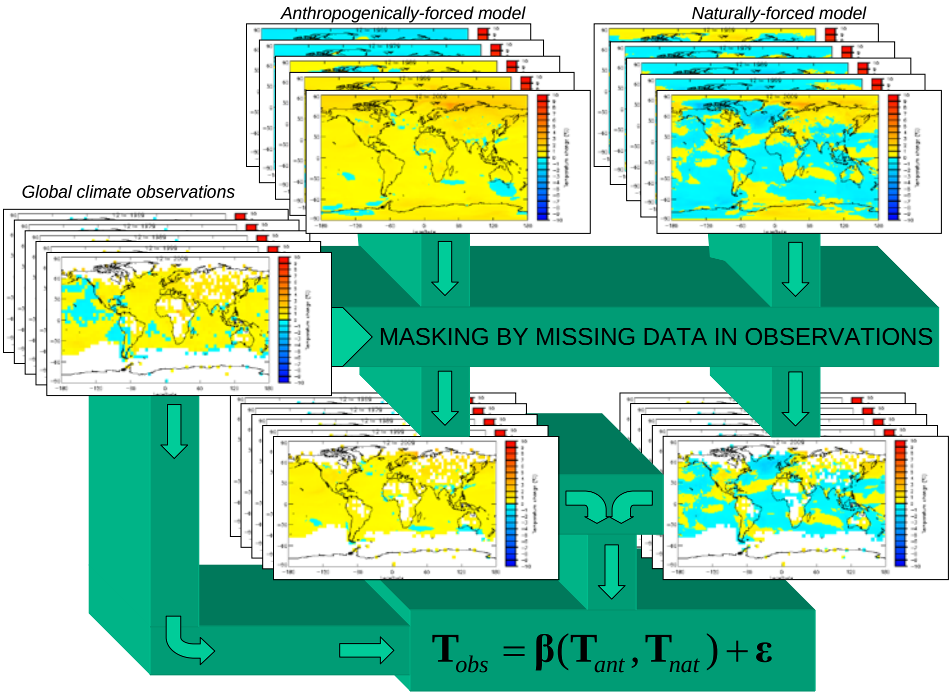

Figure 10.2: Schematic of a detection and attribution analysis on multiple signals employing a linear regression based approach. In the example given here two signals are employed (anthropogenic and natural) and five spatial patterns make up each fingerprint.

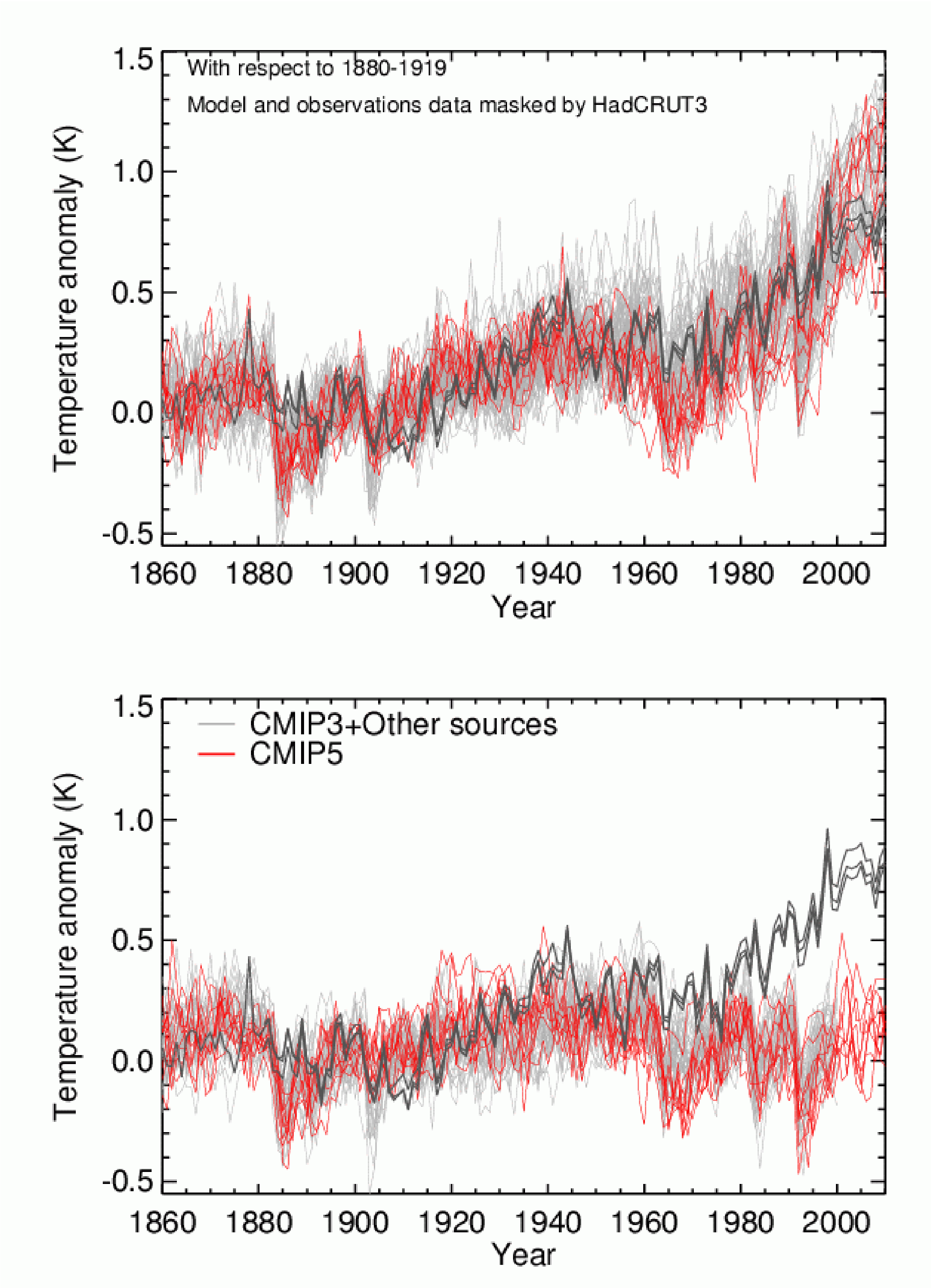

Figure 10.3: [PLACEHOLDER FOR FIRST ORDER DRAFT, to be updated with more CMIP5 model data and new observational datasets when available] Three observational estimates of global mean temperature (dark grey lines) from HadCRUT3, NASA GISS, and NOAA NCDC, compared to model CMIP3 simulations (light grey) and CMIP5 simulations from HadGEM2-ES and CanESM2 (red) with natural forcings only (lower panel) and anthropogenic and natural forcings (upper panel). All data were masked using the HadCRUT3 coverage, and global average anomalies are shown with respect to 1881–1920, where all data are first calculated as anomalies relative to 1961–1990 in each grid box.

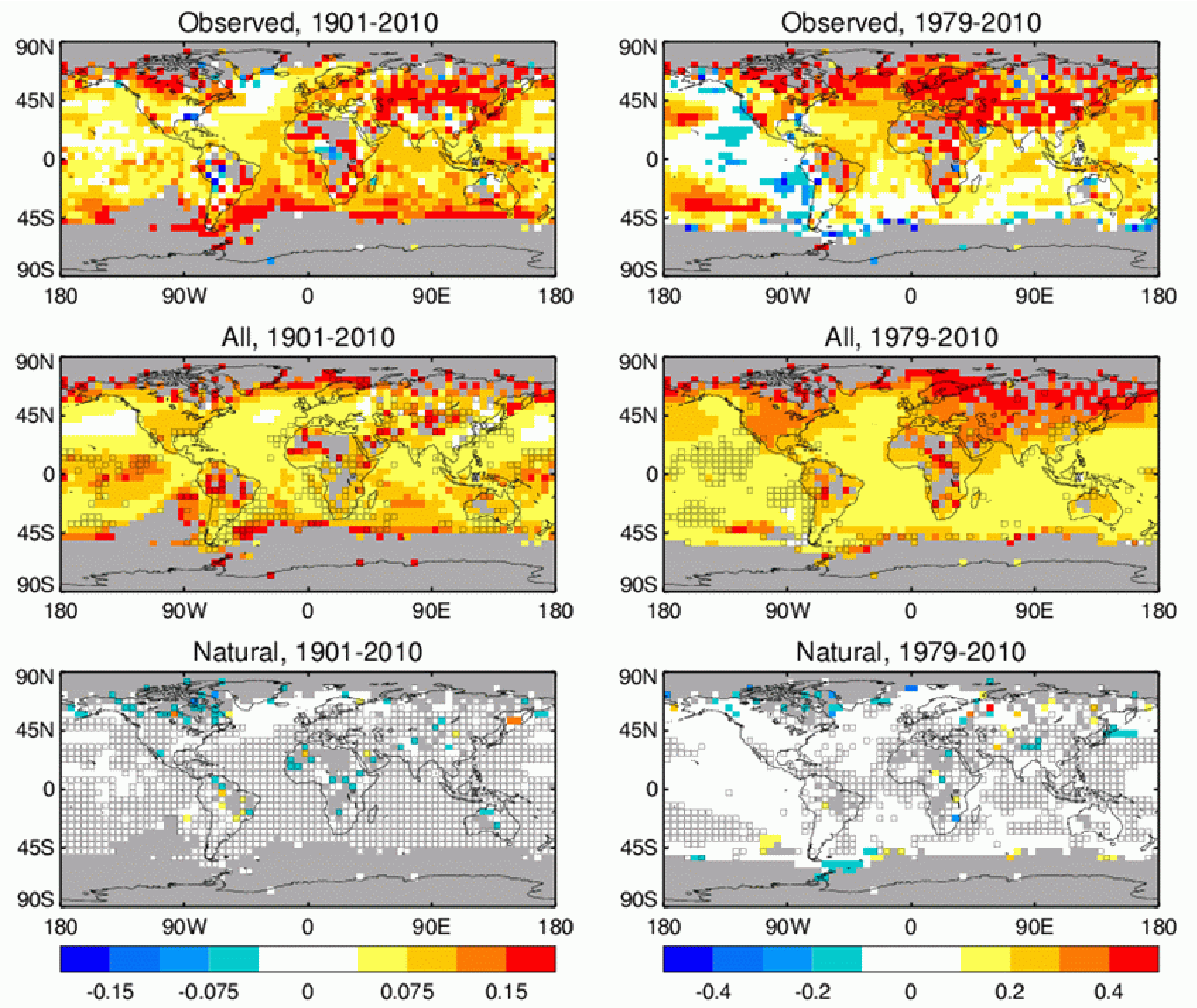

Figure 10.4: [PLACEHOLDER FOR FIRST ORDER DRAFT, to be updated with more CMIP5 model data and new observational datasets when available] Trends in observed and simulated changes (oC per decade) over the 1901–2010 period (left hand column) and the 1979–2010 periods (right hand column). Top row: Trends in observed temperature changes averaged over the HadCRUT3, NASA GISS, and NCDC datasets. Second row: Trends averaged over the CMIP3 and available CMIP5 datasets when they include anthropogenic and natural forcings. Third row: Trends averaged over the model datasets when they include natural forcings only. Data shown only where observational data are available in the HadCRUT3 dataset. Boxes in 2nd and 3rd rows show where 5 to 95 percentile of model range lies above or below observational value at that grid box.

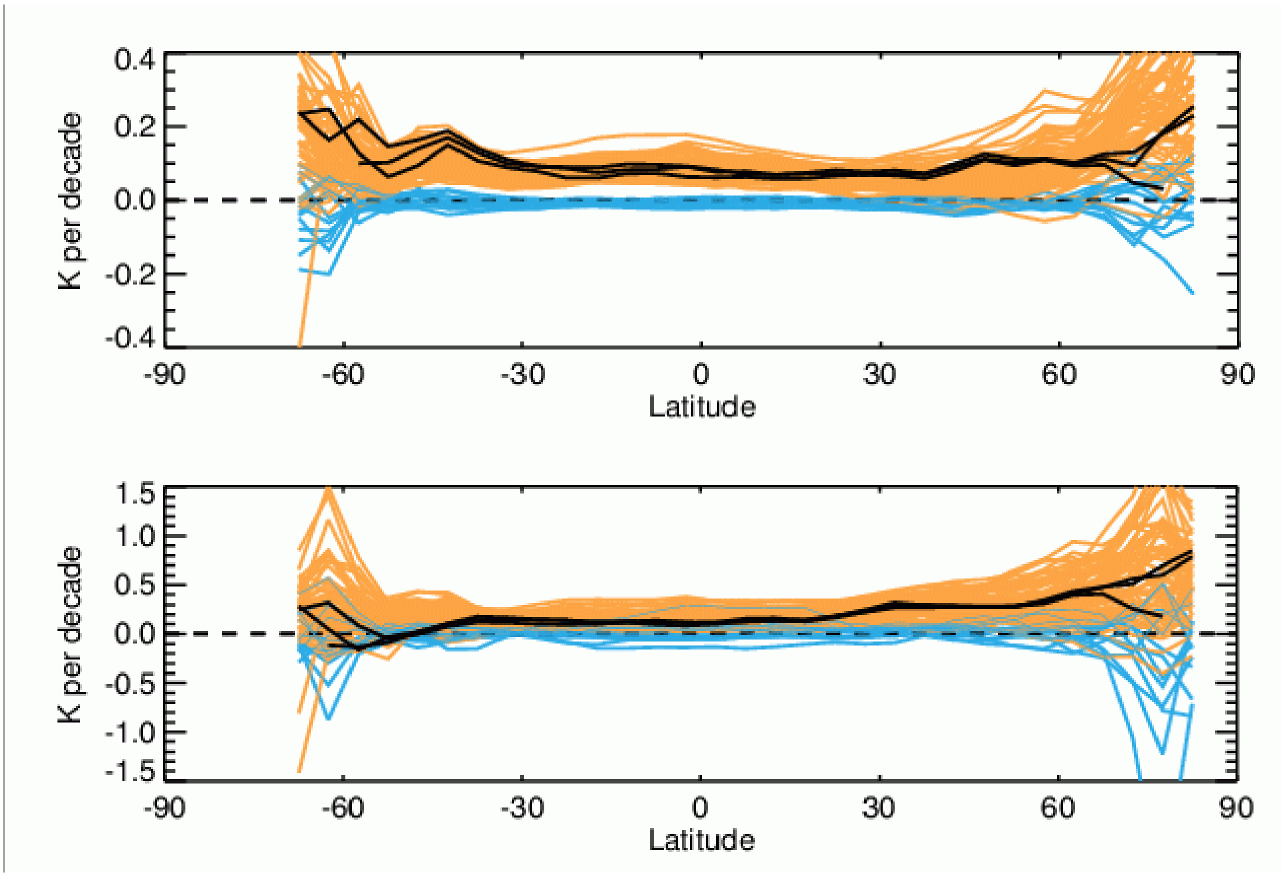

Figure 10.5: [PLACEHOLDER FOR FIRST ORDER DRAFT, to be updated with more CMIP5 model data and new observational datasets when available] Zonal mean temperature trends over 1901–2010 period (top) and 1979–2010 period (bottom). Black lines show HadCRUT3, NASA GIS and NCDC observational datasets, orange lines models with anthropogenic and natural forcings, blue lines models with natural forcings only. All data masked to HadRUT3 mask.

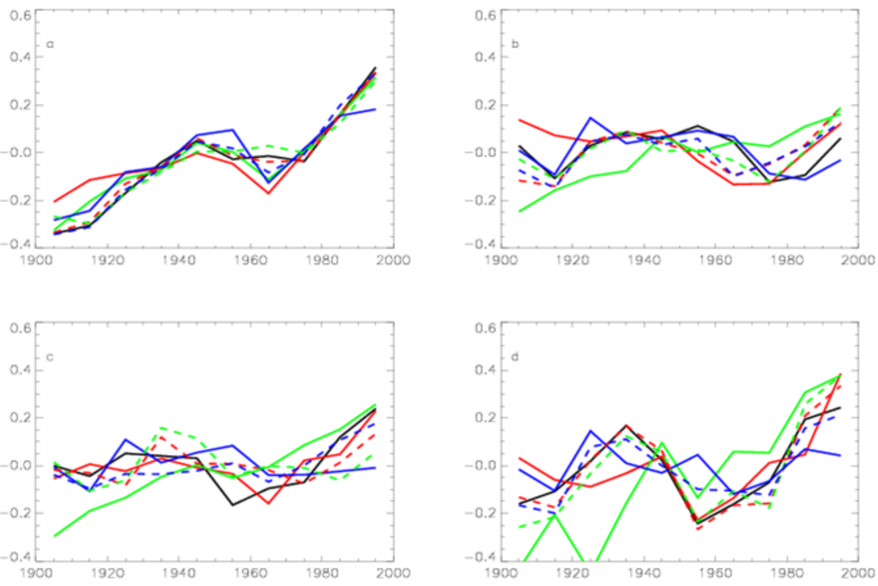

Box 10.1, Figure 1: [PLACEHOLDER FOR FIRST ORDER DRAFT, to be updated with CMIP5 models] Components of large scale temperature response a) global mean, b) northern hemisphere average minus southern hemisphere average, c) land average minus ocean average, d) meridional temperature gradient) for three models (HadCM3, GFDL, PCM, solid lines) and after scaling by optimal detection using observational constraints (dashed lines). Adapted from (Stott et al., 2006).

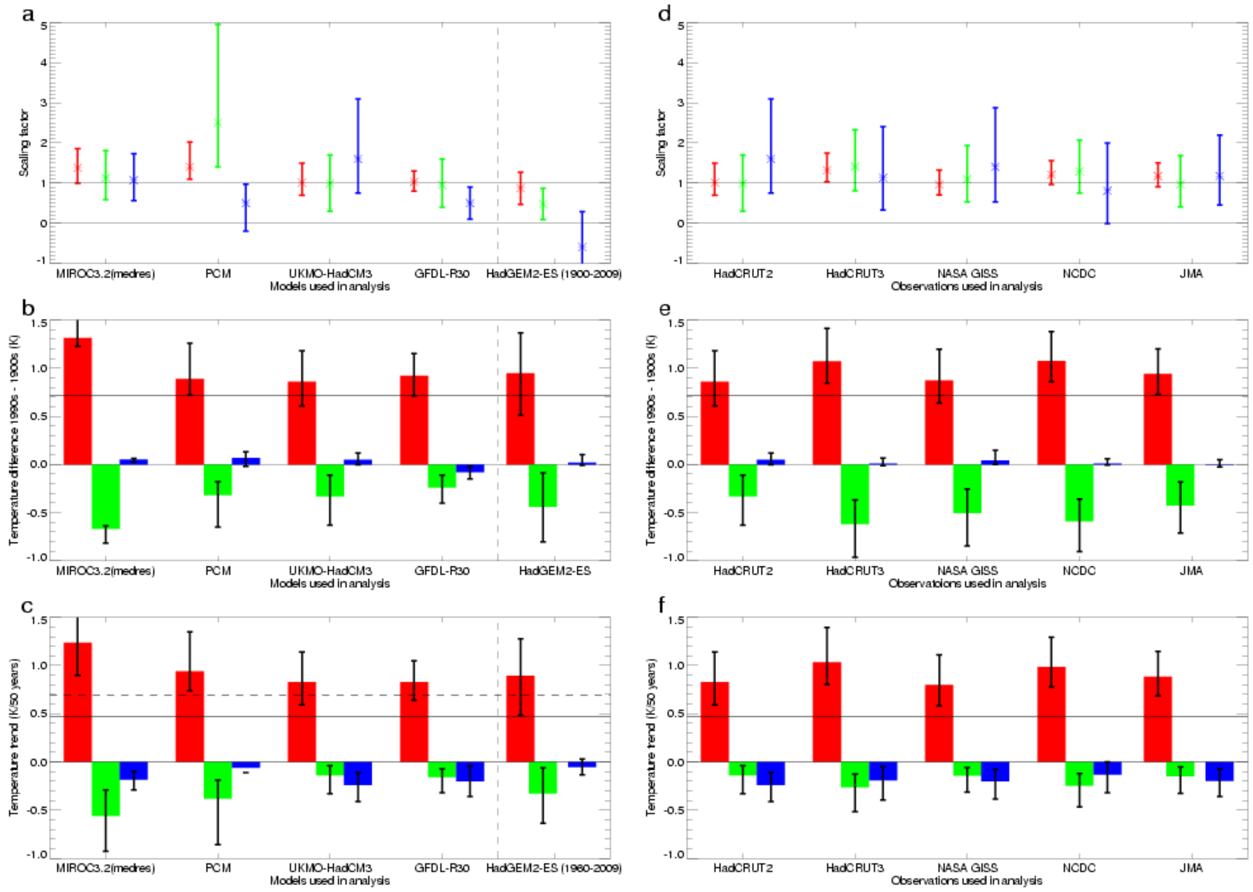

Figure 10.6: [PLACEHOLDER FOR FIRST ORDER DRAFT**,** to be updated with CMIP5 model analyses for updated period to include 21st century data] Estimated contributions from greenhouse gas (red), other anthropogenic (green) and natural (blue) components to observed global surface temperature changes. **a)** 5 to 95% uncertainty limits on scaling factors based on an analysis over the 1900–1999 period (leftmost 4 sets of bars) and 1900–2009 period (rightmost set of bars). **b)** The corresponding estimated contributions of forced changes to temperature changes over the 20th century expressed as the difference between 1990 to 1999 mean temperature and 1900 to 1909 mean temperature. **c)** Estimated contribution to temperature trend over 1950–1999 (leftmost 4 sets of bars) and over 1960–2009 (rightmost set of bars). The solid horizontal black lines in b) and c) show the corresponding observed temperature changes from HadCRUT2v (Parker et al., 2004) and the dashed line in c) show the observed temperature trend over 1960–2009 HadCRUT3v (Brohan et al., 2006). Five different analyses are shown using different models (MIROC3.2, PCM, HadCM3, GFDL-R30, HadGEM2-ES) which are explained in more detail in the text. From (Stott et al., 2010) adapated from (Hegerl et al., 2007). **d)** to **f)** Parallel plots to a) to c) but entirely for 1900–1999 period, for HadCM3 model and for five different observational datasets; (HadCRUT2v, HadCRUT3v, NASA GISS, NCDC, JMA). From (Jones et al., 2011, in prep). (Jones, G. S., The sensitivity of the choice of observational dataset on the detection of anthropogenic changes to near surface temperatures).

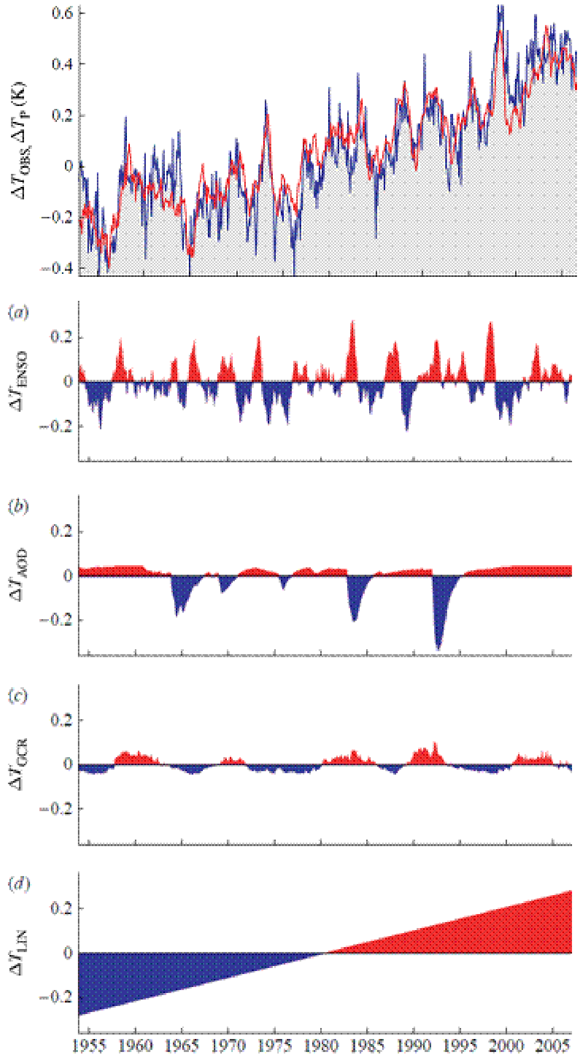

Figure 10.7: Top: the variations of the observed global mean air surface temperature anomaly (blue line) and the best multivariate fit (red line). Below: the contributions to the fit from a) ENSO, b) volcanoes, c) solar contribution, d) a linear drift. From Lockwood (2008).

Figure 10.8: [PLACEHOLDER FOR FIRST ORDER DRAFT, to include CMIP5 simulations] Plot of temperature and precipitation on sub-continental regions illustrating greater signal to noise and separation of anthropogenically and naturally forced CMIP climate model simulations.

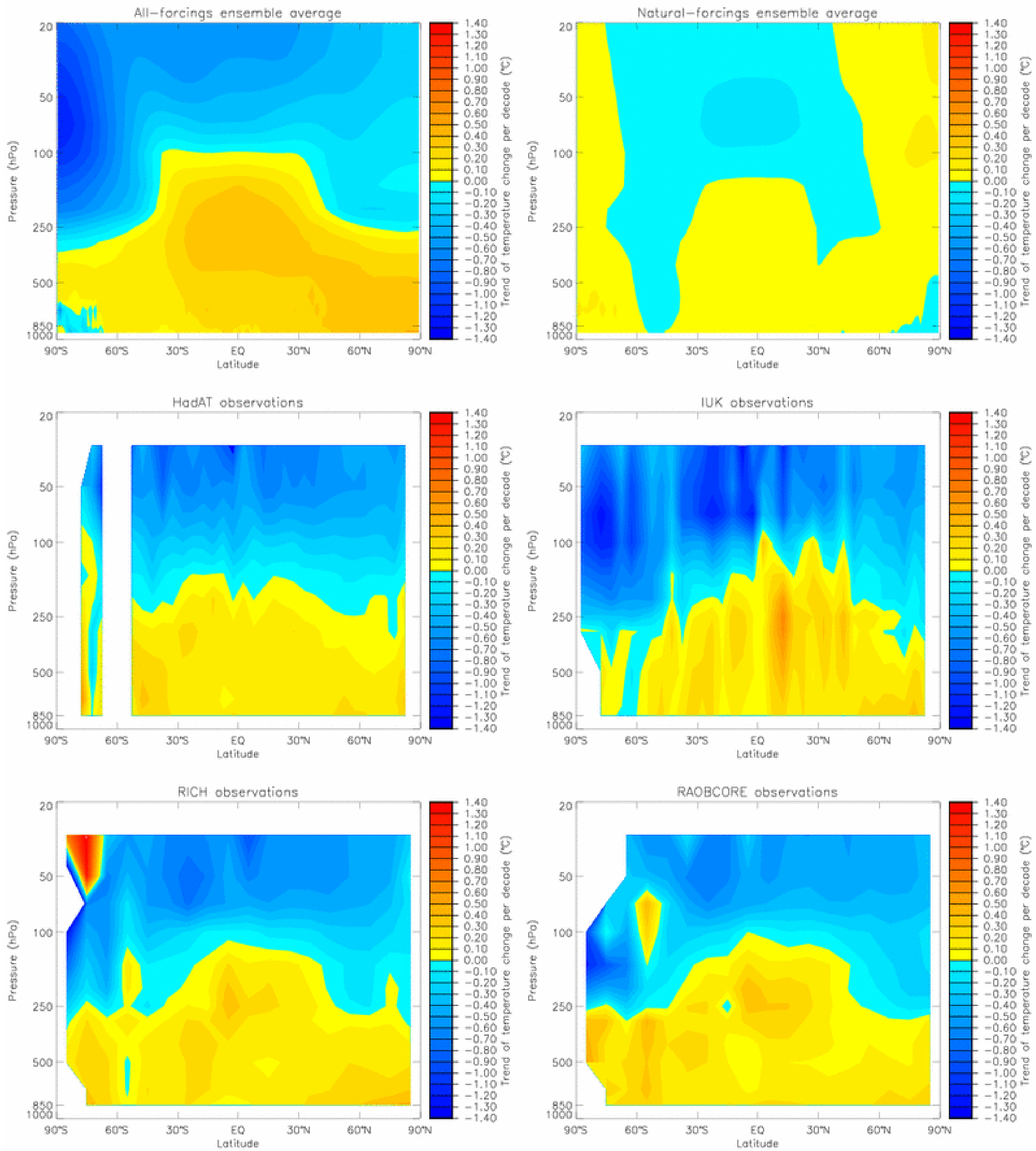

Figure 10.9: [PLACEHOLDER FOR FIRST ORDER DRAFT, to be updated with CMIP5 models] Latitude-height sections of simulated and observed zonal mean temperatures trends from December 1957 to November 2009 for all data except for IUK which is only available to 2006. Shown are the ensemble mean of all forcing and natural forcing simulations for HadGEM1 (top row), and four radiosonde data sets. One data point at a given latitude is considered sufficient to generate zonal means in this figure. From Lott et al., 2011 (in preparation).

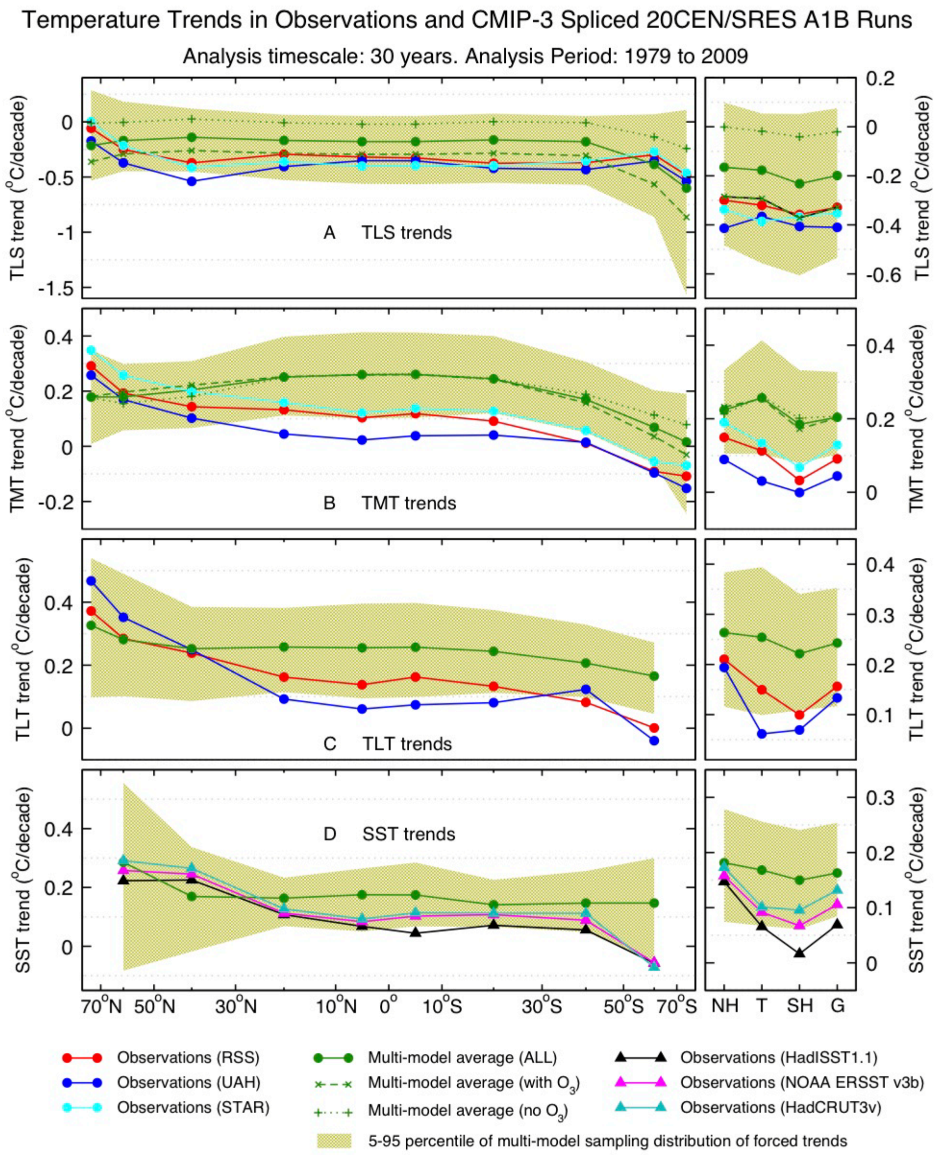

Figure 10.10: [PLACEHOLDER FOR FIRST ORDER DRAFT, to be updated with CMIP5 models] Comparison of the latitude/altitude structure of 30-year temperature trends in observations and in CMIP3 models. Results are for the lower stratosphere (TLS; A), the mid- to upper troposphere (TMT; B), the lower troposphere (TLT; C), and SST (D). Modeled and observed trends were calculated over the common period 1979–2009. The analysis period contains only two samples of overlapping 30-year trends (for the periods 1979–2008 and 1980–2009). Each observed trend (bo) is the average of these two trend samples. Since 50 individual realizations of the 1979–2009 period are available from the spliced 20CEN/SRES A1B runs, each multi-model average trend, << bm >>, is based on 50 × 2 samples of overlapping 30-year trends. The 5–95 percentiles of these sampling distributions are shaded. Results in the left column are for individual latitude bands (82.5°N-70°N, 70°N-50°N, 50°N-30°N, 30°N- 10°N, 10°N-0°N, etc.), and are plotted on the sine of the center of the latitude band. Results in the right column are for temperatures averaged over 4 different regions: the NH, the tropics (20◦N-20◦S), the SH, and the globe. Because of differences in the latitudinal extent of observational MSU datasets, the RSS spatial coverage was used as the basis for calculating all spatial averages of TLS, TMT, and TLT (see SI Appendix). Spatial averages in A-C data use both land and ocean data. The model TLS and TMT results were stratified according to the presence or absence of stratospheric ozone depletion in the CMIP3 20CEN runs. Since "with O3" and "no O3" trends are virtually identical lower in the atmosphere, "ozone-stratified" results are not shown for TLT and SST. From Santer et al., 2011 (in preparation).

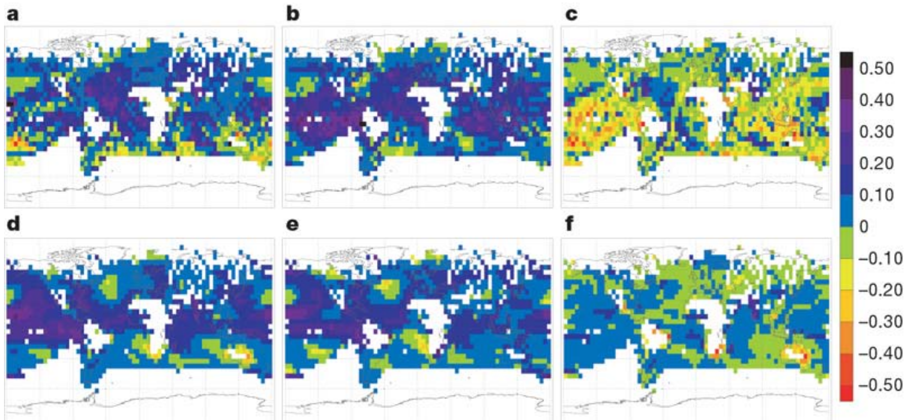

Figure 10.11: Observed (top row) and simulated (bottom row) trends in specific humidity over the period 1973–1999 in g/kg per decade. Observed specific humidity trends a) and the sum of trends simulated in response to anthropogenic and natural forcings d) are compared with trends calculated from observed b) and simulated e) temperature changes under the assumption of constant relative humidity; the residual (actual trend minus temperature induced trend is shown in c) and f) (Willett et al., 2007).

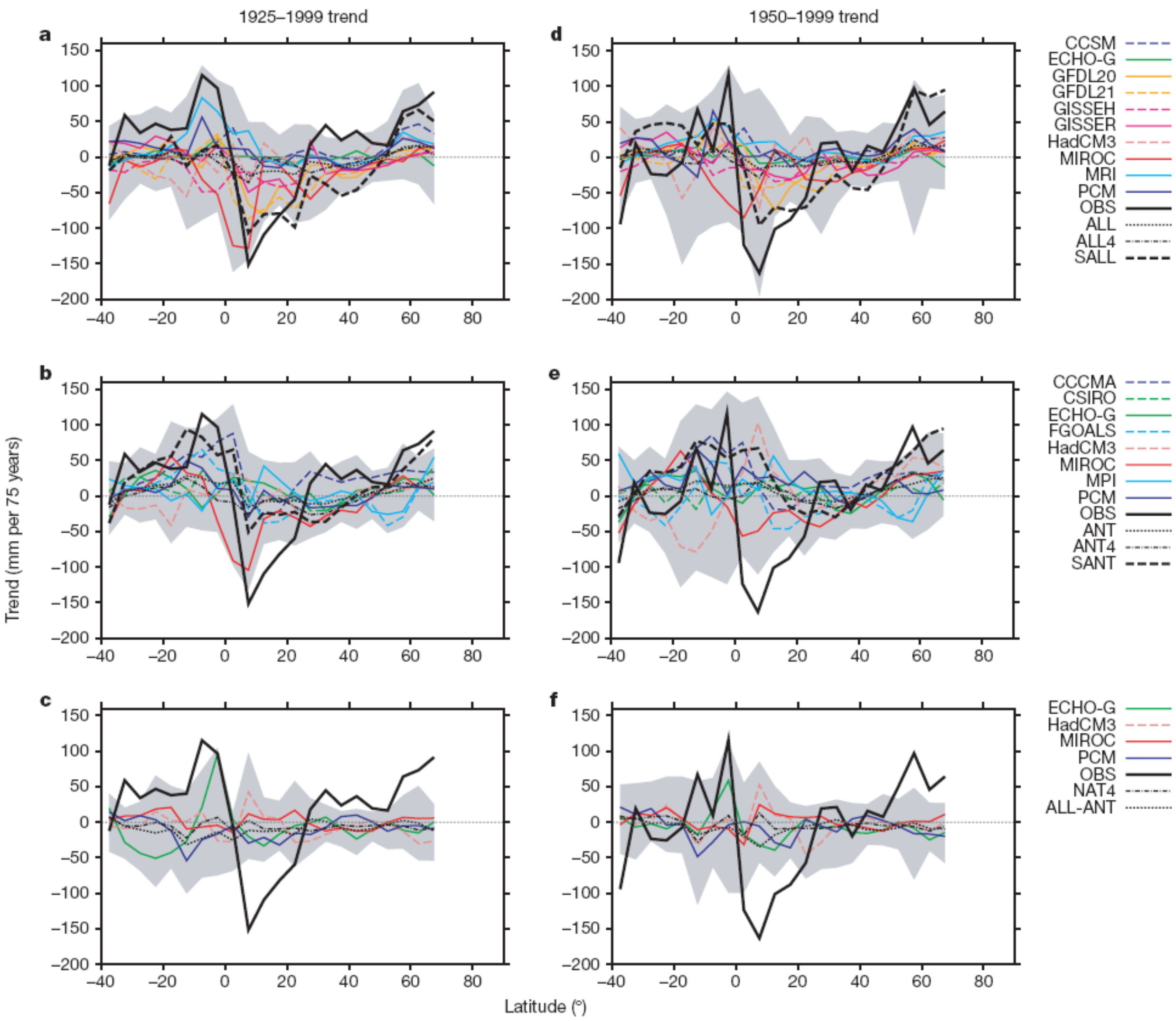

Figure 10.12: Comparison between observed (solid black) and simulated zonal mean land precipitation trends for 1925–1999 (left) and 1950–1999 (right). Black dotted lines indicate the multi-model means from all available models (ALL in top row, ANT in middle row, and NAT in bottom row), and black dash-dotted lines those from the subset of 4 models which simulated the response to each of the forcing scenarios (ALL4, ANT4 and NAT4). The model simulated range of trends is shown shaded. Black dashed lines indicate ensemble means of ALL and ANT simulations that have been scaled (SALL and SANT) to best fit the observations based on a 1-signal analysis. Coloured lines indicate individual model mean trends (Zhang et al., 2007).

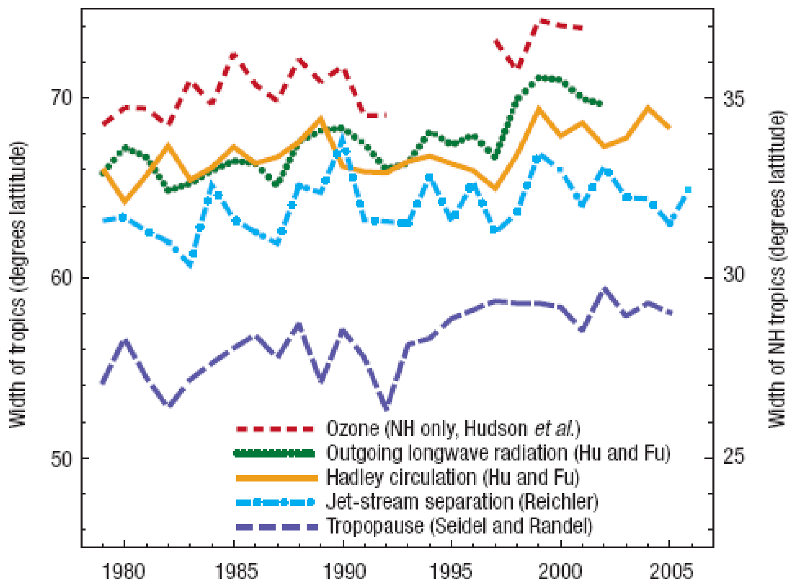

Figure 10.13: [PLACEHOLDER FOR FIRST ORDER DRAFT, will be replaced by a model-observation comparison figure] Changes in the tropical belt, estimated from different quantities as marked in the plot Adapted from (Seidel et al., 2008).

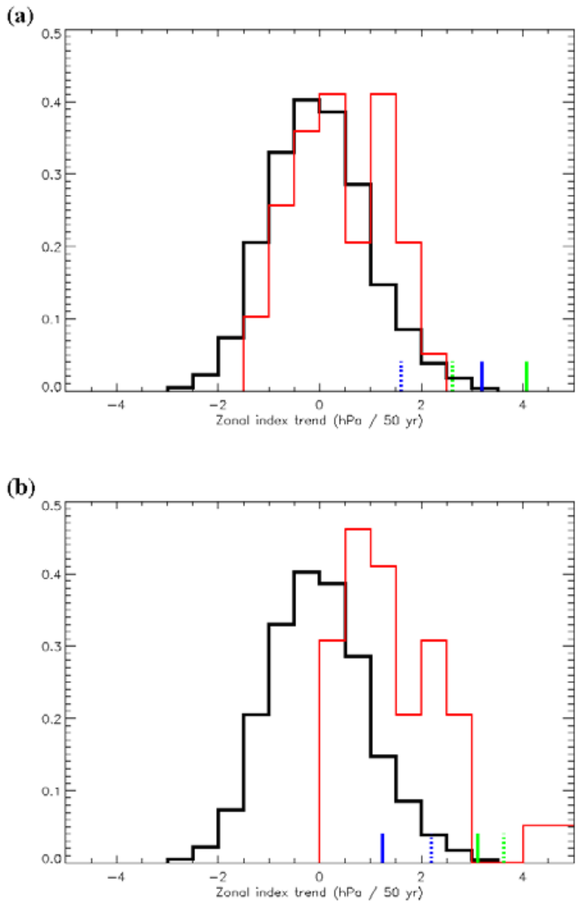

Figure 10.14: DJF zonal index trends over 50-year periods. Panel a) shows the 50-year DJF trend in an index of meridional pressure gradient derived by subtracting mean SLP poleward of 45°N from mean SLP equatorward of 45°N in HadSLP2r (blue) and the NCEP reanalysis (green) over the period 1955–2005 (solid), and 1961–2011 (dotted). This zonal index is closely related to the NAM index. The black line shows a histogram of trends simulated in overlapping segments of control simulation from nine CMIP3 models, while the red line is a histogram of 1955–2005 trends in the historical simulations of nine CMIP3 models including greenhouse gas changes, sulphate aerosol changes, natural forcings and stratospheric ozone depletion. Panel b) shows equivalent 50-year DJF zonal index trends for the Southern Hemisphere, closely related to SAM index trends. Updated from Gillett (2005).

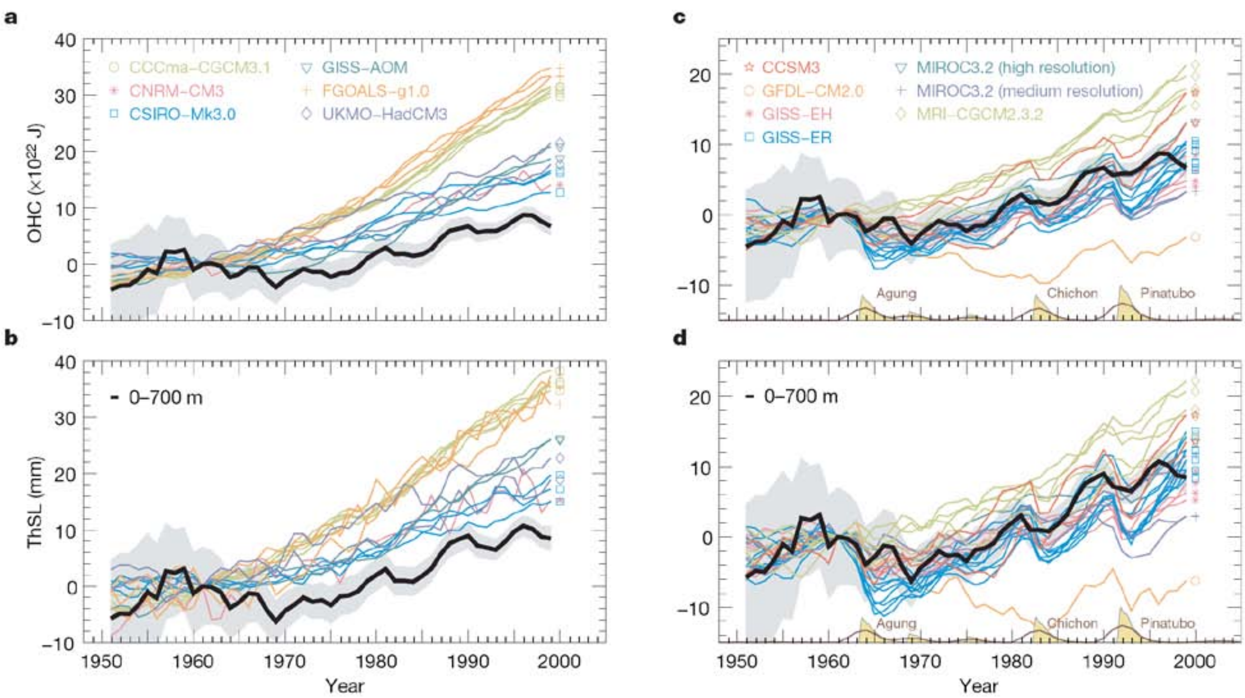

Figure 10.15: Comparison of observed and simulated ocean heat content (OHC) and thermosteric sea level (ThSL) estimates for the upper 700 m. a) and b): Models without volcanic forcing. c) and d): Models with volcanic forcing (Domingues et al., 2008).

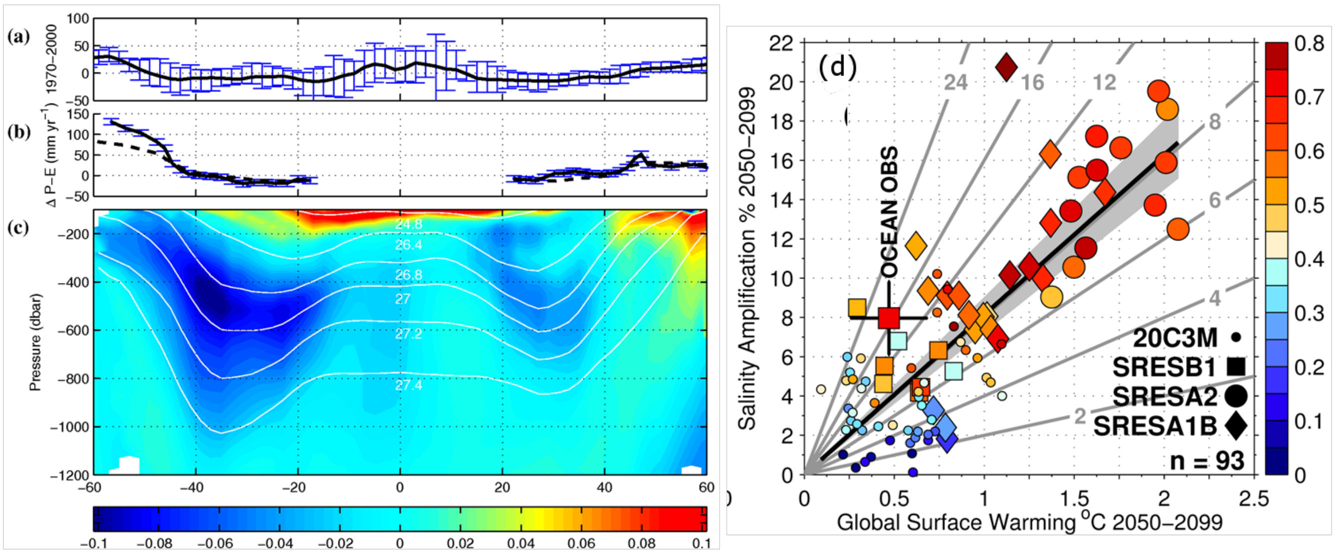

Figure 10.16: Ocean salinity change observed in the ocean (panel c) and estimated surface precipitation minus evaporation (panel b), and comparison with coupled climate change model projections of precipitation minus evaporation from 10 IPCC AR4 models (panel a), and the salinity pattern amplification (see text) from coupled GCM with all forcings and from 20th century simulations and observations as a function of global surface temperature change (panel d). Panel a),b), and c) are from Helm et al. (2010) and panel c) is from Durack and Wijffels (2011, in prep).

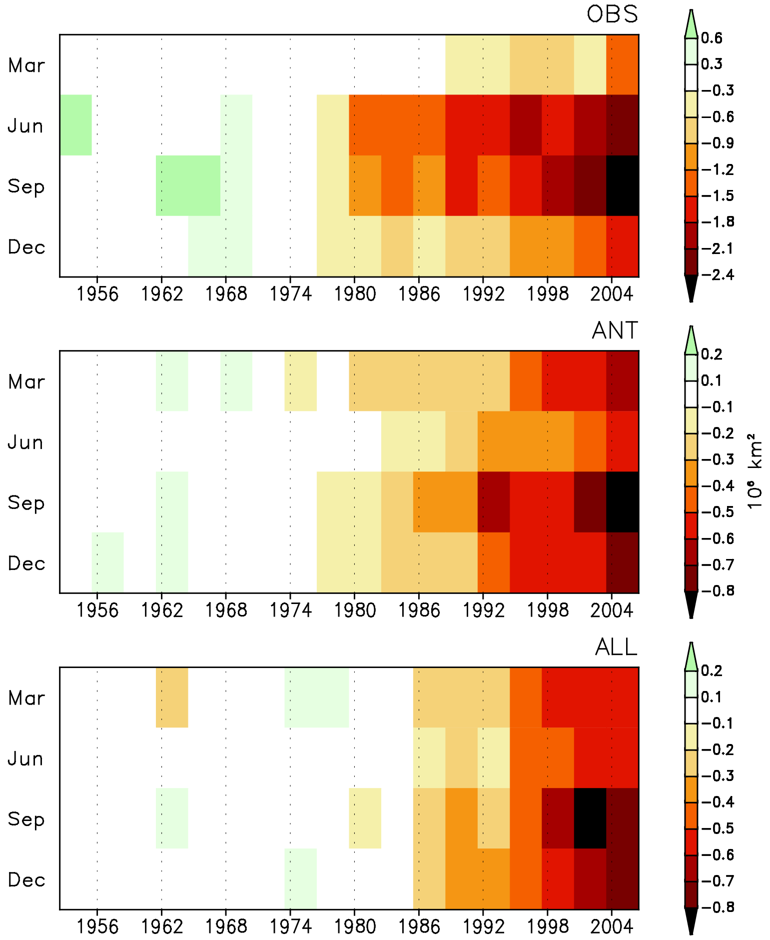

Figure 10.17: Seasonal evolution of observed and simulated Arctic sea ice extent over 1953–2006. Anomalies are displayed relative to the 1953–1982 means from observations (OBS) and model simulations with anthropogenic only (ANT) and natural plus anthropogenic (ALL) forcings. These anomalies were obtained by computing non-overlapping 3-year mean sea ice anomalies for March, June, September, and December separately. Note different color scales between the observed and modeled patterns. Units: $\times 10^6$ km^2 (Min et al., 2008).

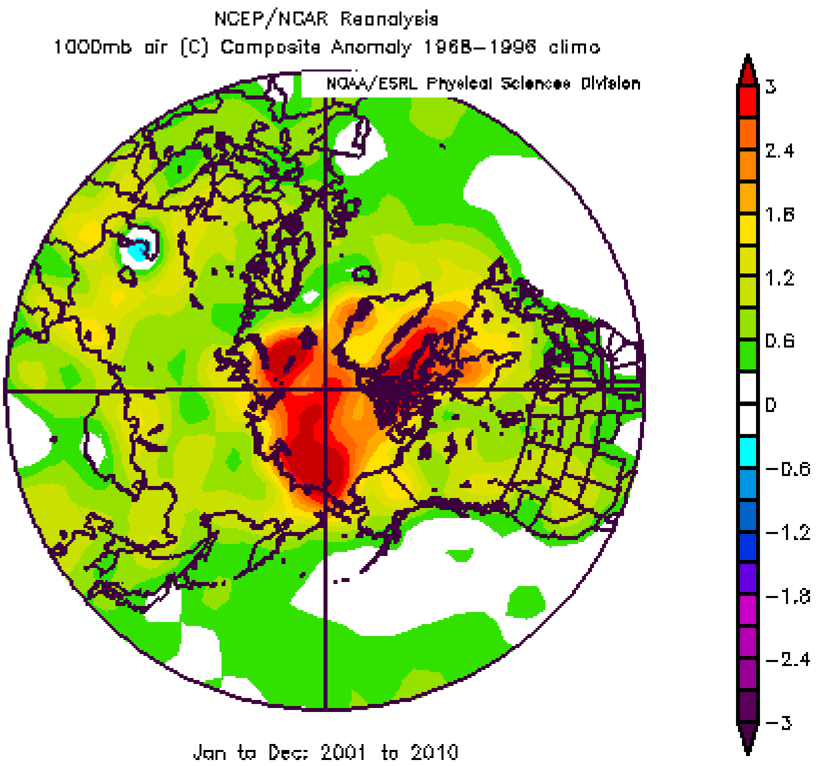

Figure 10.18: Near surface (1000 hPa) air temperature anomaly multiyear composites (°C) for 2001–2010. Anomalies are relative to 1968–1996 mean and show an Arctic amplification of recent air temperatures. Data are from the NCEP–NCAR Reanalysis through the NOAA/Earth Systems Research Laboratory, generated online at www.cdc.noaa.gov.

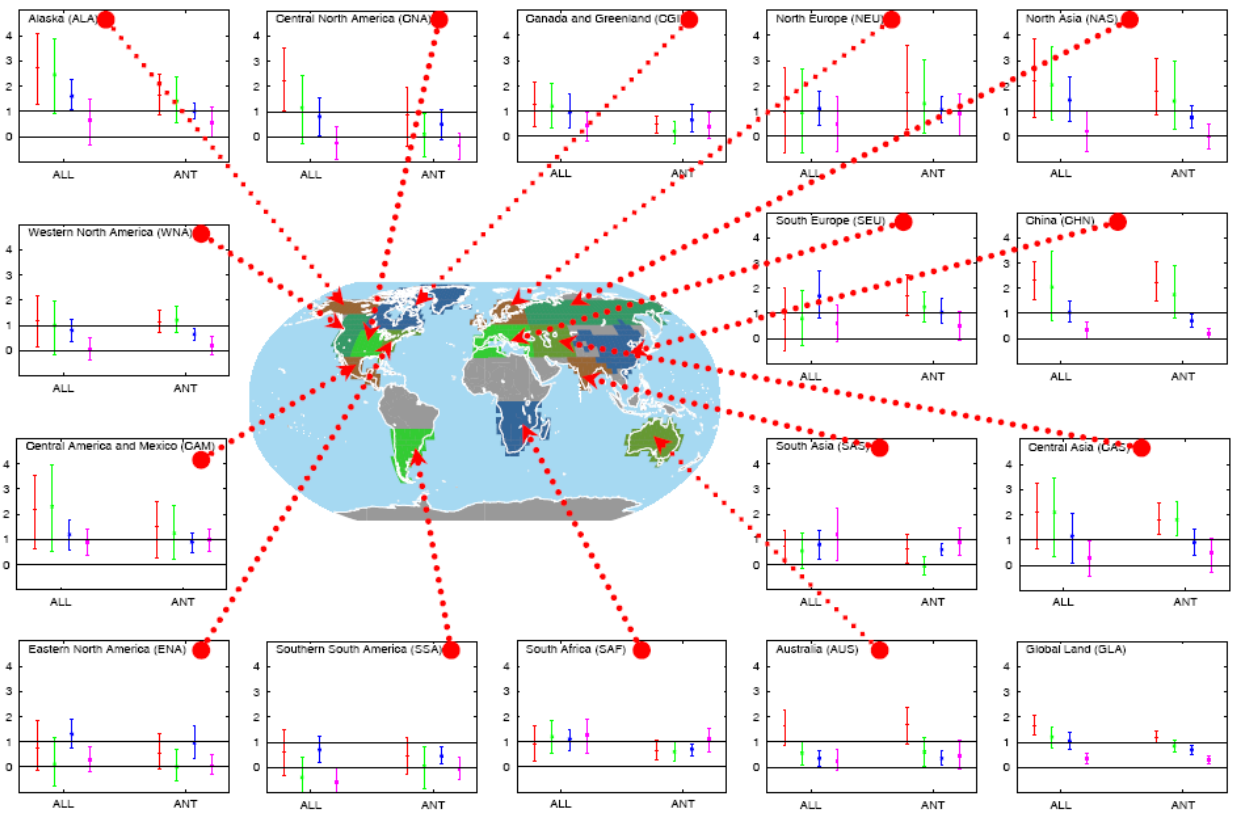

Figure 10.19: Scaling factors and their 90% confidence intervals for annual extreme temperatures for ALL and ANT forcings for period 1961–2000. Red, green, blue, pink error bars are for TNn, TXn, TNx, and TXx respectively. Detection is claimed at the 10% significance level if the 90% confidence interval of a scaling factor is above zero line (Zwiers et al., 2011).

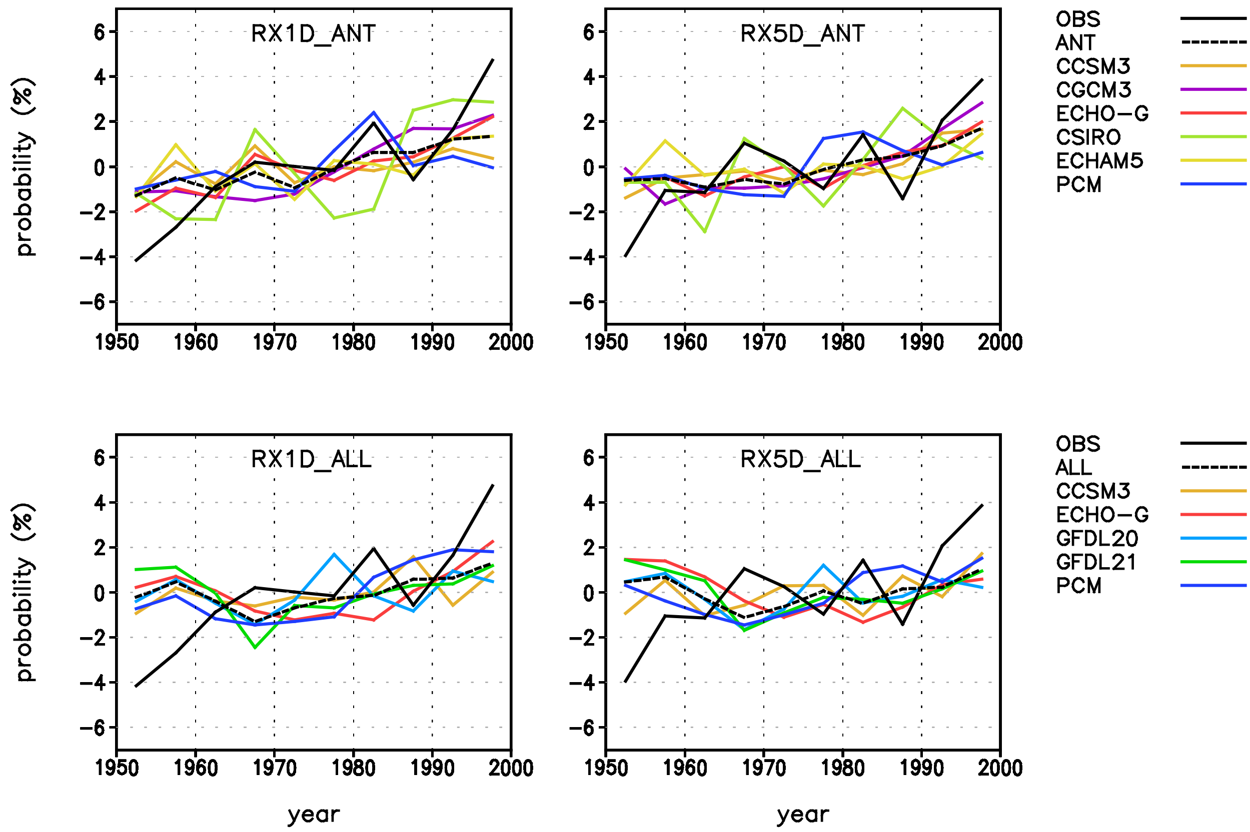

Figure 10.20: Time series of five-year mean area-averaged extreme precipitation indices anomalies for 1-day (RX1D, left) and 5-day (RX5D, right) precipitation amounts over Northern Hemisphere land during 1951–1999. Model simulations with anthropogenic (ANT, upper) forcing; model simulations with anthropogenic plus natural (ALL, lower) forcing. Black solid lines are observations and dashed lines represent multi-model means. Coloured lines indicate results for individual model averages (see Supplementary Table 1 of Min et al. (2011) for the list of climate model simulations and Supplementary Fig. 2 of Min et al. (2011) for time series of individual simulations). Annual extremes of 1-day and 5-day accumulations were fitted to the Generalized Extreme Value distribution which was then inverted to map the extremes onto a 0-100% probability scale. Each time series is represented as anomalies with respect to its 1951–1999 mean (Min et al. 2011).

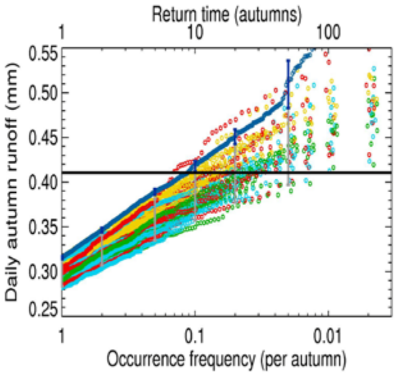

Figure 10.21: Return times for precipitation-induced floods aggregated over England and Wales for conditions corresponding to October to December 2000 with boundary conditions as observed (blue) and under a range of simulations of the conditions that would have obtained in the absence of anthropogenic greenhouse warming over the 20th century – colours correspond to different AOGCMs used to define the greenhouse signal, black horizontal line to the threshold exceeded in autumn 2000 – from Pall et al. (2011). [This figure will also include a Panel b: corresponding figure for precipitation- and snow-melt-induced floods in 4 catchments across the UK for conditions corresponding to January to March 2001, from Kay et al., 2011 (in preparation). This would probably look similar to the above, but with most of the non-industrial distributions above the industrial one.]

a)

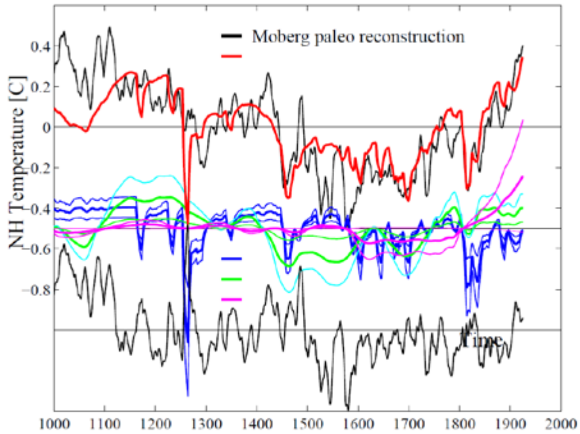

b)

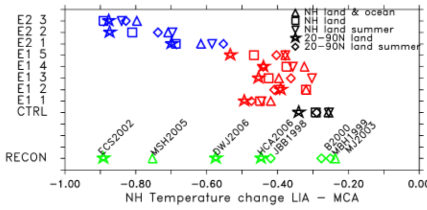

c)

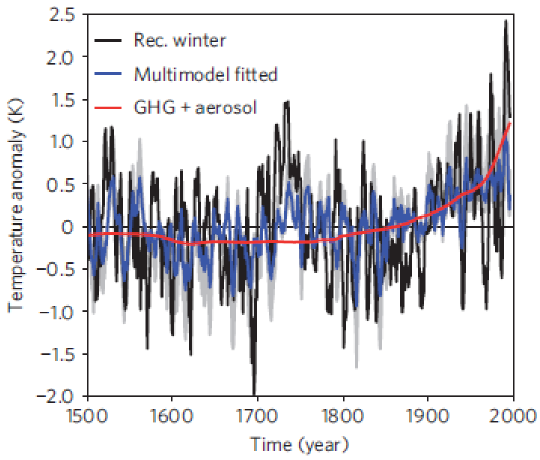

Figure 10.22: [REVIEWERS NOTE THAT ALL FIGURES WILL BE REDONE USING THE CMIP5 ARCHIVE AND MORE COMPLETE DATA] Role of external forcing for hemispheric (a,b,) and European (c) temperature variability. **a)** Reconstructed changes in NH mean temperature (30-90N) reconstructed by Moberg et al. (2005), black compared to best fit simulation from OAGCM [NOT YET SHOWN] and an Energy Balance Model Simulation (red; highly significantly detectable). Middle panel: estimated contribution from volcanic (blue, detectable based on EBM and OAGCM), solar (detectable for EBM) and greenhouse gas forcing (detectable based on OAGCM). The fingerprints are based on EBM simulations [SHOWN] and GCM simulations [NOT YET SHOWN]. Bottom shows the unexplained residual; figure after Hegerl et al., 2007b. **b)** shows an analysis focusing on the Northern Hemispheric temperature difference between the coldest 30-year period during the Little Ice Age 1550–1750 and the warmest 30-year period during the Medieval Warm Period (900–1300) from reconstructions (green symbols, see Jansen et al., 2007) compared to climate model simulations without forcing (black), all forcings included using present best estimate solar forcing (red) and the same using high solar forcing estimates (blue; from Jungclaus et al., 2010). Panel **c)** shows a reconstruction of European mean winter temperature (Luterbacher et al., 2004) compared to a best estimate of the fingerprint for all forcings combined (detectable at the 10% level, uncertainty range shown grey) from OAGCMs, and the detectable contribution to the long-term evolution by greenhouse gas plus aerosol forcing from an Energy Balance Model (red). From Hegerl et al. (2011).

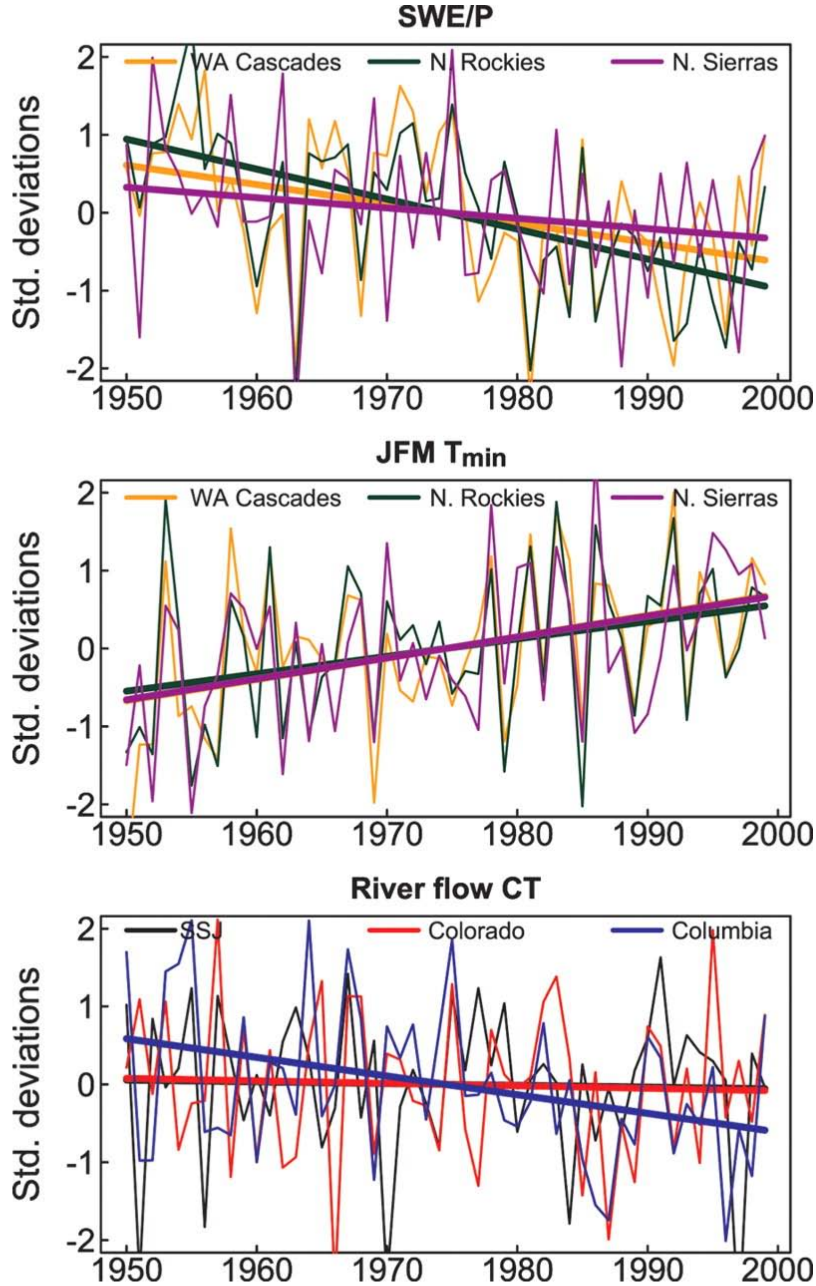

Figure 10.23: Observed time series of selected variables (expressed as unit normal deviates) used in the multivariate detection and attribution analysis. Taken in isolation, seven of nine SWE/P, seven of nine JFM Tmin, and one of the three river flow variables have statistically significant trends (Barnett et al., 2008).

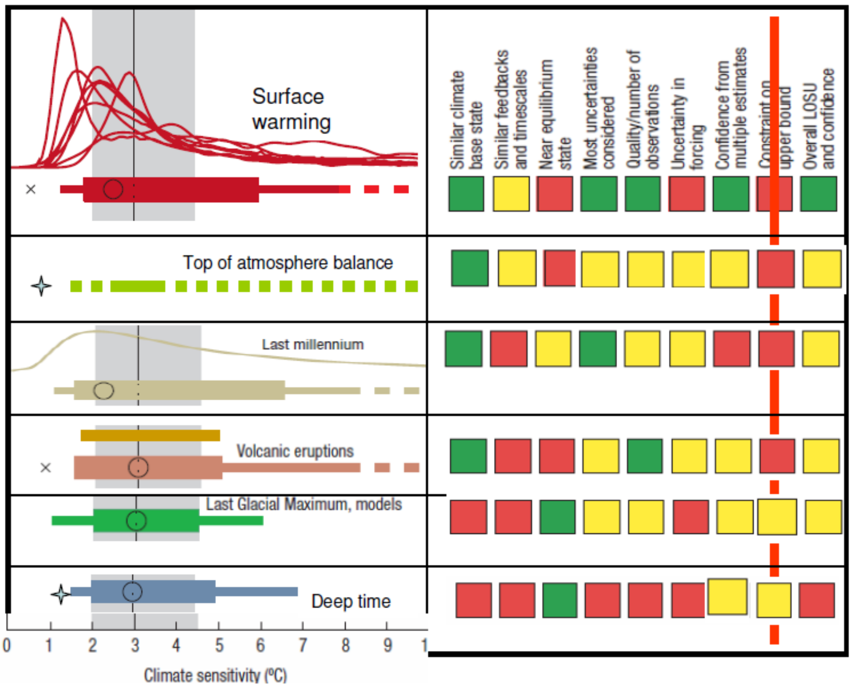

Figure 10.24: [PLACEHOLDER FOR FIRST ORDER: DRAFT / SKETCH OF FIGURE IN PLAN] Estimates of equilibrium climate sensitivity from observed / reconstructed changes in climate compared to overall assessed range (to be determined; grey). The estimates are generally based on comparisons of model evidence (ranging from 0-D EBMs through OAGCMs) with given sensitivity with data for climate change and are based on instrumental changes including surface temperature; estimates based on changes in top-of-the atmosphere radiative balance (2nd row); climate change over the last millennium; volcanic eruptions; changes in the last glacial maximum (only showing model-based estimates since these more completely account for uncertainty), and deep time studies (see chapter 5). The boxes on the right hand side indicate if a condition is fullfilled (green), partly fulfilled (yellow) or problematic (red); assessing advantages and shortcomings/uncertainties of different lines of evidence (Knutti and Hegerl, 2008).

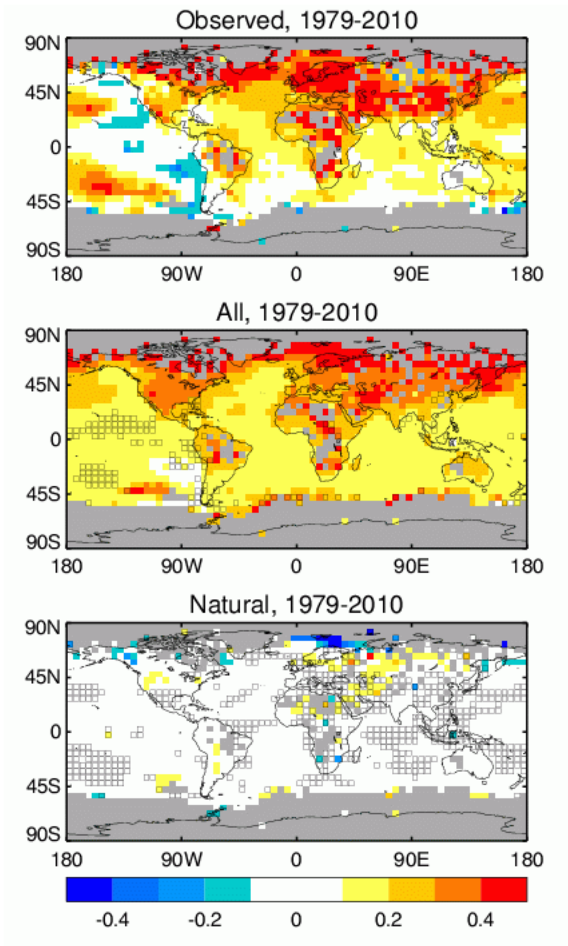

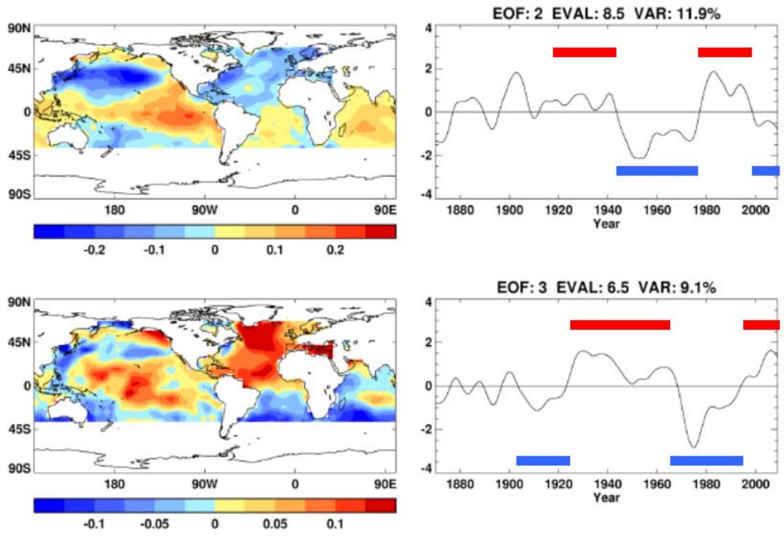

FAQ 10.1, Figure 1: Top part: Comparison between trends over 1979–2010 as observed (top row) and as averaged over the CMIP3 and available CMIP5 datasets when they include anthropogenic and natural forcings (middle row) and when they include only natural forcings (bottom row). Data shown only where observational data are available in the HadCRUT3 dataset. Boxes in 2nd and 3rd rows show where 5 to 95 percentile of model range lies above or below observational value at that grid box. Bottom: Observed pattern of temperature response associated with PDO/IPO (top row) and AMO (bottom row) and their associated timeseries. After (Parker et al., 2007).

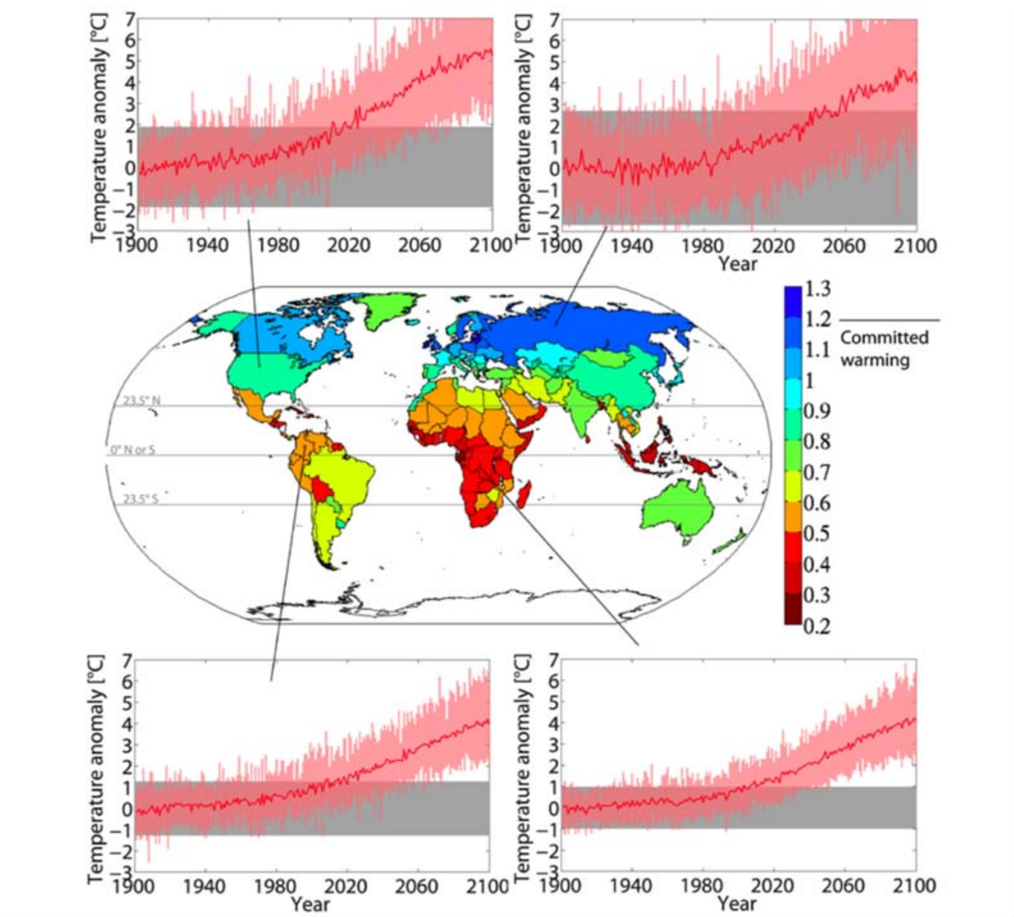

FAQ 10.2, Figure 1: The map shows the global temperature increase (^{o}C) needed for a single location to undergo a statistical significant change in average summer seasonal surface temperature, aggregated on a country level. The black line near the colorbar denotes the committed global average warming if all atmospheric consistuents were fixed at 2000 levels. The small panels show the interannual summer-season variability during the base period (1900–1929) (±2 standard deviations shaded in gray) and the multi model summer surface temperature (red line) of one arbitrarily chosen grid cell within the specific country. The shading in red indicates the 5% and 95% quantiles across all model realizations. From Mahlstein et al. (2011, submitted to PNAS).